Università degli Studi di Ferrara

DOTTORATO DI RICERCA IN

"SCIENZE BIOMEDICHE E BIOTECNOLOGIE"

CICLO XXIX

COORDINATORE Prof. Paolo Pinton

Safety and efficacy of gene therapy for Pompe disease

Settore Scientifico Disciplinare BIO/11

Dottorando

Dott. Puzzo Francesco

Tutore

Prof. Mingozzi Federico

Co-tutor

Prof. Bernardi Francesco

Anni 2014/2017

Contents

1. Introduction

Chapter I

Whole-body correction of Pompe disease with AAV vector-mediated liver delivery of a novel secretable GAA transgene

2. Results

Chapter II

Long-term exposure to Myozyme results in a decrease of anti-drug antibodies in late-onset Pompe disease patients

5. Results

1. Introduction

1.1 Glycogen storage disease type II (Pompe disease)

Glycogen-storage type II, or Pompe disease, (OMIM #232300) is an autosomal recessive disorder, belonging to the family of lysosomal storage disease (LSD). This pathology was described for the first time, in 1932, by a Dutch physician, J.C. Pompe, in a 7 months-old infant who died of idiopathic hypertrophy of the heart; additionally this child also presented a generalized muscle weakness. Dr. Pompe was in fact the first who associated the baby's symptoms with the massive vacuolar glycogen in tissues. In 1954, Pompe disease was classified as glycogen storage disease and only in the 1963 a Belgian biochemist, Henri-Gery Hers, found out that this disease was due to the deficiency of a lysosomal enzyme, the maltase, which is, nowadays, commonly known as acid α-glucosidase (GAA) [1].

Pompe disease is caused by mutations in the gene encoding for GAA, which catalyzes the hydrolysis of α-1,4 and α-1,6 bonds in lysosomal glycogen. GAA, as many other lysosomal enzymes, is intracellularly produced in the rough endoplasmic reticulum (ER) as precursor (110kDa), and during its trafficking to lysosome it undergoes sugar chains modifications and proteolytic cleavages. This maturation process produces the intermediate (95kDa) and mature (76/70kDa) forms of the enzyme [2]. In the Golgi, the addition of mannose-6-phosphate (M6P) allows GAA to bind the cation-independent mannose-6-phosphate (CI-M6P) receptor, which transports the enzyme in the early and late endosome. GAA, therefore, leaves the Golgi apparatus through vesicles which deliver the enzyme in early/late endosomes and lysosomes. Once in late endosome, ligand (GAA)-receptor (CI-M6P) binding is disrupted, by the strong decrease of pH, and the GAA can be released in lysosome [3].

Moreover, even if the mature form (76/70kDa) is reported as the most active, the precursor (110kDa) has an enzymatic activity by itself. As lysosomal enzyme, GAA is not thought to be secreted, however 10% of the protein (110kDa form) is found in circulation, and it can be taken up by the nearby cells through CI-M6P receptor [4], [5]. This mechanism is at the basis of the enzyme replacement therapy which will be discussed in the next paragraph.

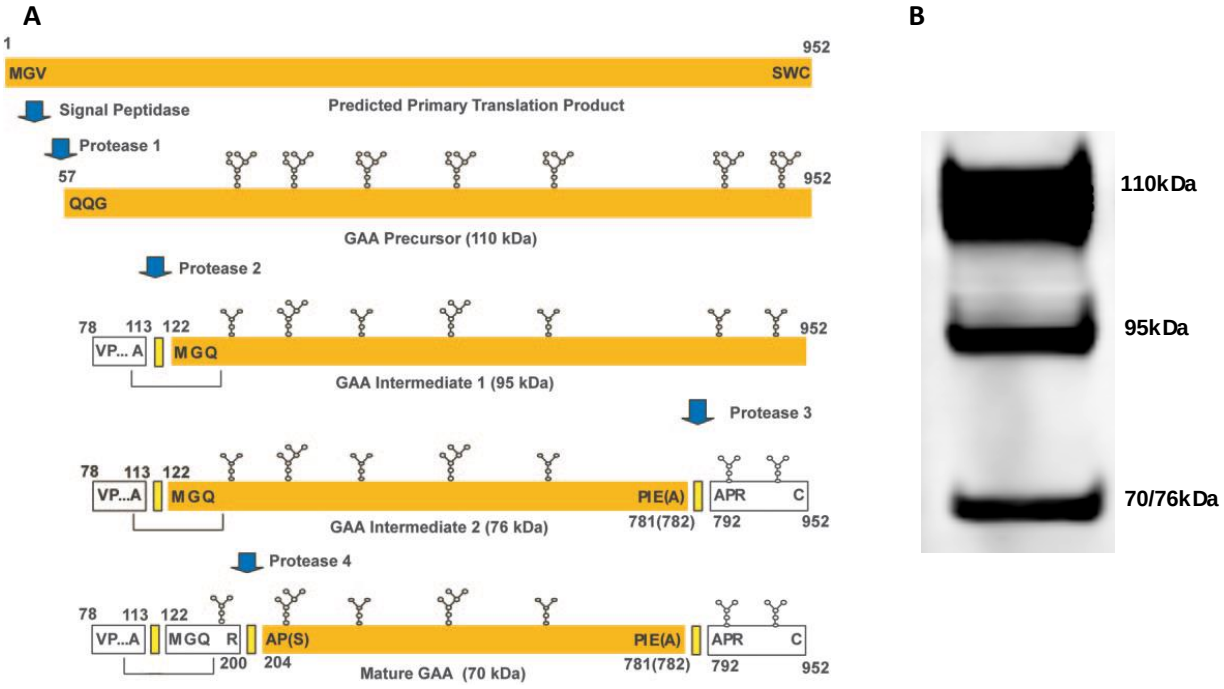

(A) Schematic overview of the GAA maturation process. (B) Representative western blot using an anti-human GAA antibody of liver-derived human cell line lysate (HuH7) transfected with a plasmid expressing GAA protein. Shown are the three intracellular forms of the human GAA.

Diagnosis for Pompe disease is made by sequencing the *GAA* locus in subjects suspected to be affected, and depending on the type of mutation it may lead to i) a complete lack of the GAA expression or ii) a reduction of the enzyme activity. The enzyme deficiency leads to the pathological accumulation of glycogen and lysosomal alteration in virtually all tissues, mainly resulting in cardiac, respiratory and skeletal muscle dysfunction with an estimated frequency of 1:40000 new-born [6]. Based on the residual activity of GAA, the disease can be broadly classified into i) infantile-onset Pompe disease (IOPD), resulting from an almost complete lack of residual GAA activity (less than 1%), associated with generalized hypotonia, and cardio-respiratory failure, due to a severe cardiomegaly, leading to death in the first year of life; and ii) late-onset Pompe disease (LOPD), characterized by residual levels of GAA activity (between 10-30%) and a much less severe cardiac phenotype with progressive limb muscle weakness and respiratory insufficiency [6], [7]. Thurberg and colleagues described in detail all the stages of IOPD pathogenesis which is initially characterized by small glycogen-filled lysosomes between intact myofibrils (stage 1), an increase in cytoplasmic glycogen and the size and numbers of

lysosomes combined with fragmentation of myofibrils constitute stage 2; after that, glycogen-filled lysosomes are tightly packed, whereas some of them show membrane rupture, and only few myofibril fragments remain in stage 3; finally, in stages 4 and 5, most of the glycogen is cytoplasmic, the contractile elements of muscle cells are completely lost, and the cells bloat due to the influx of water [8].

In 2006 the Food and Drugs Administration (FDA) board approved the first therapeutic product for the treatment of Pompe disease, Myozyme®. Myozyme is the recombinant human GAA (rhGAA) precursor produced in chinese hamster ovary (CHO) cells [9]. The Myozyme-based enzyme replacement therapy (ERT) is described in paragraph 1.3.

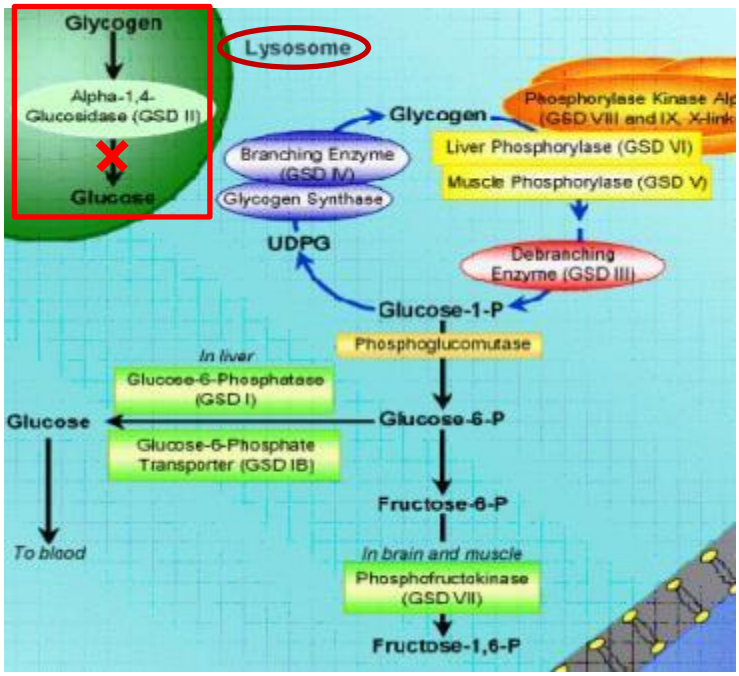

Schematic representation of metabolic pathways implicated in the onset of different glycogenosis. In the red square is highlighted the lysosomal pathway of glycogen degradation which is affected in Pompe disease.

1.2 Animal models of Pompe disease

Since the Pompe disease was described for the first time, researchers made a lot of efforts in order to find reliable models for studying the pathology in depth. To this end, in the early 80' a German group tried to induce the disease by injecting α-acid glucosidase inhibitor (Acarbose) in rats [10], [11]. In these animals, the effect of the acarbose resulted in the formation of characteristic vacuoles in liver, spleen, and soleus.

In the same period, a dog suspected to be affected by Pompe disease was described [12]. Recently, a new study carried out on those same samples confirmed the diagnosis. In fact, by sequencing the canine *gaa* gene, researchers found a mutation which is present in the most severe form of the disease in IOPD patients [13].

In 1983, was described a particular type of Japanese quails in which Pompe disease naturally occurred [14]. Thus, for two decades, the quail has been the only available and reliable animal model for Pompe disease, and it was also the first model used to test several therapeutic strategies (remarkably, it was the animal model on which was tested for the first time the enzyme replacement therapy (ERT) injecting a recombinant human GAA) [15]–[17]. In 2003, using this animal model, McVine-Wylie and colleagues published a study in which was reported a complete clearance of glycogen in heart and pectoralis muscles by liver specific expression of the hGAA using an adenoviral vector [18]. Moreover, this study demonstrated the feasibility to cross-correct the muscle pathology by liver-specific expression of the hGAA. However, in the 1998 there was a breakthrough in the field of the Pompe disease, when the Raben's group generated the first transgenic mouse model ($GAA^{-/-}$ mice) [19]. These mice were extensively characterized in order to assess whether they could resemble the human phenotype of the disease. They do not have any detectable Gaa activity in tissues and, start to build-up glycogen since the third week of life. Extensive glycogen accumulation was found in cardiac and skeletal muscle, peripheral and central nervous system [20]. $Gaa^{-/-}$ mice develop an early and significant cardiomegaly and progressive muscle weakness as reported in Pompe patients, although the onset of the symptoms in mice occurs later (7-8 months of age) if compared with the human disease. These mice, actually, can be considered as a hybrid model of Pompe disease, since they develop an early heart hypertrophy as IOPD patients, while the late onset of the respiratory and skeletal muscle might reflect the LOPD patient's condition Finally, these animals are also

immunologically classified as cross-reactive immunological material (CRIM) negative since they do not express the Gaa protein (Gaa null) and when treated by ERT they develop an humoral response against the rhGAA with very high antibody titers [21].

Overall, this mouse model of Pompe disease, since it presents all the characteristics that can be found in Pompe patients, is the gold standard to study the pathology and its related immunological features in order to find therapeutic strategies for the treatment of this disease.

1.3 Enzyme replacement therapy (ERT)

The enzyme replacement therapy (ERT) as a treatment for Pompe disease significantly prolonged the lifespan of infantile patients [22] and resulted in stabilization of the disease in late-onset patients [23], [24]. In fact, rhGAA is been demonstrated to effectively restore the heart hypertrophy in very young patients who are affected by the most severe form of the disease. However, it was reported a high variability concerning the response to the treatmet, since ~50% of these very young subjects became dependent on invasive ventilation, while the rest of them did not require any artificial ventilation support [25]. In particular, many long-term survivors, among IOPD patients undergoing ERT show signs of disease progression including debilitating skeletal muscle myopathy and also develop new previously unrecognized symptoms such as ptosis, hypernasal speech, osteopenia, hearing loss and gastroesophageal reflux [25]–[27].

Follow-up studies of late-onset Pompe patients who underwent ERT, instead, showed that after an initial phase of amelioration, these subjects were stabilized with no further improvement of the symptoms [28]–[30].

ERT is based on cross-correction mechanisms, as the GAA enzyme infused in the circulation can be taken up by the exposed tissues via binding to the CI-M6P receptor on the cell surface and trafficked to the lysosome [6]. However, while being a life-saving therapy, ERT suffers from several limitations, leading to treatment failures and limited long-term efficacy. Additionally, ERT with rhGAA is inconvenient and very costly, mainly due to the short half-life of the recombinant enzyme in circulation [31] which requires biweekly infusions of large doses of rhGAA (20-40 mg/kg). Furthermore, there is a variable and an overall low uptake of rhGAA in skeletal muscle, likely due to the variable amount of the CI-M6P receptor on the cell surface of different muscle groups [6], [32]. Moreover, the progressive impairment of autophagy [33]

strongly limit the ability of ERT to fully rescue Pompe disease since the impaired cell trafficking hampers the recombinant enzyme to reach the lysosomal compartment. Additionally, the inability of rhGAA to cross the blood-brain barrier makes this strategy highly ineffective to restore the pathology in the central nervous system [34].

1.4 Immune responses in Pompe disease

One of the major issue for the treatment of Pompe disease is the high immunogenicity of the therapeutic protein rhGAA, which often results in acute infusion reactions [24] and development of anti-GAA antibodies in response to ERT [35], [36]. This represents an important issue in infantile subjects who undergo to ERT. In fact, cross-reactive material (CRIM)-negative patients frequently develop high-titer antibodies that are hard to manage and lead to poor prognosis [35]. CRIM-positive Pompe patients also may develop anti-rhGAA antibodies in response to ERT, which in rare cases are associated with neutralizing activity [36]. The presence of cross-reactive immunological material is determined in part by the residual expression of the GAA protein epitopes in Pompe disease patients [37]. Since CRIM-negative Pompe disease patients have a complete deficiency of GAA, the immune system is naïve to the therapeutic protein, recognizes GAA as foreign antigen, and develops anti-GAA B- and T-cells responses [38]. During the development of the immune system, immune cells are exposed to antigens expressed within the body and autoreactive B- and T-cells are eliminated to prevent autoimmunity. In the periphery, antibody generation results from interactions between professional antigen-presenting cells (APCs) such as dendritic cells, CD4+ T helper cells, and B-cells. Presentation of processed antigens by myeloid APCs and B-cells on major histocompatibility complex II (MHCII), with appropriate cytokine signaling and co-stimulation, results in CD4+ T-cell activation. The cross-talk between B and T-cells ultimately drives B-cell activation and antibody production, thereby establishing a humoral response and antigen-specific plasma cells [39]. Recently, Van Gelder and colleagues assessed i) the relationship between antibody formation and the patient's CRIM status and ii) the impact of antibody formation on the patient's clinical outcomes in infantile Pompe patients [40]. This study confirmed that the CRIM-negative status is associated with a poor prognosis and the counteracting effect is possibly determined by the antibody-enzyme

molecular stoichiometry. Moreover, early ERT administration (within 2 months of age) seems to minimize the immune response against the infused recombinant enzyme.

ERT for the treatment of LOPD patients was approved few years later that of IOPD patients and the characterization of immunological response in these subjects is not totally clear due to the heterogeneous response to ERT. Moreover, in several studies were reported life-threatening allergic reactions during infusions of rhGAA [21], [36], [41]. Despite the fact that LOPD patients are CRIM-positive it has been described that they can develop antibodies against the rhGAA which most of the time do not seem to have neutralizing activity [40]. Only few case reports about LOPD patients show rhGAA neutralizing activity, sometimes in subjects that already had an allergic reaction during the infusion of the enzyme [36]. In fact, in an *in vitro* experiment, pre-incubation of rhGAA with a neutralizing serum abrogated the uptake of the enzyme in $GAA^{-/-}$ fibroblasts [36]. Moreover, another study has been carried out to characterize the immunological response in LOPD patients. Analyses of peripheral blood mononuclear cells (PBMCs) showed a dose-dependent increase of interferon gamma (INFγ) and tumor necrosis factor alpha (TNFα) in response to ERT [42].

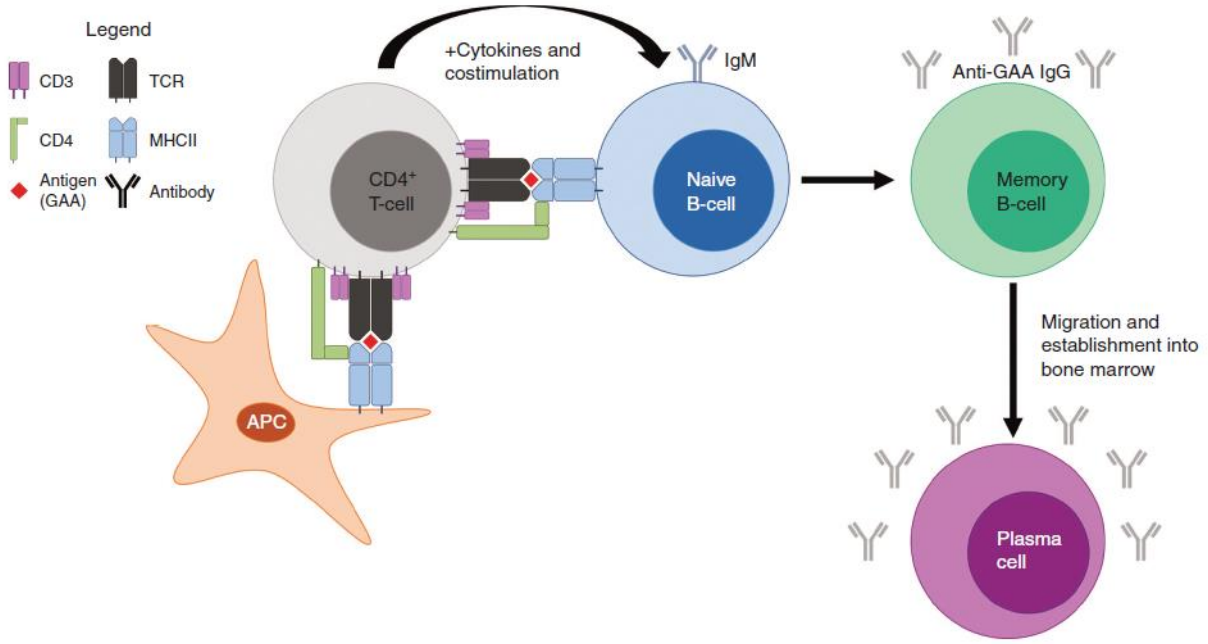

Generation of a humoral immune response. CD4+ T-cells engage MHCII loaded with antigen (GAA) on APCs or naive B-cells via TCR. The CD4 co-receptor also binds and facilitates the appropriate signaling through CD3. During the immune response, additional cytokines and costimulatory molecules drive the generation of memory B-cells which undergo Ig class switching from immature IgM to affinity matured

IgGs directed against the antigen. Memory B-cells then migrate into the bone marrow and develop into antigen-specific plasma cells which perpetually produce antibodies.
APC, antigen-presenting cell; GAA, acid α-glucosidase; Ig, immunoglobulin; MHCII, major histocompatibility complex II; TCR, T-cell receptor. **(Doerfler PA et al., 2016)**

Recent progresses in the use of drugs which prevents the formation of anti-IgG demonstrated the efficacy of this approach in pre-clinical and clinical settings [43]. In the context of ERT regimen for Pompe disease many strategies have been investigated in order to preclude the formation of anti-GAA antibodies.

In combination with ERT, a low dose of methotrexate was used as immunosuppressive drug which succeeded to prevent the formation of anti-GAA antibodies. In a related study, the combinatorial use of methotrexate, gamma globulin and rituximab have showed a successful prevention of antibody formation in an ERT regimen [44], [45]. Administration of intravenous gamma globulin was used as immune modulator, furthermore, since rituximab induces generalized severe B-cell suppression, gamma globulin was needed also to preserve normal immune function [45]. Despite the efficacy demonstrated by these immune modulatory approaches, either T cells (methotrexate) or B-cells depletion (rituximab) pose concerns for the safety and the possible toxicity of these compounds.

Other immune modulatory strategies, not including chemotherapeutics agents that globally weaken the global immune system have been also investigated in order to specifically block survival factors and to inhibit antibody formation potentially harmful for patients who undergo ERT The use of B-cell activating factor (BAFF) inhibitors succeeded to prevent development of anti-GAA antibodies in the mouse model of Pompe disease [46]. BAFF is a pleiotropic cytokine responsible for the B-cells maturation, and its inhibition effectively prevents GAA-specific plasma cells from maturing and migrating to the bone marrow [47]. Moreover, rapamycin was also used to halt the antibody formation although its function on B-cells is still poorly understood [48]. However, a combination of rapamycin and rituximab was successfully administered to Pompe patients who, because of the immune suppression, did not exhibit any hypersensitivity reaction during the infusion of the recombinant enzyme [49].

Furthermore, targeting of T-cells co-receptors has been demonstrated effective for the prevention of anti-GAA antibodies in ERT regimen. In $Gaa^{-/-}$ mice, treatment with anti-CD3 antibody

succeeded to block the immune response against the rhGAA [50], [51]. This treatment, actually, led to a marked decrease of CD4+ and CD8+ T-cells and the ratio between regulatory and effector cells was redirected toward T_{regs} that are essential to induce immunological tolerance to transgenes [52]. Among the strategies to induce antigen-specific tolerance toward the rhGAA, there are two studies carried out in mouse model of Pompe disease that need to be mentioned for their novelty. The first study was based on taking advantage of the gut-associated lymphoid tissue (GALT) which possesses specialized cells that under normal conditions are capable to induce oral tolerance [53]. Su and colleagues expressed in plant cell lines a fusion protein of human GAA conjugated with the cholera-toxin B (CTB) subunit which could strongly reduce the development of anti-GAA antibodies by activating mechanisms of oral tolerance [54]. Another approach relied on the fact that red blood cells (RBCs) were found out as a novel carrier to induce specific immune tolerance [55]. Researchers developed a tool for the bioencapsulation of RBC, and, therefore, they encapsulated the rhGAA that is currently used for ERT in clinic. This approach resulted very effective in $Gaa^{-/-}$ mice,since the rhGAA encapsulated in RBCs was able to block the formation of anti-GAA antibodies [56].

Others strategies which have been adopted to induce antigen-specific tolerance will be discussed in the paragraph concerning gene therapy.

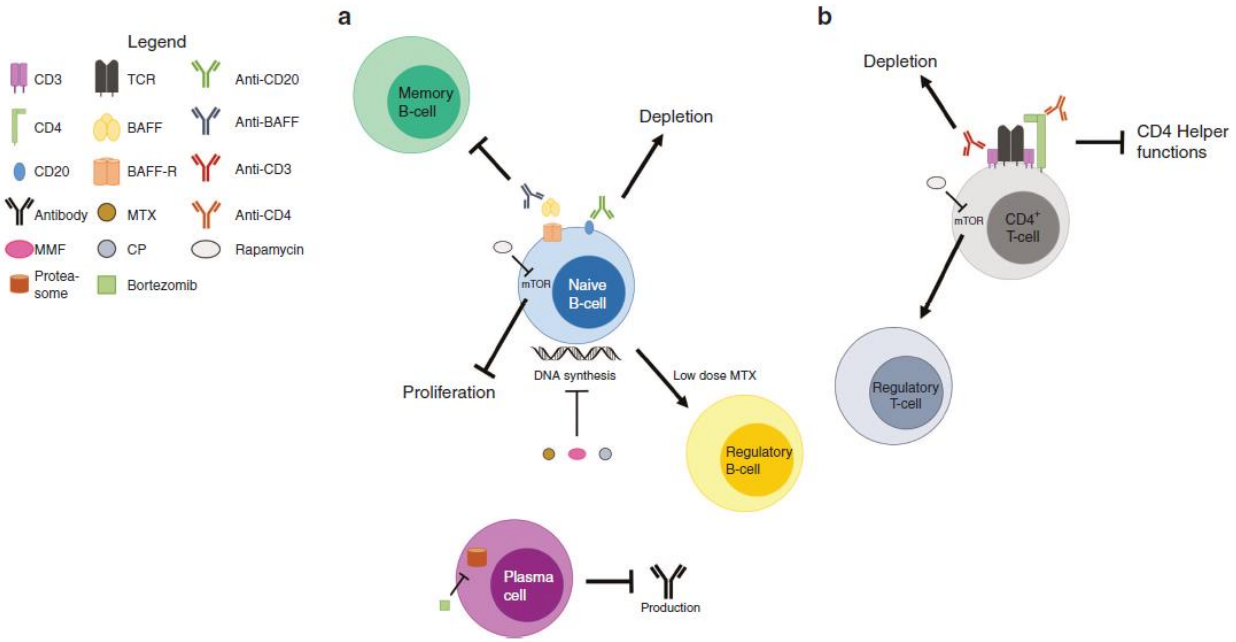

Targets for immune modulatory therapy. (a) ***B-cell targets****. Targeting of BAFF prevents binding to BAFF-R, which inhibits the maturation of antigen-specific memory B-cells. DNA-damaging agents such as CP, MMF, and MTX result in B-cell depletion. Treatment with anti-CD20 also results in B-cell depletion. Blocking mTOR signaling through rapamycin treatment inhibits B-cell proliferation. Proteasome inhibitors, such as bortezomib, inhibit the recycling of proteins that would be used to generate antibodies in plasma cells, inducing senescence. (b)* ***T-cell targets****, such as CD3 or CD4, induce the depletion of T-cells or prevent the activation of B-cells to produce antibodies, respectively. Treatment with rapamycin induces a signaling cascade that skews T-cells into a regulatory phenotype capable of antigen-specific immune suppression.*

BAFF, B-cell activating factor; BAFF-R, BAFF receptor; CP, cyclophosphamide; MMF, mycophenolate mofetil; mTOR, mammalian target of rapamycin; MTX, methotrexate. **(Doerfler PA et al., 2016)**

1.5 Adeno-associated virus (AAV)

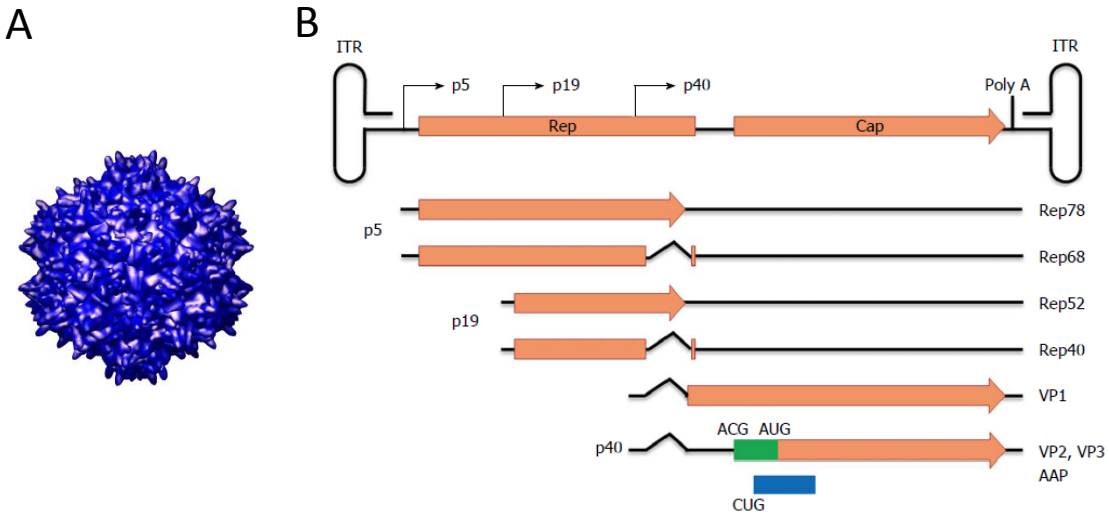

(A) 3D reconstruction of the icosahedral adeno-associated virus capsid. (B) Genomic structure of wild-type AAV. Several transcript are generated from the REP and CAP genes, although the 5' and 3' inverted terminal repeat (ITR) are the only portion of wild-type genome that are required for virus packaging. In addition, the VP2/VP3 mRNA codes for an assembly-activating protein (AAP) which is not present in the mature capsid. **(Chen H, 2015, *World journal of medical genetics*)**

Adeno-associated virus (AAV) is a small (25 nm) virus composed by a non-enveloped icosahedral capsid (protein shell) that contains a linear single-stranded DNA genome of about 4.7 Kb. AAV belongs to the family of Parvoviridae, genus Dependovirus, as it can replicate in the nucleus of target cells only in the presence of helper viruses such as adenovirus or herpes virus [57]. The AAV genome is flanked by two palindromic inverted terminal repeats (ITR, ~145 bp) and includes two open reading frames, rep and cap. Rep encodes proteins involved in: i) replication of the viral DNA; ii) transcriptional control of viral genes; iii) packaging of newly synthetized single-stranded AAV genomes into the capsid; and iv) site-specific genome integration in the host cell DNA [57] Cap encodes for the VP1, VP2 and VP3 proteins that form the capsid, and for the assembly activating protein (AAP) that is required for the starting of capsid assembly in the nucleus [57] AAV viruses naturally infect humans; usually exposure to the wild-type virus occurs at around one-three years of age [58]–[60] and is not associated with any known disease or illness [60]. AAV viruses infect both dividing and non-dividing cells and

remain latent in the host cell DNA by integration into specific chromosomic loci [Adeno-associated virus integration sites (AAVS)] unless a helper virus provides the functions for its replication [57]. In the genome of recombinant AAV vectors, the only viral sequences that are retained are the two ITRs (cis packaging signals) while the sequences encoding rep and cap are exchanged with the exogenous DNA of choice (that is flanked by the ITRs and it is referred to as the transgene). Rep and cap are nonetheless required for the production of AAV vectors and to this aim they are provided in *trans* to the packaging cells together with the adenoviral helper functions [61], [62]. AAV vectors can be produced at high yields by transient triple transfection of mammalian cells [63] or infection of packaging eukaryotic [64] and insect cells [65]. Transduction of cells by AAV vectors occurs by a series of sequential events, including: interaction of the viral capsid with receptors on the surface of the target cell, internalization by endocytosis, intracellular trafficking through the endocytic/proteasomal compartment, endosomal escape, nuclear import, virion uncoating and viral DNA double-strand conversion leading to the transcription and expression of the transgene [66]. The conversion of the AAV genome from single-stranded to double-stranded DNA occurs by both de novo synthesis of the complementary DNA strand (second strand synthesis) and base pairing of complementary single-stranded AAV genomes derived from separate AAV viruses co-infecting the same cell and carrying plus and minus genomes (strand annealing). The frequency and efficiency of strand annealing has been reported to increase proportionally by increasing the dose of AAV vector per cell [66]. Unlike the wild type virus, the genome of the recombinant AAV vectors does not undergo site-specific integration in the host DNA but mainly remains episomal in the nucleus of transduced cells, while random integration events are observed with a low frequency (0.1 to 1% of transduction events) [60], [67], [68]. To date, 12 different AAV serotypes and 108 isolate (serovars) have been identified and classified [57], [69]. The versatility of the AAV production system allows to easily generate hybrid AAV vectors composed by the same transgene flanked by the ITRs from serotype 2 [70] (so far the most commonly used) and any of the available AAV capsid [57]. Since the capsid interacts with receptors on target cells and impact on the post-entry transduction steps, AAV vectors bearing different capsids have different transduction features (i.e. cell tropism and kinetic of transgene expression) and the user can choose the most appropriate to target the cell of interest [57], [71]. So far, AAV vectors have been generated from many naturally occurring serotypes [57], [71]. More recently, engineered AAV vectors have

been generated carrying novel capsids derived from rational design or directed evolution, significantly expanding the AAV vector toolkit [71]–[74]. AAV engineering has not only involved the capsid but also the genome of the vector. These efforts have been aimed at overcoming some of the key limitations of AAV vectors, such as the slow onset of gene expression (due to the time-consuming conversion of single-stranded to double-stranded AAV genome) and the limited DNA cargo capacity (~5 Kb). In particular, McCarty and colleagues showed that the second-strand synthesis step in AAV vector transduction can be circumvented by using self-complementary (sc) AAV vectors [75]. However the scAAVs have a packaging capacity much more limited than the single strand AAV, because only transgenes expression cassette up to ~2,400 base pair in length could be used to generate scAAVs, significantly limiting the number of applications of this platform [75]. Overall, the small packaging capacity of AAV vectors (~4.75 Kb) precludes the AAV-based delivery of several genes which exceed this length and/or the use of large physiologic regulatory elements [76]. However, the AAV genome size limitation can be currently bypassed by using two main strategies: oversized AAV vectors and dual AAV vectors [76]–[78].

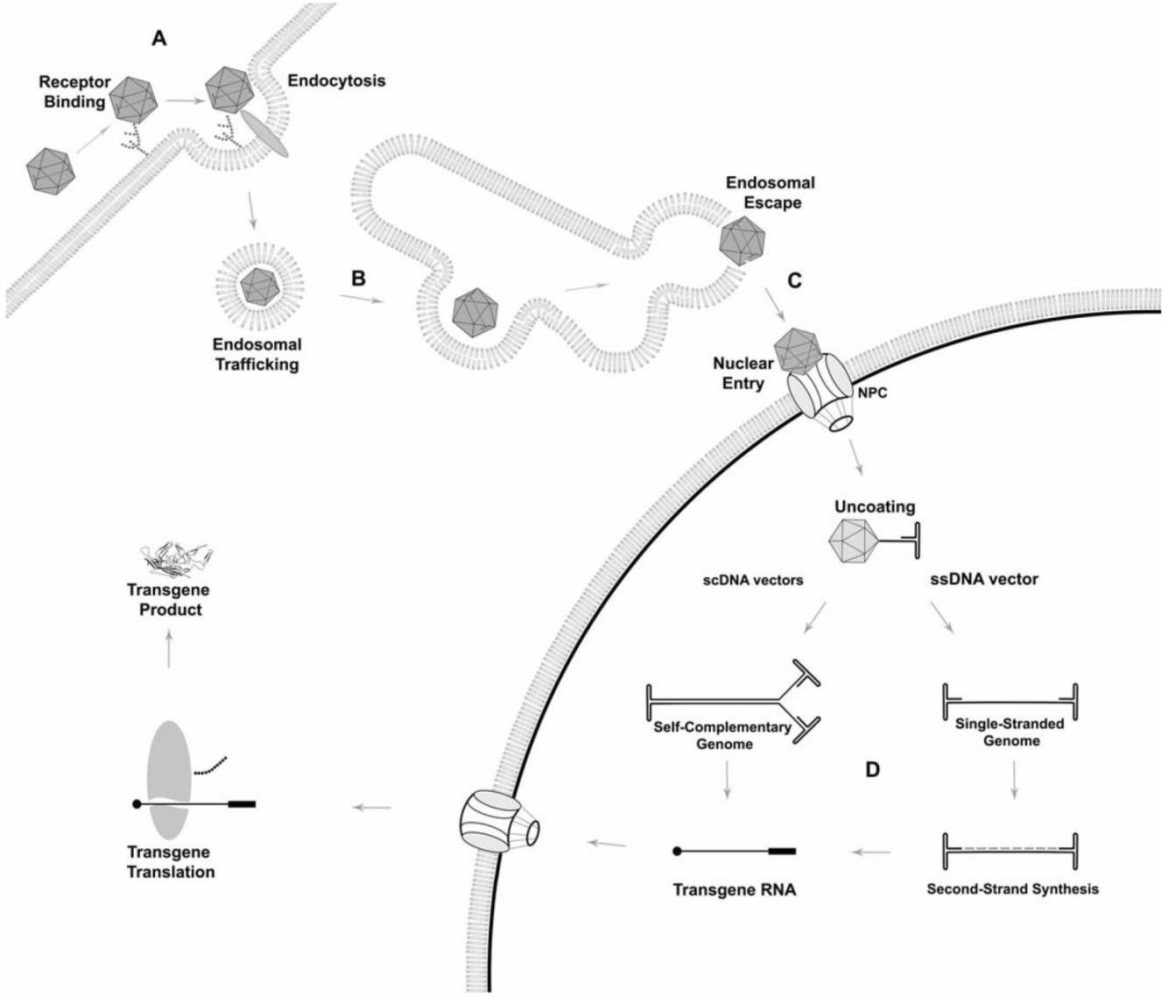

The picture shows the AAV vector infectious pathway describing the virus binding to the cell surface receptor (A), the trafficking through the endosomal system (B), the escaping from the endosomal compartment and consequent tethering to the nuclear pore complex (NPC) (C), and the virus uncoating in the nucleus (D). **(Salganik M. et al., 2015)**

1.6 AAV in the clinic

AAV-based gene therapy has been tested in over 60 clinical trials (http://www.gemcris.od.nih.gov/). Notably, in 2012 the European Commission has granted marketing authorization for the first gene therapy drug, Glybera® (http://www.unicure.com) [79]. This medication is, actually, an AAV-1 vector encoding for lipoprotein lipase (LPL) which is injected intramuscularly and it has been shown to somewhat improve the condition of patients with LPL deficiency (LPLD) [80]–[82]. Notably, when Glybera® was approved there were no cure available for LPLD, therefore, patients had to follow a very restrictive low-fat diet in order to avoid pancreatitis which in some cases could be fatal.

Clinical experience with AAV vectors in the context of several diseases like hemophilia [83] and congenital blindness [84] have established this platform as one of the safest and more effective for in vivo gene transfer [85]. In fact, several trials have been carried out for the treatment of Leber's congenital amaurosis (LCA) which demonstrated visual acuity improvement in treated subjects [84], [86]–[89]. Moreover, the therapy demonstrated an excellent safety profile, as none of the subjects treated had severe adverse effects nor developed high titer antibodies against transgene (RPE65) or vector capsid. Similar data are emerging from hemophilia B trials, in which stable expression of coagulation factor IX (FIX) transgene resulted in efficient correction of the bleeding diathesis [90]. Hemophilia B has always been considered as a relatively "easy" disease to target, since a very small correction of FIX activity (~5 % of normal circulating levels of the enzyme) significantly ameliorates symptoms of the disease. Nevertheless, hemophilia B trial will be detailed in the next paragraph.

The table at the end of the paragraph shows the AAV-based clinical trials directed to diseases affecting various organ systems and using different routes of administration, including the lung via the airway, direct injection to muscle, brain and liver.

Disease	Description	Transgene	Route of administration:	AAV serotype	Reference
Familial Lipoprotein Lipase Deficiency	Disorder that impairs breakdown of fatty acids.	Lipoprotein Lipase -LPL	Intramuscular	AAV1	[91]; [81]
Cystic fibrosis	Lethal autosomal disease that affects mostly the lungs but also the pancreas, liver, kidneys and intestine.	Cystic fibrosis transmembrane conductance regulator -CFTR	Lung, via aerosol	AAV2	[92]–[98]
Hemophilia B	Blood clotting disorder leads to an increased propensity for hemorrhage.	Factor IX -FIX	Intravenous, Intramuscular, Hepatic	AAV8	[83], [90], [99]
Batten's disease	Fatal autosomal recessive neurodegenerative disorder that begins in childhood.	Neuronal ceroid lipofuscinosis -CLN2	Intracranial	AAV2, AAV rh10	[100]
Canavan's disease	Most common degenerative cerebral diseases of infancy.	Aspartoacylase -ASPA	Intracranial	AAV2	[101]
Parkinson's Disease	Degenerative disorder of the central nervous system mainly affecting the motor system.	Glial cell line-derived neurotrophic factor –GDNF or Neurturin -NTN or Aromatic L-amino acid decarboxylase -AADC	Intracranial	AAV2	[102]–[105]
Giant Axonal Neuropathy	Chronic neurodegenerative disease fatal by the third decade of life	Gigaxonin -GAN	Lumbar intrathecal injection	AAV9	
Mucopolysaccharidosis	Lysosomal storage disease associated with developmental delay, severe hyperactivity, spasticity, motor	N-acetylglucosaminidase –NAGLU or		AAV9	

	dysfunction, death by the second decade.	Heparan sulfamidase - SGSH			
Galactosialidosis	Autosomal recessive lysosomal storage disorder with a broad spectrum of clinical manifestations.	Protective protein cathepsin A -PPCA	Intravenous infusion	AAV8	
Homozygous Familial Hypercholesterolemia	Severe elevation of serum LDL leading to premature and lethal coronary artery disease	Low-density lipoprotein (LDL) receptor LDLR	Hepatic artery	AAV8	
Prader-Willi syndrome	Genetic disorder characterized by low muscle tone, short stature, cognitive disabilities and a chronic feeling of hunger that can lead to life-threatening obesity.	Brain-derived neurotrophic factor -BDNF		AAV2	
Heart Failure	Wide range of abnormalities that impair normal cardiac function.	Sarcoplasmic endoplasmic reticulum calcium ATPase - SERCA2a	Intracoronary	AAV1	[106], [107]
Becker Muscular Dystrophy	X-linked recessive inherited disorder characterized by slowly progressive muscle weakness of the legs and pelvis.	Follistatin 344 - FS344	Intramuscular	AAV1	[108]
Spinal Muscular Atrophy Type 1	Autosomal recessive disease of early childhood leading to progressive muscle wasting and mobility impairment.	Survival motor neuron protein - SMN	Intravenous peripheral limb vein	AAV9	[109]
Limb Girdle Muscular Dystrophy type 2D	Progressive muscle wasting which affects predominantly hip and shoulder muscles.	Alpha-sarcoglycan -SGCA	Intramuscular or femoral artery limb perfusion	AAV1, AAV8	[110]

Duchenne Muscular Dystrophy	Recessive X-linked disease, which results in muscle degeneration and premature death.	Mini-dystrophin or GalNAc transferase - GALGT2	Intramuscular	AAV2 rh74, AAV5	[111], [112]
Dysferlinopathy	Autosomal recessive neuromuscular disorder characterized by progressive muscle wasting.	Dysferlin -DYSF	Intramuscular	AAV6	[113]
Flexor Tendon Injury	Inability to bend fingers.	Vascular endothelial growth factor -VEGF	Intramuscular	AAV2	[114]
Pompe Disease	Glycogen storage disease, which damages muscle and nerve cells throughout the body.	acid alpha-glucosidase -GAA	Intramuscular, diaphragm	AAV1	[115]
Alpha-1 Antitrypsin Deficiency	Genetic disorder provoking respiratory problems and impaired liver function.	Alpha-1 Antitrypsin -AAT	Isolated Limb Infusion; Intramuscular	AAV1	[116], [117]
Leber Congenital Amaurosis	Autosomal recessive disorder associated with multiple genes and leading to severe vision loss or blindness.	Retinal pigment epithelium-specific 65 kDa protein - RPE65	Subretinal	AAV2	[84], [86]–[89]
Leber Hereditary Optic Neuropathy	Mitochondrially inherited degeneration of retinal ganglion cells and their axons that leads to loss of central vision in young adult males.	NADH ubiquinone oxidoreductase subunit 4 -ND4	Intravitreal	AAV2	
X-linked Retinoschisis	Early onset retinal degenerative disease leading to juvenile macular degeneration in males.	Retinoschisin -RS1	Intravitreal	AAV2tYF	

Choroideremia	X-linked, recessive, degenerative disease of the retina leading eventually to blindness	Rab escort protein 1 REP1 or Retinal pigment epithelium-specific 65 kDa protein - RPE65 or	Intraocular	AAV2	[79], [118], [119]
Neovascular Age-Related Macular Degeneration	Disease characterized by a growth of new blood vessels beneath the retina, which leakage causes damage to retinal cells and create blind spots in central vision	VEGF receptor - FLT01 or sFlt-1	Subretinal	AAV2	[120]
Congenital Achromatopsia	Retinal disorder characterized absence of daylight vision from birth, photophobia and a slowly progressing loss of cone photoreceptors.	Cyclic nucleotide gated channel beta -CNGB3	Subretinal	AAV2tYF	
Rheumatoid arthritis	Long lasting disorder that primarily affects joints. It typically results in warm, swollen, and painful joints.	TNFR-Fc	Intra-articular	AAV2	[121], [122]

1.7 Liver directed gene therapy

Several reasons make liver a very attractive organ for gene therapy: i) it is one of the major biosynthetic organs in the body; ii) pre-clinical studies in small and large animal models demonstrated that it is easily targeted by injecting AAV intravenously [83], [123]; iii) despite the episomal persistence of the virus genome in hepatocytes, long-term expression of a donated transgene is achieved [124], [125]; iv) liver-restricted expression induces tolerance to the transgene product by activating CD4+ regulatory T cells [126]–[129]; v) a number of pre-clinical studies demonstrated that liver-directed gene therapy can be applied to treat not only plasma protein deficiencies, but also metabolic disorders; vi) most importantly, clinical trials showed that the liver can be targeted with AAV gene transfer to express a transgene long-term.

Historically, the initial clinical trials were carried out using an AAV2 expressing human FIX, which demonstrated for the first time the feasibility of liver gene therapy in humans [99]. Furthermore, this trial allowed identifying some limitations of this approach related to vector immunogenicity [130] and pre-existing immunity to AAV vectors [131]. In fact, one of the challenges in AAV gene therapy is the formation of neutralizing antibodies directed to the capsid which prevent re-administration of the vector. However, some years later, a successful liver gene therapy for Hemophilia B was carried out using an AAV8 expressing a codon optimized version of the human FIX, and the patients showed long-term therapeutic levels of FIX after AAV treatment [83]. Notably, in AAV-treated subjects, a transient spike of circulating hepatic enzymes was kept under control by treating patients with corticosteroids which allow maintaining therapeutic levels of circulating protein. Moreover, recently new data were released from a clinical trial concerning a liver-directed therapy for the treatment of the acute intermittent porphyria [132]. In this trial, patients did not show significant correction of the disease, possibly due to poor efficiency of the transgene expression cassette used in the study. Despite the vector doses were similar to the Hemophilia B trial [83], except for one patient, all the subject did not show any sing of hepatotoxicity with unchanged levels of circulating hepatic enzyme. However, clinical improvements were achieved since the duration and number of hospitalization were reduced in most of all the treated patients. Interestingly, even the number of heme infusions (the only available treatment nowadays for this pathology) was reduced.

1.8 Gene therapy for the treatment of Pompe disease

Several alternative therapies have been proposed to treat Pompe disease, including gene therapy. In the context of Pompe disease, several AAV-based gene therapy approaches directly targeting the diseased muscle have been proposed, and one clinical trial of direct intra-diaphragmatic gene transfer has been completed [133]. However, in studies published thus far, AAV vector-mediated GAA expression in muscle resulted in incomplete correction of Pompe disease and anti-transgene immunogenicity [134], [135]. Recently, the research group that conducted the AAV-based clinical trial, tried to overcome the immunogenicity concern of muscle gene transfer by taking advantage from the liver-mediated transgene tolerance [136]. Basically, during the transfection step of vector production, two different GAA expression cassettes are used to be co-

packaged into a unique AAV vector preparation. These two GAA expression cassettes are respectively under control of a muscle- and liver-specific promoter in order to achieve, both a therapeutic effect in the target tissues, muscles, and immune tolerance to GAA by strong expression in the liver [126], [137]. However, after gene transfer of co-packaged AAV vector in $GAA^{-/-}$ mice by intravenous administration the animals still developed antibodies against the transgene, although at lower levels than those measured in animals treated with a vector expressing GAA only in muscle. Furthermore, in a second setting of experiments it was showed that this co-packaged vector was able to attenuate pre-existing immune response in $GAA^{-/-}$ mice. The application of this gene therapy strategy to Gaa-/- mice lead to low levels of GAA in skeletal muscle- as quadriceps- and nervous system that were below those measured in wild type animals. Finally, since in this study the accumulation of glycogen in treated $GAA^{-/-}$ mice was not evaluated it is not possible to fully understand its therapeutic potential

Therefore, due to immunological concerns for the muscle directed expression of GAA, liver gene transfer with AAV vectors is potentially an attractive strategy to achieve immune tolerance and whole-body correction of Pompe disease because liver has been successfully targeted with AAV vectors in a variety of preclinical and clinical studies, leading to long-term efficacy [85]. Furthermore, hepatic expression of transgenes, including GAA, has been shown to induce antigen-specific immunological tolerance [126], [138], a highly attractive feature in the case of Pompe disease. Liver expression of GAA in Pompe mice has resulted in increased enzyme activity in peripheral tissues via cross-correction like in ERT [139], [140]. However, although some of skeletal muscles have been successfully treated, a complete correction of glycogen accumulation in refractory tissues -such as triceps- with liver gene transfer has not been achieved. The use of a chimeric GAA transgene containing a heterologous signal peptide from alpha-1 antitrypsin has been reported to provide better correction of glycogen accumulation in Pompe mice at vector doses $>1x10^{12}$ vg/kg, with more extensive clearance observed at $\sim1x10^{13}$ vg/kg [141] . Nevertheless, high vector doses potentially pose a challenge for the clinical translation of proof-of-concept results, as they enhance risk of vector-related immunotoxicities making the potential therapeutic product ineffective [142].

An *ex-vivo* approach has been also investigated by using lentiviral vectors (LV) expressing hGAA [143]. In this case, hematopoietic stem cells (HSCs) were collected from bone marrow of $Gaa^{-/-}$ mice and transduced with LV before being re-transplanted in mice. This approach does not

trigger any immune response to GAA as reported in the paper. In fact, this mechanism is thought to resemble the process of central tolerance, since thymocytes develop from the lymphoid progenitors derived from transduced HSCs. In this case, GAA expression within cortical and medullary thymic epithelial cells is orchestrated by SIRTUIN 1, a deacetylase, and also an autoimmune regulator which facilitates central tolerance to autoantigens and negative selection of auto-reactive T-cells [144]–[146]. On the other hand, the reconditioning regimen in mice relied on sublethal radiation doses of 6Gy in order to totally ablate the bone marrow; Pompe patients may not afford this regimen of total body irradiation. Nevertheless, this attempt resulted only in a partial correction of glycogen accumulation, with no apparent therapeutic efficacy in the central nervous system. This strategy failed to treat Pompe disease most likely due to the low expression level of GAA as reported by the authors [143]. Future optimizations for *ex-vivo* gene therapy need to account the achievement of therapeutic enzyme levels in target tissue in order to efficiently clear lysosomal glycogen.

In the last years has been also proposed a pharmacological therapy by using chaperones molecules in addition to the ERT regimen [147]. Chaperone molecules have been demonstrated to increase the half-life of rhGAA used for ERT. Thus, a clinical trial has been carrying out, in which chaperones were supplied during ERT infusion in Pompe patients [148]. First results confirmed the improved half-life of the circulating rhGAA, although the follow-up of the participants to the trial is still ongoing (https://clinicaltrials.gov/ct2/show/NCT02675465?term=atb200&rank=1).

However, as supporting therapy it does not effectively overcome the several limitations of the ERT (e.g. immunogenicity of GAA, biodistribution of the enzyme, etc.), therefore novel and effective therapeutic strategies for Pompe disease are urgently needed.

CHAPTER I

Whole-body correction of Pompe disease with AAV vector-mediated liver delivery of a novel secretable GAA transgene

2. Results

2.1 A novel engineered human GAA for cross-correction-based Pompe gene therapy

GAA is a lysosomal enzyme not efficiently secreted by cells [149]. To enhance therapeutic efficacy of GAA gene transfer, we developed a highly-secretable, codon-optimized version of the human GAA transgene by performing sequential modifications of its coding sequence (CDS, **Fig. S1A**). First, we performed an *in-silico* analysis of the GAA sequence [150]. Based on this, we predicted that a deletion of at least 8 amino acids in N-terminus of the pro-peptide region of the enzyme would enhance its secretion score (D-score, **Fig. S1B**). An initial set of deleted GAA (Δ8) constructs were cloned based on the wild-type (wt) or codon-optimized (co) CDS of GAA. Additionally, the native signal peptide of GAA was replaced by that of the human α-1 antitrypsin enzyme (sp2, **Fig. S1C**) [141]. The engineered GAA transgenes were then cloned in the same liver-specific expression cassette [151] and transiently transfected into the human hepatoma cell line HuH7 (**Fig. 1A**). GAA activity in medium, measured 48 hours post-transfection, showed a slight, non-significant increase in enzyme activity levels in cells transfected with co, sp2-co, or sp2-wt constructs vs. the wt GAA construct (**Fig. 1A**). Conversely, the deleted versions (Δ8) of the sp2 GAA constructs displayed a significant enhancement of secretion in conditioned media (**Fig. 1A**).

To further improve and expand our toolkit of highly-secretable engineered GAA constructs, we generated five additional Δ8 versions of GAA carrying signal peptides that were either synthetic

or from secreted proteins (sp3-8, **Fig. S1C**) and tested them in vitro (**Fig. 1B-C**). This screening allowed us to identify two additional engineered GAA constructs, sp7-Δ8-co and sp8-Δ8-co, which provided significantly higher GAA activity in the cell culture media when compared to both co and wt GAA (**Fig. 1B**). Representative western blot analysis with an anti-GAA antibody on cell lysates and media from transfected HuH7 cells confirmed that higher levels of secreted GAA were achieved using sp2-, sp7- and sp8-Δ8-co constructs compared to wt and co GAA constructs, that are mainly retained in the cell (**Fig. 1C**). Deletions up to 42 amino acids (**Fig. S1B**) resulted in higher secretion of GAA with no loss of enzyme specific activity (**Fig. S2A**), as predicted by the cleavage of the pro-peptide during protein maturation within the endosomal compartment [5].

Then, to assess whether the use of an engineered deleted GAA transgene would provide a significant advantage in the setting of *in vivo* gene therapy, we treated *Gaa* knock-out ($Gaa^{-/-}$) mice by intravenous injection of AAV8 vectors encoding for the sp7-Δ8-co GAA, sp7-Δ42-co GAA, and the corresponding non-deleted GAA form (sp7-co), as control (**Fig. 1 D-F** and **Fig. S2B-D**). Analysis at 3 months post-treatment showed that the GAA protein was correctly secreted into the circulation (**Fig. 1D**), but that only the sp7-Δ8-co vector provided higher circulating GAA activity than the non-deleted vector (sp7-co) (**Fig. 1E**). This resulted in significantly higher GAA activity levels in the heart of sp7-Δ8-co treated mice (**Fig. 1F**), and generally higher levels of uptake of GAA in sp7-Δ8-co treated mice vs. animals from other treatment groups (**Fig. 1F**). Activity of GAA normalized for antigen levels was identical for all transgenes (**Fig. S2B**). In the liver of treated animals, GAA activity (**Fig. S2C**) and vector genome copies (**Fig. S2D**) were not significantly different. These results indicated that the novel engineered highly-secretable GAA transgene provides higher levels of circulating and tissue GAA activity in $Gaa^{-/-}$ mice.

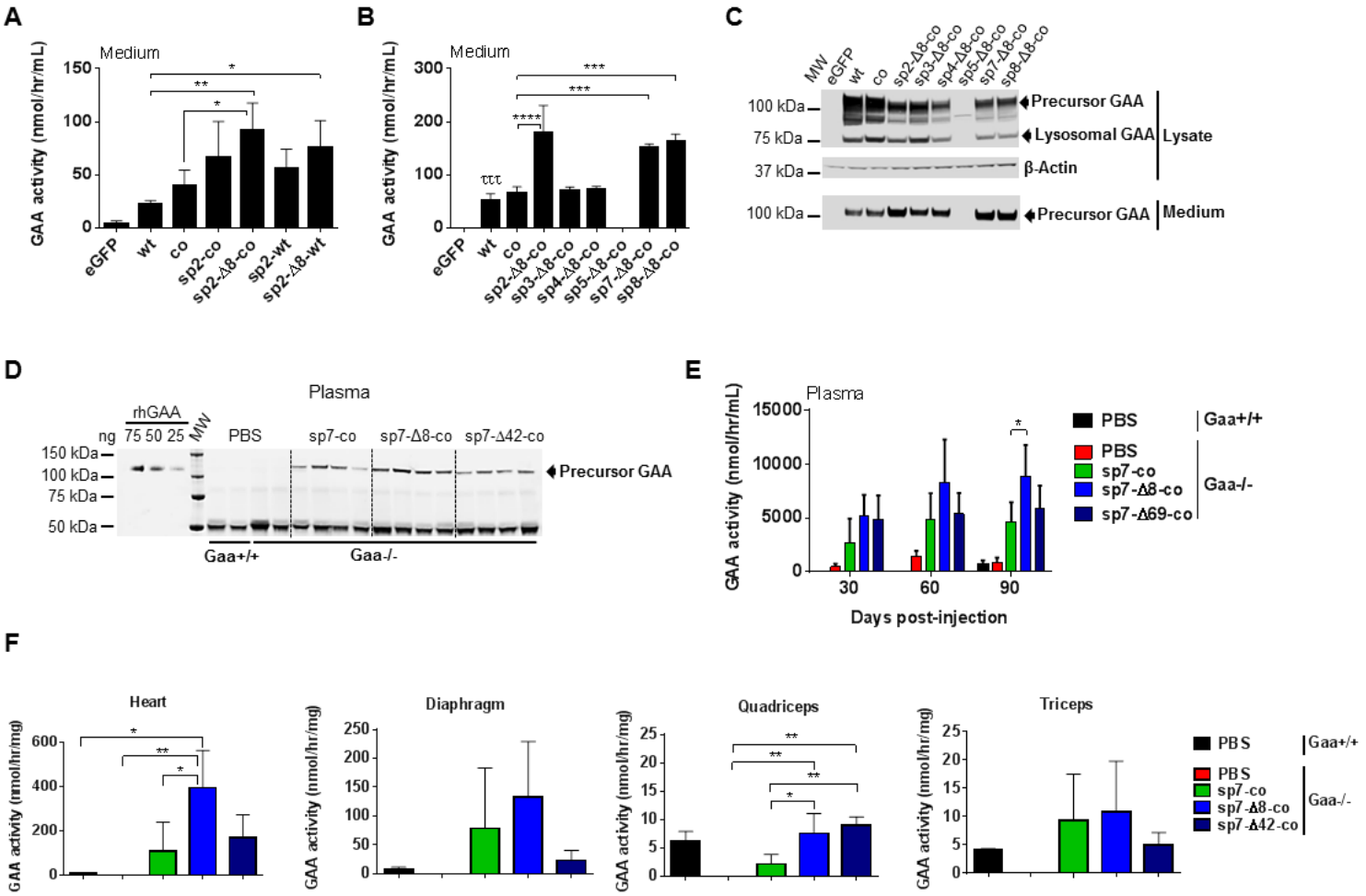

Fig. 1. Selection of engineered human GAA transgenes in vitro and in vivo. *(A-B) GAA activity in media of HuH7 cells 48 hours after transfection with plasmids encoding for engineered human GAA transgenes. A plasmid encoding for eGFP was used as negative control. Data are shown as mean ± standard deviation of 3 independent experiments. (C) Representative GAA Western blot analysis of media and lysates of transfected HuH7 cells. An anti-β-actin antibody was used as loading control. wt, native human GAA; co, codon-optimized human GAA; sp, signal peptide; Δ, truncated human GAA. (D-F) In vivo testing of AAV vectors expressing secretable GAA transgenes. Four-month-old mice were treated with PBS or with 2x10^{12} vg/kg of AAV8 vectors and followed for 3 months. Gaa$^{+/+}$-PBS (n=2), PBS-treated wild-type littermates; Gaa$^{-/-}$-PBS (n=3), untreated control; sp7-co (n=4), AAV8-hAAT-coGAA treated Gaa$^{-/-}$ mice; sp7-Δ8-co (n=4), AAV8-hAAT-sp7-Δ8-coGAA treated Gaa$^{-/-}$ mice; sp7-Δ42-co (n=4), AAV8-hAAT-sp7-Δ42-coGAA treated Gaa$^{-/-}$ mice. (D) Western blot analysis of plasma from treated mice. rhGAA was used as standard. MW, molecular weight marker. (E) GAA activity in plasma and in (F) heart, diaphragm, quadriceps, and triceps. Statistical analysis: one-way ANOVA with Tukey's post hoc (A, B, F) or two-way ANOVA (treatment, time) with Dunnett's post hoc. Error bars represent standard deviation of the mean. In (B) τττ, p<0.001 vs. sp2-, sp7-, sp8-Δ8- coGAA.*

2.2 AAV-mediated liver gene transfer with an engineered secretable GAA provides higher enzymatic activity and dose- and time- dependent complete clearance of glycogen in muscle

Based on the results from the initial screening, we generated AAV8 vectors encoding for two best-candidate Δ8 secretable GAA constructs under the control of the apolipoprotein E hepatocyte control region enhancer and the human α-1 antitrypsin (hAAT) promoter, AAV8-hAAT-sp2-Δ8-coGAA and AAV8-hAAT-sp7-Δ8-coGAA (sp2-Δ8-co and sp7-Δ8-co, respectively, **Fig. 2** and **Fig. S1C**). Vectors were tested *in vivo* in comparison to the codon-optimized GAA construct encoding for the native GAA protein (co). In all the *in vivo* studies, $Gaa^{-/-}$ mice or wild-type littermates ($Gaa^{+/+}$) were used.

Three independent studies were conducted in which mice were treated at 4 months of age and followed up for 3 or 10 months, i) a 3-month study at a low vector dose ($5x10^{11}$ vg/kg), ii) a 3-month study at a high vector dose ($2x10^{12}$ vg/kg), and iii) a 10-month study at the high vector dose (**Fig. 2**). Following vector delivery, circulating GAA transgene activity reached plateau levels within 3 months and remained stable for the duration of the observation period (**Fig. S3A**). Circulating GAA transgene activity was higher in $Gaa^{-/-}$ mice treated with the secretable sp-Δ8-co vectors than in mice treated with native co vector [~2 times at $5x10^{11}$ vg/kg and 3 to 7 times at $2x10^{12}$ vg/kg (**Fig. 2A**, **Fig. S3A** and **Tables S1-S3**)]. The differences in enzyme activity between vectors expressing secretable sp-Δ8-co GAA and native co GAA trangenes were significant in plasma (**Fig. 2A, Fig. S3A**) but not in liver (**Fig. S3B**), where the GAA transgenes were efficiently expressed from all vectors. Accordingly, similar levels of liver transduction were measured in liver (**Fig. S3C**). These results indicate that the engineered secretable GAA transgenes allow for higher circulating enzyme activity following liver gene transfer compared with their native counterpart.

At sacrifice, 3 and 10 months after gene transfer, GAA transgene activity was increased in heart, diaphragm, quadriceps, and triceps of $Gaa^{-/-}$ mice treated with the AAV8-GAA vectors, indicating uptake of both native and engineered secretable GAA proteins from the circulation into the tissues (**Fig. 2B** and **Tables S1-S3**). However, GAA activity levels in mice treated with AAV vectors encoding for secretable GAA transgenes at a dose of $2x10^{12}$ vg/kg were significantly higher than the endogenous activity measured in $Gaa^{+/+}$ littermates and, in some cases, higher than the activity levels measured in co-treated mice (**Fig. 2B** and **Tables S1-S3**).

As previously reported [140], [141], [152], we found that GAA transgene product was preferentially taken up by heart and diaphragm, compared with quadriceps and triceps (**Fig. 2B**). Detection of GAA transgene activity in tissues reflected a generalized correction of glycogen accumulation (**Fig. 2C**). In the short-term, 3 months after gene transfer, a vector dose-dependent correction of glycogen levels was observed in all tissue, with lower glycogen accumulation observed at $2x10^{12}$ vg/kg vs. $5x10^{11}$ vg/kg (two-way ANOVA dose per treatment, dose $p<0.0001$). Additionally, at $5x10^{11}$ vg/kg, complete correction of glycogen levels in heart was achieved only in mice treated with vectors encoding for secretable GAA transgenes (**Fig. 2C**), supporting the hypothesis that these vectors have higher therapeutic potential than the native GAA transgene.

In parallel to the dose-dependent correction of glycogen accumulation, long-term follow up of animals treated at $2x10^{12}$ vg/kg also highlighted a time-dependent correction of the Pompe phenotype in affected animals, which reflected a more efficient clearance of glycogen from tissues at 10 months vs. 3 months post-treatment (two-way ANOVA time per treatment, triceps, time $p<0.001$, **Fig. 2C** and **Tables S2-S3**). Ten months after liver gene transfer, complete clearance of glycogen accumulation was observed in all tissues, including quadriceps and triceps which are known to be more refractory to GAA treatment (**Fig. 2C** and **Tables S2-S3**). These results suggest that there is a threshold of steady circulating GAA activity that leads to complete long-term rescue of glycogen accumulation in muscle, which can be more easily achieved with engineered secretable GAA transgenes.

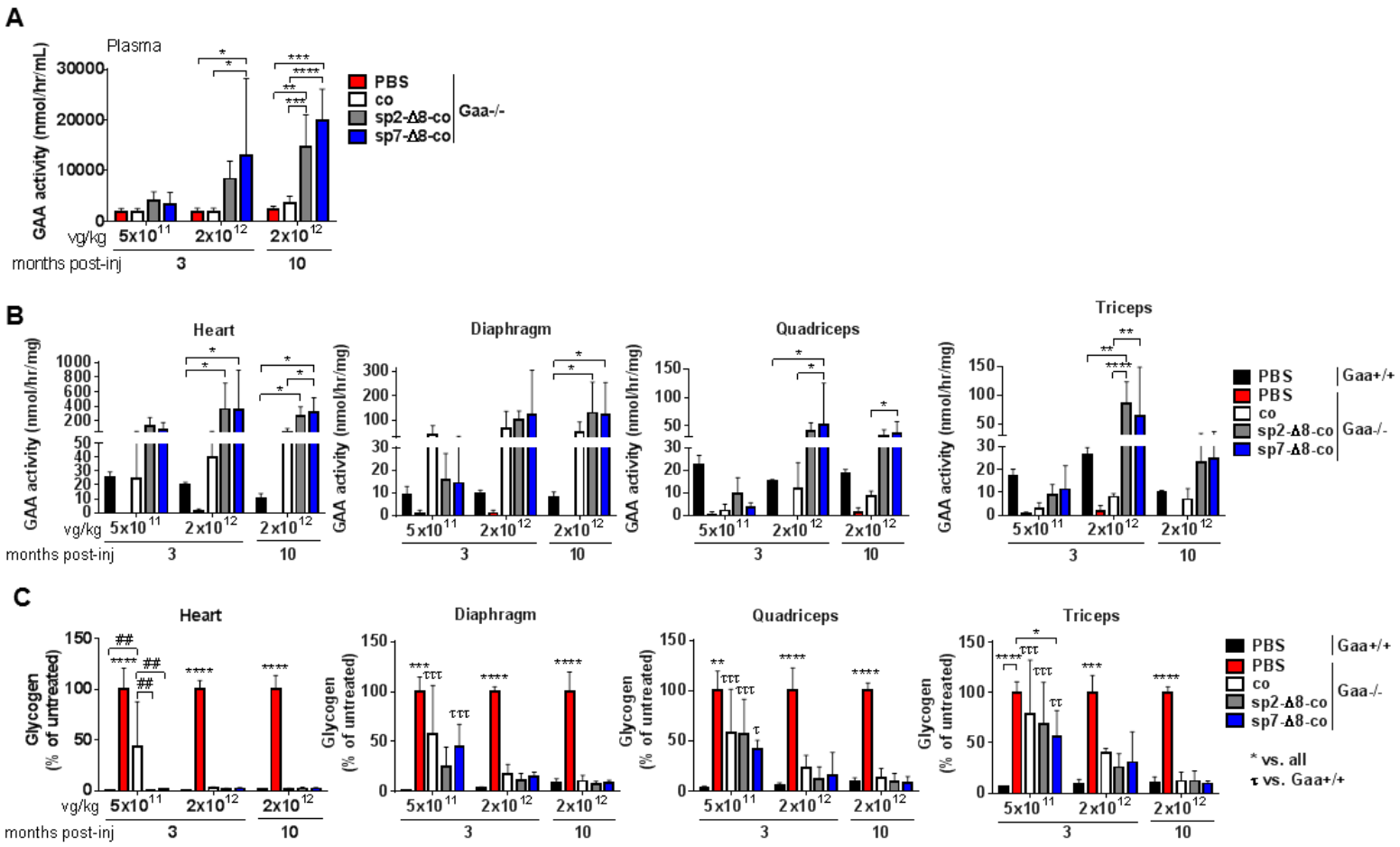

Fig. 2. GAA activity levels and tissue glycogen in vivo. (A-C) *Four-month-old mice were treated with PBS or at the vector doses indicated and followed for 3 months (n=4/5 per cohort) or 10 months (n=8/9 per cohort; n=3 $Gaa^{-/-}$-PBS cohort). $Gaa^{+/+}$-PBS, PBS-treated wild-type littermates; $Gaa^{-/-}$-PBS, untreated control; co, AAV8-hAAT-coGAA treated $Gaa^{-/-}$ mice; sp2-Δ8-co, AAV8-hAAT-sp2-Δ8-coGAA treated $Gaa^{-/-}$ mice; sp7-Δ8-co, AAV8-hAAT-sp7-Δ8-coGAA treated $Gaa^{-/-}$ mice. co, codon-optimized human GAA; sp, signal peptide; Δ, truncated human GAA. (A) GAA transgene activity in plasma. (B) GAA transgene activity in heart, diaphragm, quadriceps, and triceps. (C) Glycogen content in heart, diaphragm, quadriceps, and triceps reported as percentage of PBS-treated $Gaa^{-/-}$ mice (untreated control). (A-C) Statistical analysis: two-way ANOVA with Tukey's post hoc (treatment, dose). Error bars represent standard deviation of the mean. (C) Stars (*) indicate significant differences vs. all groups; tau symbols (τ) indicate significant differences vs. $Gaa^{+/+}$-PBS. * or τ, $p<0.05$; ** or ττ, $p<0.01$, *** or τττ, $p<0.001$, **** or ##, $p<0.0001$. vg, vector genomes*

2.3 AAV-mediated liver gene transfer of secretable GAA preserves muscle structure and normalizes autophagy

As we observed a complete clearance of glycogen from muscle of $Gaa^{-/-}$ mice after long-term treatment, we asked whether this was accompanied with a normalization of muscle histology and autophagic build-up. Hematoxylin and eosin (HE) staining of muscle confirmed that the histology of fibers in AAV-treated $Gaa^{-/-}$ mice were similar to those of $Gaa^{+/+}$ mice (**Fig. 3A, Fig. S4**). This was accompanied with the disappearance of the periodic acid-Schiff (PAS) staining (**Fig. 3A** and **Fig. S4**), which corroborated the results of the analysis of glycogen content (**Fig. 2C**). These results correlated with the presence of both the precursor and lysosomal forms of GAA in muscle (**Fig. 3B-D** and **Fig. S5A-C**). Notably, the amount of lysosomal GAA protein was significantly higher in triceps treated with the sp7-Δ8-co vector than with the co vector (**Fig. 3B-D**). Based on these results, trafficking of GAA to lysosomes did not seem to be impaired [33]in AAV-treated animals. Next, we evaluated autophagic build-up [153] in skeletal muscle. Skeletal muscle from AAV-treated mice, alongside with untreated $Gaa^{-/-}$ controls and $Gaa^{+/+}$ littermates, was analyzed (**Fig. 3C-E** and **Fig. S5B-D**). A Western blot was used for the quantification of the p62 protein in triceps, a recognized marker of autophagic build-up [153], [154]. Significant accumulation of this autophagy substrate in PBS-treated $Gaa^{-/-}$ mice was measured compared to $Gaa^{+/+}$ littermates (**Fig. 3C-E**). The pathological accumulation of p62 was significantly reduced to normal levels in $Gaa^{-/-}$ mice treated by liver gene transfer (**Fig. 3C-E**). A similar normalization of autophagic build-up was found in quadriceps (**Fig. S5B-D**). These results show that the long-term expression of optimized and engineered GAA transgenes from the liver via AAV vectors at a clinically relevant dose can cross-correct both pathological glycogen accumulation and secondary defects in refractory skeletal muscles in the mouse model of Pompe disease.

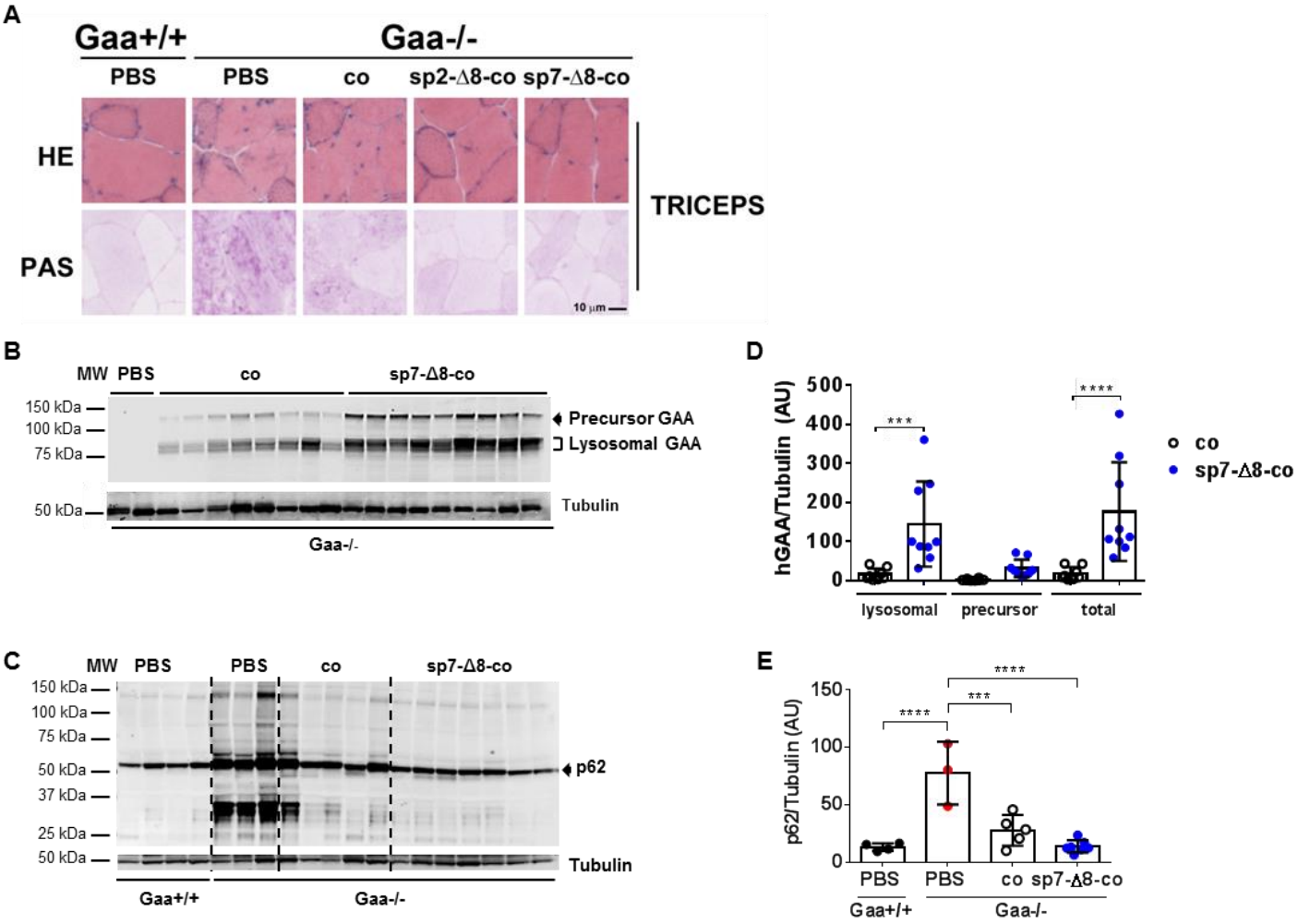

Fig. 3. Histology, GAA uptake, and autophagic build-up in triceps of treated Gaa$^{-/-}$ mice and controls. (A-E) *Analysis of triceps in mice 10 months after treatment. Gaa$^{+/+}$-PBS, PBS-treated wild-type littermates; Gaa$^{-/-}$-PBS, untreated control; co, AAV8-hAAT-coGAA treated Gaa$^{-/-}$ mice; sp2-Δ8-co, AAV8-hAAT-sp2-Δ8-coGAA treated Gaa$^{-/-}$ mice; sp7-Δ8-co, AAV8-hAAT-sp7-Δ8-coGAA treated Gaa$^{-/-}$ mice; Vector dose, 2x10^{12} vg/kg. co, codon-optimized human GAA; sp, signal peptide; Δ, truncated human GAA. (A) Representative images of hematoxylin and eosin (HE, top panels) and periodic acid-Schiff (PAS, bottom panels) staining of triceps. The scale bar is depicted. (B-C) Western blot analysis of triceps lysates using anti-GAA (B) or anti-p62 (C) monoclonal antibodies. An anti-tubulin antibody was used as loading control. MW, molecular weight marker. (D-E) Quantification of GAA (D) or p62 (E) bands from the corresponding Western blots. Statistical analysis: (D) multiple t-tests, with Sidak-Bonferroni post hoc c. Gaa$^{-/-}$-PBS, n=2; Gaa$^{-/-}$-co, n=8; Gaa$^{-/-}$-sp7-Δ8-co n=9. (E) One-way ANOVA with Tukey's post hoc. Gaa$^{+/+}$-PBS, n=4; Gaa$^{-/-}$-PBS, n=3; Gaa$^{-/-}$-co, n=5; Gaa$^{-/-}$-sp7-Δ8-co, n=7. Error bars represent the standard deviation of the mean.*

2.4 AAV-mediated liver gene transfer of engineered secretable GAA significantly improves the disease phenotype of central and peripheral nervous system

Aside from muscle involvement, several reports of central nervous system (CNS) and motor neuron involvement in Pompe disease are available in the literature [155], [156]. Therefore, we investigated whether native (co) or secretable GAA proteins, expressed by liver gene transfer, could be taken up by cells in the nervous system, leading to the correction of the disease phenotype. Western blot analyses of brain (**Fig. 4A**) and spinal cord (**Fig. 4B**) lysates showed the presence of GAA in these tissues. Accordingly, quantification of glycogen in brain also showed a significant reduction in AAV-treated $Gaa^{-/-}$ mice compared with PBS-treated $Gaa^{-\backslash-}$ mice (**Fig. 4C**). Like for muscle (**Fig. 2C**), prolonged exposure to the enzyme (10 months), together with the higher circulating levels provided by the engineered secretable GAA transgenes, significantly improved glycogen clearance (**Fig. 4C**). Conversely, 3 months post-treatment only a mild amelioration of the brain phenotype was observed (**Fig. 4C**). Importantly, the native GAA transgene (co) failed to achieve statistically significant correction of glycogen in the brain at 3 and 10 months post-treatment (**Fig. 4C**), despite the fact that GAA activity was found in the brain at both time points (**Tables S2-S3**). Immunofluorescence analysis of the cervical, thoracic, and lumbar regions of the spinal cord also showed significant increased survival of motor neurons (ChAT staining, **Fig. 4D-E**), significantly reduced number of Iba1+ cells (**Fig. 4F-G**), and normalization of astrogliosis (GFAP, **Fig. 4H-I**) in treated $Gaa^{-/-}$ mice. In particular, neuroinflammation, measured by quantification of GFAP and Iba1 staining in the grey matter of the spinal cords, was better controlled by treatment with secretable GAA transgenes, while no significant amelioration of the pathological phenotype was observed in mice treated with vectors expressing the native GAA transgene (co, **Fig. 4H-I**).

Together, these results demonstrate that liver gene transfer for secretable GAA drives a time-dependent clearance of glycogen from CNS, and results in normalization of the Pompe phenotype in the spinal cord.

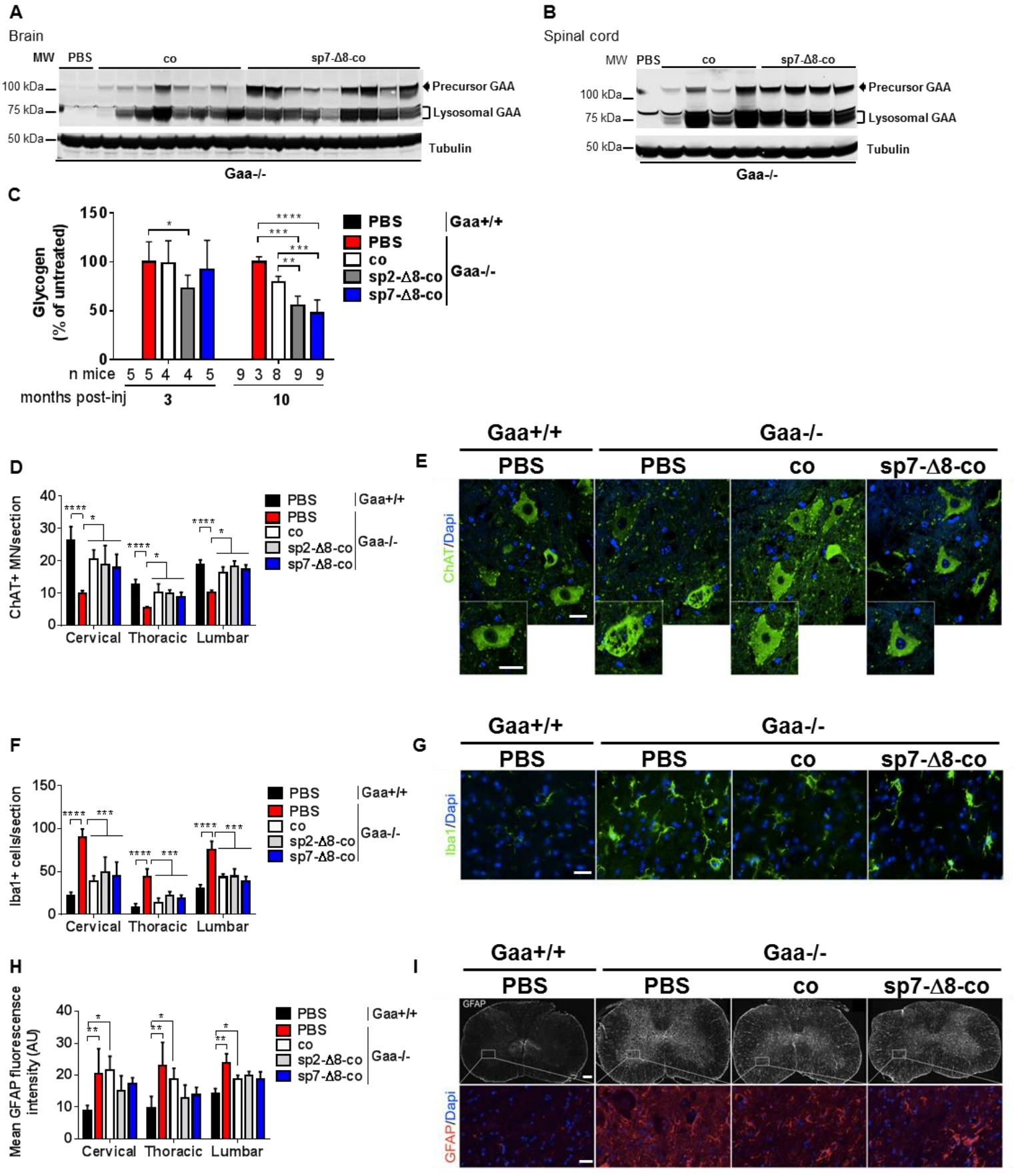
A
Brain
MW
PBS
co
sp7-Δ8-co
100 kDa
75 kDa
50 kDa
Precursor GAA
Lysosomal GAA
Tubulin
Gaa-/-
B
Spinal cord
C
Glycogen (% of untreated)
n mice 5 5 4 4 5 9 3 8 9 9
months post-inj 3 10
PBS
Gaa+/+
co
sp2-Δ8-co
sp7-Δ8-co
Gaa-/-
D
ChAT+ MN/section
Cervical
Thoracic
Lumbar
E
Gaa+/+
Gaa-/-
ChAT/Dapi
F
Iba1+ cells/section
G
Iba1/Dapi
H
Mean GFAP fluorescensce intensity (AU)
I
GFAP
GFAP/Dapi

Fig. 4. Analysis of brain and spinal cord of treated Gaa$^{-/-}$ mice and controls. (A-I) *Four-month-old mice were treated with PBS or with 2x10^{12} vg/kg of AAV8 vectors and followed for 3 months (n=4/5 per cohort) or 10 months (n=8/9 per cohort; n=3 Gaa$^{-/-}$-PBS per cohort). Gaa$^{+/+}$-PBS, PBS-treated wild-type littermates; Gaa$^{-/-}$-PBS, untreated control; co, AAV8-hAAT-coGAA treated Gaa$^{-/-}$ mice; sp2-Δ8-co, AAV8-hAAT-sp2-Δ8-coGAA treated Gaa$^{-/-}$ mice; sp7-Δ8-co, AAV8-hAAT-sp7-Δ8-coGAA treated Gaa$^{-/-}$ mice. co, codon-optimized human GAA; sp, signal peptide; Δ, truncated human GAA. Western blot analysis of brain (A) and cervical spinal cord (B) lysates 10 months after treatment using a monoclonal anti-GAA antibody. An anti-tubulin antibody was used as loading control. MW, molecular weight marker. (C) Quantification of glycogen content in brain 3 and 10 months after treatment. The quantification is reported as percentage of Gaa$^{-/-}$ mice treated with PBS. (D) Count of ChAT+ motor neurons in spinal cord 10 months after treatment. (E) Representative images of ChAT staining. (F) Count of Iba1+ cells in the grey matter of spinal cord 10 months after treatment. (G) Representative images of Iba1 staining. (H) GFAP fluorescence quantification in the grey matter of the spinal cord 10 months after treatment. (I) Representative images of GFAP staining. In all images, nuclei were stained by Dapi. Scale bars correspond to 200 μm (I, upper panel), 25 μm (E, G, I lower panel). (D-I) Gaa$^{-/-}$-PBS n=2, n=3 for the other cohorts. Error bars represent standard deviation of the mean. Statistical analysis: (C) two-way ANOVA with Tukey's post hoc (treatment, time); (D, F, H) two-way ANOVA with Tukey's post hoc (treatment, region of spinal cord). MN, motor neurons; ChAT, choline acetyl transferase; GFAP, glial fibrillary acidic protein; Iba1, Ionized calcium binding adaptor molecule 1; Dapi,4',6-diamidino-2-phenylindole.*

2.5 The engineered secretable GAA transgenes are less immunogenic than their native counterpart

It is well established that the rhGAA induces neutralizing humoral immune responses in Pompe patients undergoing ERT [35]. To test the immunogenicity of the native and engineered transgenes used in the current study, we established an ELISA assay to determine the levels of anti-human GAA transgene IgG in the plasma of Gaa$^{-/-}$ mice treated with liver gene transfer. One month after vector delivery, mice treated with either 5x10^{11} or 2x10^{12} vg/kg of AAV vectors expressing secretable GAA transgenes had undetectable levels of anti-GAA IgG, while mice

treated with the native co GAA transgene developed significant levels of antibodies (up to 22 μg/mL and up to 6 μg/mL for the low and high dose cohorts, respectively, **Fig. 5A**). The evaluation of the humoral immune response to the GAA transgene product over time confirmed the significant higher immunogenicity of native GAA vs. secretable GAA transgenes; nevertheless, clearance of anti-GAA IgG was observed about 3 months post-treatment (**Fig. 5B**). These results indicate that the engineered secretable sp-Δ8-co GAA transgenes are less immunogenic than the native co GAA transgene in the context of AAV-mediated liver gene transfer. To further estimate the immunogenicity of truncated secretable GAA vs. the native GAA in more stringent setting, we expressed the native (co) and secretable (sp7-Δ8-co) GAA transgenes under the control of the muscle-specific promoter SPc5-12 [157]. One month post intravenous administration of these AAV vectors, 3 out of 4 $Gaa^{-/-}$ mice treated with the native GAA transgene (co) developed anti-GAA IgG antibody at levels >12 μg/mL, while only 2 out of 4 animals in the secretable GAA transgene cohort developed anti-IgG antibodies at ~6 μg/mL (**Fig. S6**). At 2 months, the trend for lower immunogenicity of the secretable GAA transgene was confirmed (**Fig. S6**).

Finally, to further evaluate the potential immunogenicity of the engineered secretable GAA transgene in humans, bioinformatics analysis was performed to identify potential MHC II epitopes in the GAA protein. The analysis, performed by Immune Epitope Database (www.iedb.org), identified the epitope LHDFLLVPRELSGSS as best predicted binder to the HLA allele DRB1 and particularly for haplotypes DRB1*03:01, DRB1*04:03, DRB1*07:01, DRB1*11:01, and DRB1*15:01, which represent the 50% of the human population [158]. This epitope, located at amino acid 32 of the GAA sequence, is not present in the secretable truncated version of GAA.

Thus, both in vivo and in silico prediction data suggest that the engineered secretable GAA transgenes are likely to have a low immunogenicity profile when expressed with AAV vectors in hepatocytes.

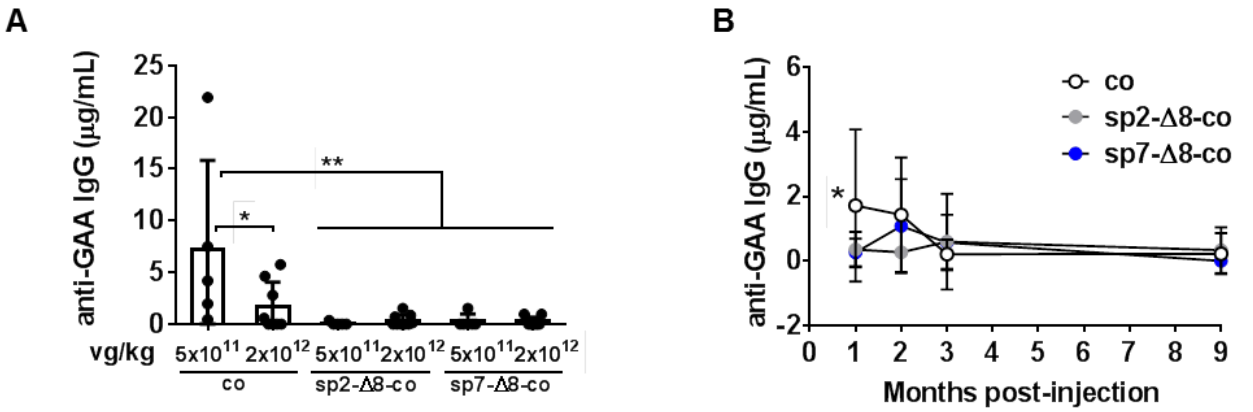

Fig. 5. Anti-human GAA transgene humoral immune responses in Gaa$^{-/-}$ mice. (A-B) *Analysis of anti-hGAA IgG in plasma samples from treated Gaa$^{-/-}$ mice. co, AAV8-hAAT-coGAA; sp2-Δ8-co, AAV8-hAAT-sp2-Δ8-coGAA; sp7-Δ8-co, AAV8-hAAT-sp7-Δ8-coGAA. (A) Anti-hGAA IgG 1 month post treatment at a dose of 5x10^{11} vg/kg (n=5 per cohort) or 2x10^{12} vg/kg (n=8/9 per cohort). (B) Anti-hGAA IgG over time in animals treated at a dose of 2x10^{12} vg/kg (n=8/9 per cohort). Error bars represent the standard deviation of the mean. Statistical analysis: (A) one-way ANOVA with Dunnett'spost hoc; (B) two-way ANOVA with Tukey's post hoc (treatment, time) (B). The star (*) in (B) indicates p<0.05 for co at 1 month vs. sp2- or sp7-Δ8-co at 1 month, and co at 1 month vs. co at 3 or 9 months.*

2.6 AAV-mediated liver gene transfer with engineered secretable GAA transgenes provides long-term survival and rescues cardiac, respiratory, and muscle function in affected animals

Long-term follow up of treated animals and controls up to 14 months of age allowed us to evaluate survival and monitor respiratory and muscle function (**Fig. 6**). Liver gene transfer of GAA significantly improved the survival of Gaa$^{-/-}$ mice, regardless of the GAA transgene version expressed (**Fig. 6A**). Accordingly, treated mice displayed normal weight gain over time (**Fig. S7**). Baseline disease state was evaluated at the time of treatment (4 months of age) in Gaa$^{-/-}$ mice and compared with wild-type littermates (**Fig. S8**). Cardiac hypertrophy was present at the time of vector infusion (**Fig. S8A**) and was significantly and completely normalized in all AAV vector-treated animals (**Fig. 6B**). Treatment with AAV vector-mediated liver gene transfer also resulted in long-term preserved muscle strength in Gaa$^{-/-}$ mice (**Fig. C-D**). In particular, PBS-treated Gaa$^{-/-}$ mice showed a progressive deterioration in the wire hang test performance

from baseline to month 10 post-treatment, while AAV treated animals remained undistinguishable from wild-type littermates (**Fig. 6C** and **Fig. S8** and **S9A**). Complete rescue in the grip test was also obtained after gene transfer (**Fig. 6D** and **Fig. S9B**). In this case, baseline assessment of $Gaa^{-/-}$ mice revealed an already decreased performance at baseline (**Fig. S8**), indicating that reversal of phenotype was achieved with gene transfer. Both in the wire hang and in the grip test, animals treated with vectors encoding for the secretable GAA sp7-Δ8-co transgene showed the most robust and significant improvements in performance (**Figs. 6C-D**). No significant differences were evidenced in the rotarod test in our Pompe mouse colony (**Fig. S9C**).

Next, respiratory function was evaluated. This measurement in $Gaa^{-/-}$ mice has been reported to be progressively impaired [155]. Measurement of tidal volume by plethysmography, showed that treatment with the engineered, secretable sp7-Δ8-co GAA transgene led to higher ventilation, compared with the native GAA (co) treatment (**Fig. 6E** and **Table S4**). In this assay, a statistically significant difference was noted between the sp7-Δ8-co and the co GAA transgene treatment groups. Due to the low survival of PBS-treated $Gaa^{-/-}$ animals (**Fig. 6A**), and the likely selection of animals with a slightly milder phenotype, the 10-month performance of PBS-treated $Gaa^{-/-}$ mice did not differ significantly from any of the other study cohorts (e.g. p=0.058 vs. sp7-Δ8-co, **Fig. 6E**).

Combined, these results show complete survival and functional rescue of mice treated with AAV-mediated liver gene transfer for GAA, in particular for cohorts treated with the secretable forms of the GAA transgene.

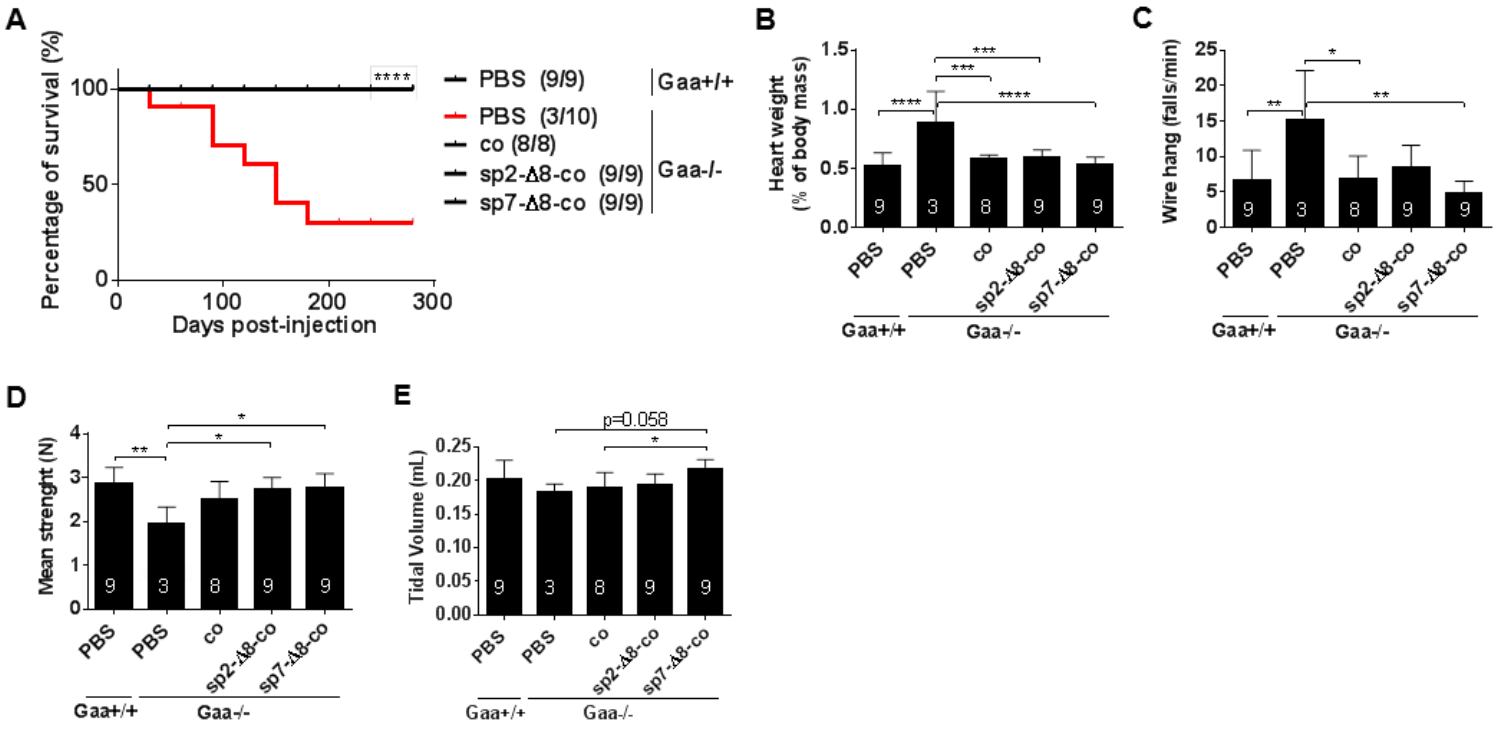

Fig. 6. Long-term outcome of gene therapy in treated Gaa$^{-/-}$ mice and controls. (A-E) *Gaa$^{+/+}$-PBS, PBS-treated wild-type littermates; Gaa$^{-/-}$-PBS, untreated control; co, AAV8-hAAT-coGAA treated Gaa$^{-/-}$ mice; sp2-Δ8-co, AAV8-hAAT-sp2-Δ8-coGAA treated Gaa$^{-/-}$ mice; sp7-Δ8-co, AAV8-hAAT-sp7-Δ8-coGAA treated Gaa$^{-/-}$ mice. Vector dose, 2x10^{12} vg/kg (A) Kaplan-Meier curve showing the percentage of survival from 4 to 14 months of age. The number of live animals per cohort at the end of the study is indicated in the legend. ****p<0.0001 vs. Gaa$^{-/-}$-PBS; log-rank Mantel-Cox test. (B) Cardiac hypertrophy showed as heart weight expressed as percentage of body mass. (C) Wire hang test shown as falls/minute. (D) Grip test as mean three independent measurements. (E) Tidal volume measured by whole-body plethysmography. (C-E) Functional tests 9 months after treatment. Statistical analysis: one-way ANOVA with Tukey's post hoc (B-D) or Dunnett's post hoc (E). The number of animals per treatment cohort is shown in the histogram bars. Error bars represent the standard deviation of the mean.*

2.7 Liver-mediated gene transfer with AAV-sp7-Δ8-coGAA leads to increased GAA activity in plasma and tissues of non-human primates

To evaluate the therapeutic potential of our cross-correction-based gene therapy strategy for Pompe disease, we treated three non-human primates (NHP, *Macaca Fascicularis*) with AAV8 vectors encoding for the engineered sp7-Δ8-co GAA transgene at the dose of $2x10^{12}$ vg/kg (**Fig. 7**). The secretion of the engineered GAA protein from the liver into the circulation was confirmed by Western blot analysis (**Fig. 7A**), which showed the presence of GAA transgene product in plasma collected at 30 and 90 days after AAV injection. No GAA was detectable at baseline, 12 days before the injection (**Fig. 7A**). In AAV-GAA treated animals, circulating GAA activity was also significantly increased by ~ 3-6 folds above the baseline levels found in NHPs (n=8), and remained stable until the end of the study (90 days after treatment, **Fig. 7B**). Since wild-type monkeys physiologically express GAA in all tissues, we used a control animal (NHP Ctrl) as reference for the endogenous GAA activity in tissues (**Fig. 7C**). At 3 months after treatment with the AAV8-sp7-Δ8-coGAA vector, enzyme activity was increased above the endogenous levels in most tissues (**Fig. 7C**). The increase was more pronounced in tissues collected from NHPs #2 and 3, which displayed the highest levels of expression (**Fig. 7A**). Circulating GAA (**Figs. 7A-B**) and GAA tissue activity (**Fig. 7C**) measured in each monkey were consistent with the efficiency of liver transduction in the 3 animals measured by vector genome copy number analysis (**Fig. S10**). These results clearly show that the engineered sp7-Δ8-co GAA transgene can be expressed in the liver of a large animal, secreted into the circulation, and taken up by peripheral tissues.

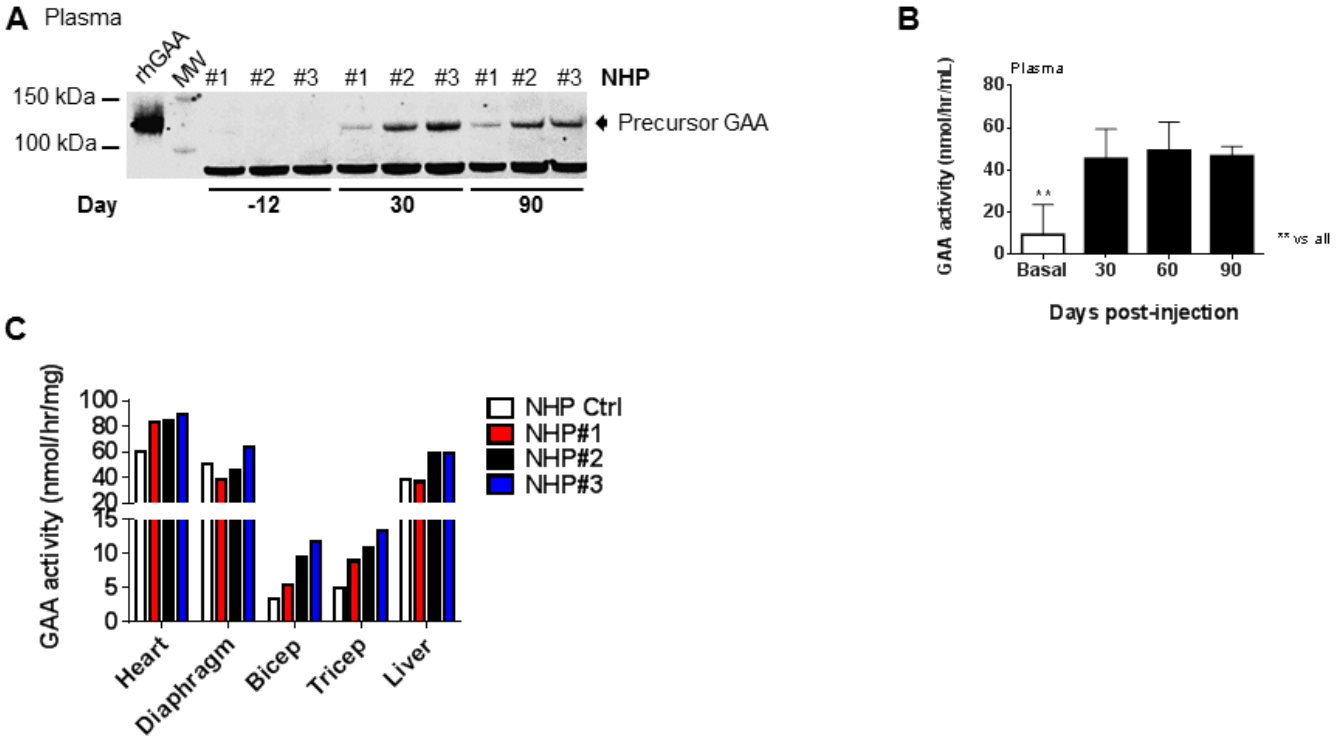

Fig. 7. Scale-up of AAV vector-mediated liver gene transfer for secretable GAA to non-human primates. (A-E) *Male cynomolgus monkeys (n=3) were treated with* $2x10^{12}$ *vg/kg of AAV8-hAAT-sp7-Δ8-coGAA and followed up for 3 months. (A) Western blot analysis of plasma using an anti-GAA antibody. Recombinant human GAA (rhGAA) was used as loading control. MW, molecular weight marker. (B) GAA activity in plasma. Basal, endogenous GAA activity in monkeys #1-3 pre-injection and 5 additional control monkeys (n=8). Statistical analysis: one-way ANOVA with Tukey's post hoc. Error bars represent the standard deviation of the mean. (C) GAA activity in heart, diaphragm, biceps, triceps, and liver. Endogenous GAA activity was measured in monkey treated with an unrelated AAV8 vector (NHP control, ctrl).*

2.8 The therapeutic potential of liver gene transfer with AAV vectors encoding for the engineered highly-secretable sp7-Δ8-co GAA transgene qualifies this strategy for clinical translation

Pompe disease is currently managed by infusions of rhGAA protein at 20 to 40 mg/kg every other week [32]. Upon infusion, the recombinant enzyme is rapidly cleared from the circulation following a classical peak and trough kinetics, and is mostly taken up by the liver and heart, and less efficiently by other tissues [6]. To evaluate if stable circulating GAA levels provided by AAV vector-mediated liver gene transfer resulted in significant accumulation of GAA in muscle, we drew a correlation between GAA activity in plasma and in heart, diaphragm, quadriceps, and triceps (**Fig. 8A** and **Tables S1-S2**). At a given GAA transgene activity in plasma, GAA activity measured in tissues was higher, suggesting an accumulation of GAA over time (**Fig. 8A**). Linear regression revealed a generally good correlation between plasma and tissue levels of GAA activity, and confirmed that GAA is preferentially taken up by heart, followed by diaphragm and skeletal muscle, as indicated by the slope of the regression curves (**Fig. 8A**).

Based on this, we wanted to correlate results obtained in AAV-treated mice and NHPs, with ERT using rhGAA. $Gaa^{-/-}$ mice received rhGAA at a high dose regimen (100 mg/kg, 2 infusions in total, given every other week, corresponding to 2.5- to 5- fold the rhGAA used in ERT [32] and sacrificed at defined time points after the last infusion. Tissues were collected for GAA activity measurement in heart (**Fig. 8B**) and triceps (**Fig. 8C**). Like for gene transfer, in the setting of ERT, rhGAA uptake was more efficient in heart vs. triceps (**Figs. 8B-C**), confirming that these two tissues represent the highest and lowest efficiency of GAA uptake, respectively. In the setting of high-dose ERT, GAA activity in tissues returned to baseline within ~30 to 40 days following the last rhGAA infusion (**Figs. 8B-C**), with an estimated half-life of GAA in heart and triceps was 5.85 and 2.03 days, respectively. To compare the therapeutic potential of our candidate sp7-Δ8-co transgene with rhGAA protein in muscle, we interpolated the values of GAA activity measured in heart and triceps of AAV-treated $Gaa^{-/-}$ mice and NHP (shown in **Figs. 2 and 7**) with those of the kinetics of clearance of rhGAA from the same tissues in the setting of ERT (**Figs. 8B-C**). The GAA activity measured in mice injected at the high vector dose ($2x10^{12}$ vg/kg) was equivalent to the activity measured in $Gaa^{-/-}$ mice ~1 day and ~3 days after the infusion of rhGAA protein in heart and triceps, respectively. At a lower vector dose, $5x10^{11}$ vg/kg, GAA activity in tissues of AAV-treated mice was similar to that measured in

NHPs, with levels equivalent to those measured in $Gaa^{-/-}$ mice ~15 days after the infusion of high doses of rhGAA protein in both heart and triceps (**Figs. 8B-C**).

These results suggest that, in NHP, liver gene transfer with AAV vectors provides stable GAA activity levels that are in the range of those achievable with ERT. Of note, the GAA activity levels achieved in muscle of $Gaa^{-/-}$ mice treated with AAV vectors encoding for the sp7-Δ8-co GAA transgene at $5x10^{11}$ vg/kg resulted in complete clearance of glycogen from heart and 50% glycogen reduction in triceps 3 months after treatment (**Fig. 2**). This suggests that the levels of GAA activity achieved in muscle in NHPs, similar to those reached in mice treated at $5x10^{11}$ vg/kg, are therapeutically relevant.

As reported in other studies, we observed that, at identical doses, AAV-based liver gene transfer led to higher transgene expression in mice than in NHP [159], [160]. At 3 months after treatment, the same vector dose of an AAV8-hAAT-sp7-Δ8-coGAA vector resulted in a GAA activity in plasma higher in $Gaa^{-/-}$ mice than in NHPs (**Fig. 2A** and **Fig. 7B**). As improving liver transduction by AAV would increase transgene expression and allow to use lower vector doses, we packaged the hAAT-sp7-Δ8-coGAA transgene expression cassette in several AAV serotypes and screened them *in vitro* using primary hepatocytes derived from NHPs (**Fig. 7D**) and human donors (**Fig. 7E**). We used as comparison the AAV8, the most characterized serotype for liver transduction in humans [83]. GAA activity was measured in the culture media 48 hours upon infection at an MOI of $1x10^5$ vg/cell. Three serotypes, AAV3B [161], AAVLK03 [159] and the newly developed serotype AAVNP59 [162], showed superior efficiency of transduction compared with AAV8, both in NHP and human primary hepatocytes (**Fig. 7D-E**).

Together, these results indicate that the engineered sp7-Δ8-co GAA transgene can be expressed and secreted by hepatocytes of mice, NHPs, and humans. Levels achieved in vivo in NHPs were therapeutically relevant, thus supporting the feasibility of our approach in patients.

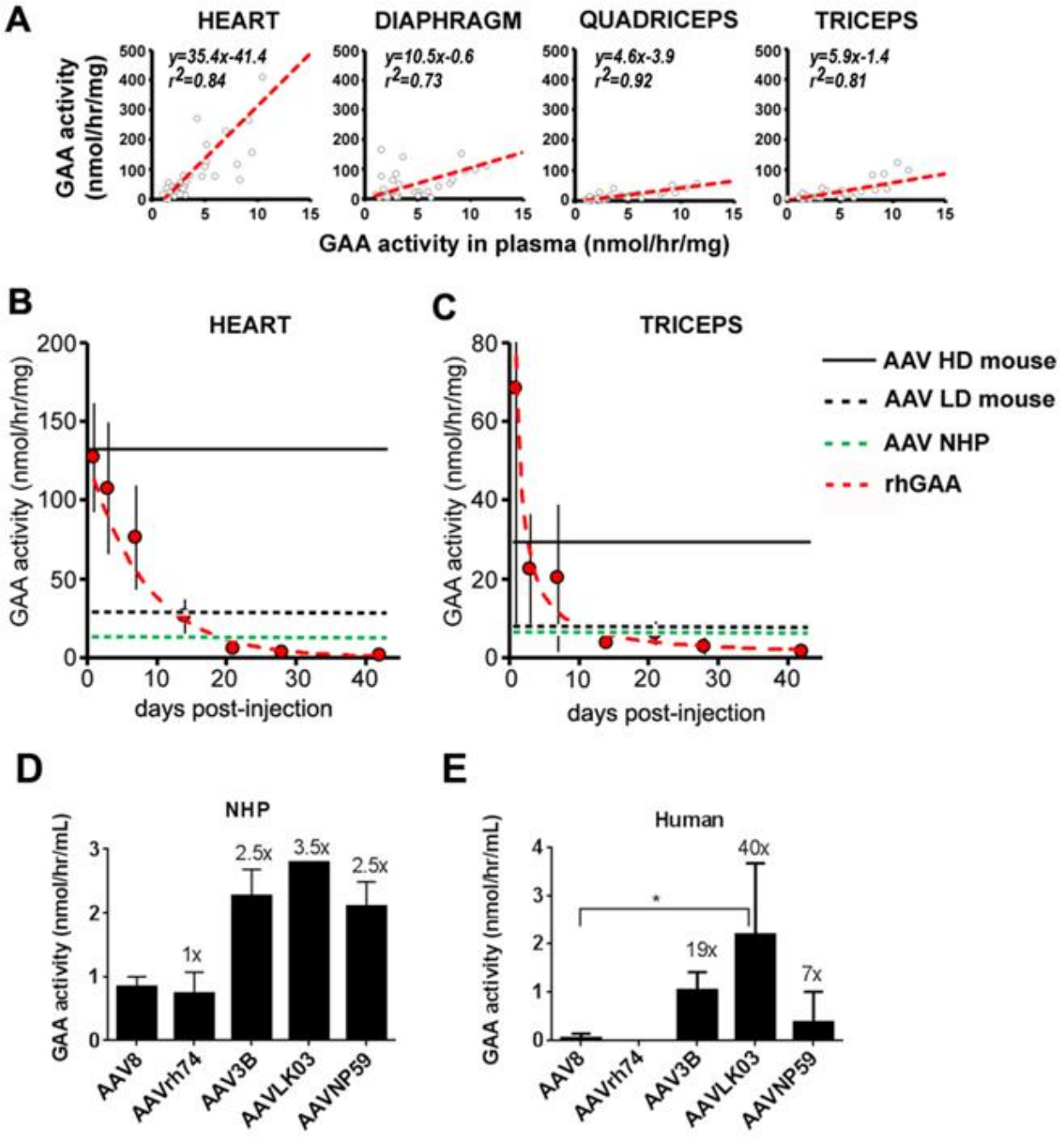

Fig. 8. Therapeutic potential of AAV vector-mediated liver gene transfer for Pompe *disease.* *(A) Regression plots showing the correlation between GAA activity measured in plasma vs. heart, diaphragm, quadriceps, or triceps in AAV-GAA treated Gaa$^{-/-}$ mice. Combined data from 3-months in vivo experiments (Tables S1-S2). The linear regression formula is depicted (B-C) Time course of GAA activity in heart (B) and triceps (C) of Gaa$^{-/-}$ mice infused with rhGAA at 100 mg/kg biweekly for a total of two infusions. Each*

time point represents the average of 4/6 animals, error bars represent standard deviation of the mean. Red lines, activity regression curves. Horizontal black lines mark the median GAA activity measured in tissues of Gaa$^{-/-}$ mice treated with AAV8-hAAT-sp7-Δ8-coGAA vectors at 2x10^{12} (HD mouse, solid line) or 5x10^{11} (LD mouse, dotted line) vg/kg. The horizontal green line indicates the mean (after baseline subtraction) GAA activity measured in tissues of monkeys treated with the same AAV8-hAAT-sp7-Δ8-coGAA vector at a dose of 2E12 vg/kg. (D-E) GAA activity measured in the culture media of primary NHP (D) or human (E) hepatocytes 48 hours post-transduction with different serotypes of AAV-hAAT-sp7-Δ8-coGAA vector a multiplicity of infection (MOI) of 1x10^{5}. The numbers above the bars indicate the fold increase of GAA activity vs. AAV8-transduced cells. Shown are mean of 2-well testing for (D). Error bars in (E) represent the standard deviation of the mean of 3 experiments except for AAVrh74 (n=1). Statistical analysis: one-way ANOVA with Dunnett's post hoc.

3. Discussion

The effective treatment of neuromuscular diseases currently represents a major challenge in human health. Pompe disease, being at the same time a neuromuscular disease and a lysosomal storage disease (LSD), represents a good model to develop and translate to the clinic novel therapeutic modalities to target the muscle body-wide. Furthermore, treating Pompe neuromuscular defects is also particularly difficult, since higher levels of enzyme have been reported to be required compared with other LSDs [163], and the therapeutic protein is highly immunogenic [35]. This therapeutic challenge can also be evinced from the fact that, despite the unmet medical need, no alternative therapies have been approved for Pompe disease since ERT ten years ago.

Here we reported the whole-body correction of Pompe neuromuscular pathology, including CNS and spinal cord, in the mouse model of the disease, and scale-up of the approach to non-human primates, using liver-directed gene transfer with AAV vectors. This unprecedented result was achieved by means of an engineered secretable GAA transgene able to mediate superior cross-correction of peripheral tissues compared with the native GAA transgene. Therapeutic levels of expression could be achieved at doses already tested in the clinic [83] and at least 1-log lower than those published in other studies [140], [164]. Furthermore, experiments in vitro with novel AAV serotypes, able to specifically target human hepatocytes [159], [161], support the feasibility of the approach in patients at even lower doses than those shown in the current study. This constitutes an important advantage of the strategy presented, as reaching therapeutic efficacy while minimizing vector doses reduces potential vector manufacturing challenges and concerns of AAV vector-related immune-mediated toxicities [142].

One key limitation of all strategies aimed at transferring a gene encoding for GAA into a target cell is the fact that the enzyme is mostly trafficked to the lysosome (90% of total) and does not follow the secretory pathway [149]. This makes the GAA transgene product poorly secreted *per se*, and perhaps accounts for the only partial efficacy observed in Pompe mice following both in vivo [139], [140], [165], [166], and ex vivo gene therapy [143]. The therapeutic candidate presented here, obtained with the deletion of 8 amino-acids in the GAA pro-peptide, combined with the addition of a heterologous signal peptide, resulted in sustained, high levels of GAA

activity measured in plasma following AAV-mediated liver gene transfer. Notably, the deleted GAA maintained specific activity equivalent to its native counterpart. This reflects the fact that the GAA pro-peptide is required neither for secretion nor for enzymatic activity, and is proteolytically cleaved during GAA maturation. Our experimental data are in agreement with extrapolations from the crystal structure of GAA, which shows an unstructured N-terminus of the protein with the first alpha-helix starting at amino acid position 100 [167]. They are also in agreement with the lack of pathological mutations in this region of the *GAA* gene (*http://cluster15.erasmusmc.nl/klgn/pompe/mutations*).

Our *in vivo* studies in Pompe mice demonstrate dose- and time- dependent glycogen clearance. Three months after treatment at low vector doses ($5x10^{11}$ vg/kg), we achieved complete clearance of glycogen in heart and about 50% reduction in diaphragm, quadriceps and triceps, while no correction was observed in the brain. A five-fold increase in vector dose ($2x10^{12}$ vg/kg) resulted in a significant glycogen clearance from muscle 3 months after treatment, demonstrating a clear dose-response in the therapeutic efficacy of the treatment. Both at low and high vector doses, the phenotypic correction was superior in animals treated with secretable GAA transgenes than in those receiving the native GAA transgene.

Aside from the vector dose-therapeutic response observed, the data presented here also highlight a more complex, perhaps unexpected specific advantage of gene therapy vs. ERT. At dose of $2x10^{12}$ vg/kg, 3 months after treatment glycogen accumulation was not corrected in the brain and incomplete in muscle groups more refractory to correction (triceps and quadriceps). Conversely, at the same vector dose, 10 months after treatment, a complete whole-body normalization of glycogen content was observed, together with a significant reduction of glycogen in brain in mice treated with the secretable GAA transgene. This indicates that not only the dose, but also the time of continuous exposure to GAA are important for reversal of the Pompe phenotype.

Whole-body clearance of glycogen allowed for the long-term preservation of muscle and respiratory function, resulting in significantly enhanced survival. Of note, mice were treated at 4 months of age, when they already had significant glycogen accumulation in all tissues [165], [168], significant cardiac hypertrophy, and mild muscle weakness. Treatment with vectors expressing secretable GAA transgenes, particularly the sp7-Δ8-coGAA, rescued the Pompe phenotype, including the diaphragmatic impairment and neural deficit of the cervical region of the spinal cord, measured with plethysmography [155].

Despite evidence that early treatment results in better outcome of ERT in Pompe [32], ongoing studies are aimed at establishing whether the enhanced circulating levels achievable with secretable GAA transgenes can rescue an advanced disease state in Pompe mice [140], [169], [170].

The analysis of muscle glycogen content in treated mice showed that there is a threshold of circulating GAA activity required for clearance, this threshold is low for the heart while increases for diaphragm, quadriceps, and triceps. This is also underlined by the survival rate of the mice treated with the non-secreted transgene, where the low amount of circulating enzyme reflects the low amount of GAA found in tissues which in turn allowed the long-term survival of those animals. Moreover, a long-term study in which a lower dose of vector was injected is ongoing and it may help highlight differences in survival of animals treated with secreted and non-secreted GAA transgenes. Similarly, in spinal cord, while the survival of motor neurons and astrogliosis were recovered by both native and secretable GAA transgenes, correction of neuro-inflammation required the higher levels of circulating enzyme activity obtained with secretable GAA transgenes. The rescue of the autophagy block in triceps followed the same pattern, as levels of p62 protein were lower in animals treated with secretable GAA-expressing vectors. These results are in agreement with what has been observed in studies when ERT is used in combination with chaperons [148], in which the longer half-life of the stabilized rhGAA protein in plasma, and the consequent higher circulating activity levels, enhanced therapeutic efficacy.

An interesting finding of our study is the presence of the GAA transgene protein in CNS and spinal cord. Like the infused rhGAA, the liver secreted protein should not be able to cross the blood-brain barrier (BBB) [34]. However, as reported for other lysosomal enzymes, high circulating levels may lead to leakage across the BBB [171]. Other mechanisms such as transport via exosomes [172] or lysosomal exocytosis at the neuro-muscular junction may also be hypothesized [173].

Previous studies in Pompe mice based on AAV-GAA liver gene transfer, using similar time points for treatment and analyses, did not report complete correction of glycogen accumulation or required vector doses up to 10 times higher than those reported here [140], [141], even when using chimeric GAA transgenes [141].

Targeting Pompe disease with AAV vectors expressing the GAA transgene directly in the affected muscle has also been proposed [135], [174]. Compared to muscle-directed gene transfer,

liver-mediated expression has several advantages. First, hepatocytes are highly metabolically active and efficient in secreting proteins into the bloodstream. The resulting dose advantage can easily be extrapolated from the literature, as for example the systemic delivery of high doses (~$5x10^{12}$ vg/kg) of an AAV9 vector expressing the GAA transgene in muscle resulted in only partial restoration of GAA activity compared to wild type animals, and incomplete clearance of glycogen accumulation in muscle [135]. Another key advantage of liver vs. muscle is that expression of antigens in hepatocytes results in induction of tolerance [126]. This has been shown in the context of Pompe disease [21], [137], [138], [175] and has been used to eradicate established immune responses to clotting factors [52]. Conversely, muscle gene transfer has been shown to be more immunogenic [135], [176].

Results presented here confirm the overall tolerogenic properties of liver-directed transgene expression. They also highlight a unique feature of secretable GAA transgenes, which is their decreased immunogenicity profile compared with native GAA transgenes, in liver but also in the stringent context of muscle-directed gene transfer. Whether this is the result of higher, more tolerogenic circulating levels of protein achieved with the secretable proteins [126], or of different mechanisms of antigen presentation, is object of further investigations. However, recently, it was published a work where Perrin and colleagues, using the well-established Ova model, demonstrated as a secreted antigen is effectively less immunogenic than a cytoplasmic one [177]. Similar to liver gene transfer, ex vivo gene therapy for Pompe disease offers the advantage of a low immunogenicity profile [143]. In summary, the work presented here is a significant advance over the current state-of-art of gene therapy for Pompe disease because it demonstrates the enhanced safety and therapeutic potential of secreted GAA transgenes. Future clinical translation efforts will have to address the potential issue of transgene persistence in liver of very young individuals [151], and eventually the need for vector readministration [178]. Nevertheless, these results can be generalized to other gene transfer modalities for Pompe, including muscle-directed and ex vivo gene transfer and, potentially, to other therapeutic proteins involved in lysosomal storage diseases [179]. The ability to scale up the approach to NHPs, for the first time in the context of AAV liver gene transfer for GAA, support the safety and feasibility of the approach in humans. Specifically, it demonstrates that circulating levels of GAA transgene, and consequent tissue uptake, in large animals are comparable to high dose ERT and likely to be therapeutic in Pompe patients

.Supplementary Figures

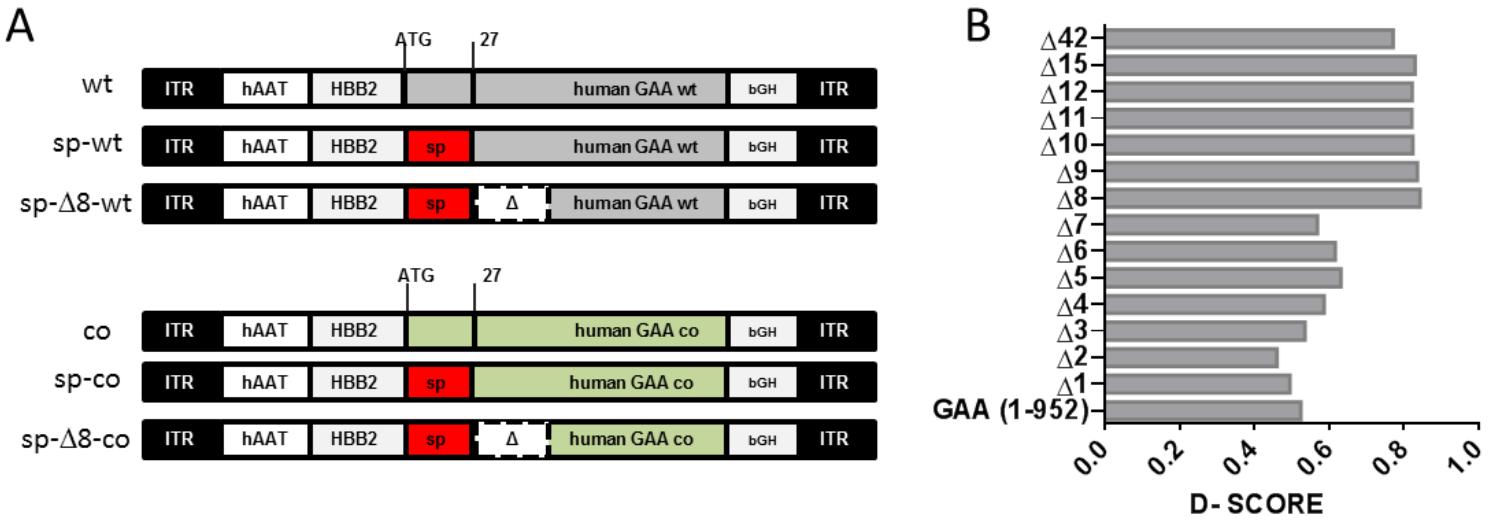

C

Expression cassette	Short name	Signal peptide	Length	Aminoacidic sequence
hAAT-HBB2-hGAA-co-bGHpA	co	native	27	MGVRHPPCSHRLLAVCALVSLATAALL
hAAT-HBB2-sp2-Δ8-hGAA-co-bGHpA	sp2-Δ8-co	alpha-1-antytripsin	26	MPSSVSWGILLLAGLCCLVPVSLAKL
hAAT-HBB2-sp3-Δ8-hGAA-co-bGHpA	sp3-Δ8-co	synthetic mut 1	16	MLLLSALLLGLAFGYS
hAAT-HBB2-sp4-Δ8-hGAA-co-bGHpA	sp4-Δ8-co	synthetic mut 3	16	MLLSFALLLGLALGYS
hAAT-HBB2-sp5-Δ8-hGAA-co-bGHpA	sp5-Δ8-co	synthetic mut 20	16	MLLEHALLLGLAHGYS
hAAT-HBB2-sp7-Δ8-hGAA-co-bGHpA	sp7-Δ8-co	chymotrypsinogen B2	18	MAFLWLLSCWALLGTTFG
hAAT-HBB2-sp8-Δ8-hGAA-co-bGHpA	sp8-Δ8-co	plasma protease inhibitor C2	22	MASRLTLLTLLLLLAGDRASS

Fig S1. Human GAA transgene engineering. *(A) Upper part: transgenes containing the wild type CDS of human GAA (wt); lower part: transgenes containing the codon-optimized CDS of human GAA (co). The native GAA signal peptide (amino acids 1-27, starting from the ATG) was removed and replaced by heterologous signal peptides [sp,* [180]*, Uniprot: Q6GPI1; Uniprot, P05155]. Amino acids 28-35 (Δ8) or 28-69 (Δ42) of the GAA pro-peptide were removed to generate the sp-Δ8 or sp-Δ42 versions of the transgene. (B) The histograms show the secretion score (D-score) predicted in silico for the full-length human GAA protein (amino acids 1-952) and its deleted versions. Amino acid residues were deleted starting from the first amino-acid after the native GAA signal peptide (Δ1=amino acidic residue 28 from the ATG). The in silico prediction was performed using SignalP 4.0. Transgene expression was under the control of the hepatocyte-specific, human alpha-1 anti-trypsin (hAAT) promoter, combined with a synthetic human beta-globin-derived (HBB2) intron* [151]*. The entire expression cassette was flanked by*

the inverted terminal repeats of AAV serotype 2 for vector packaging. bGH, bovine growth hormone polyA. (C) List of all different GAA sp-Δ8-co transgenes screened.

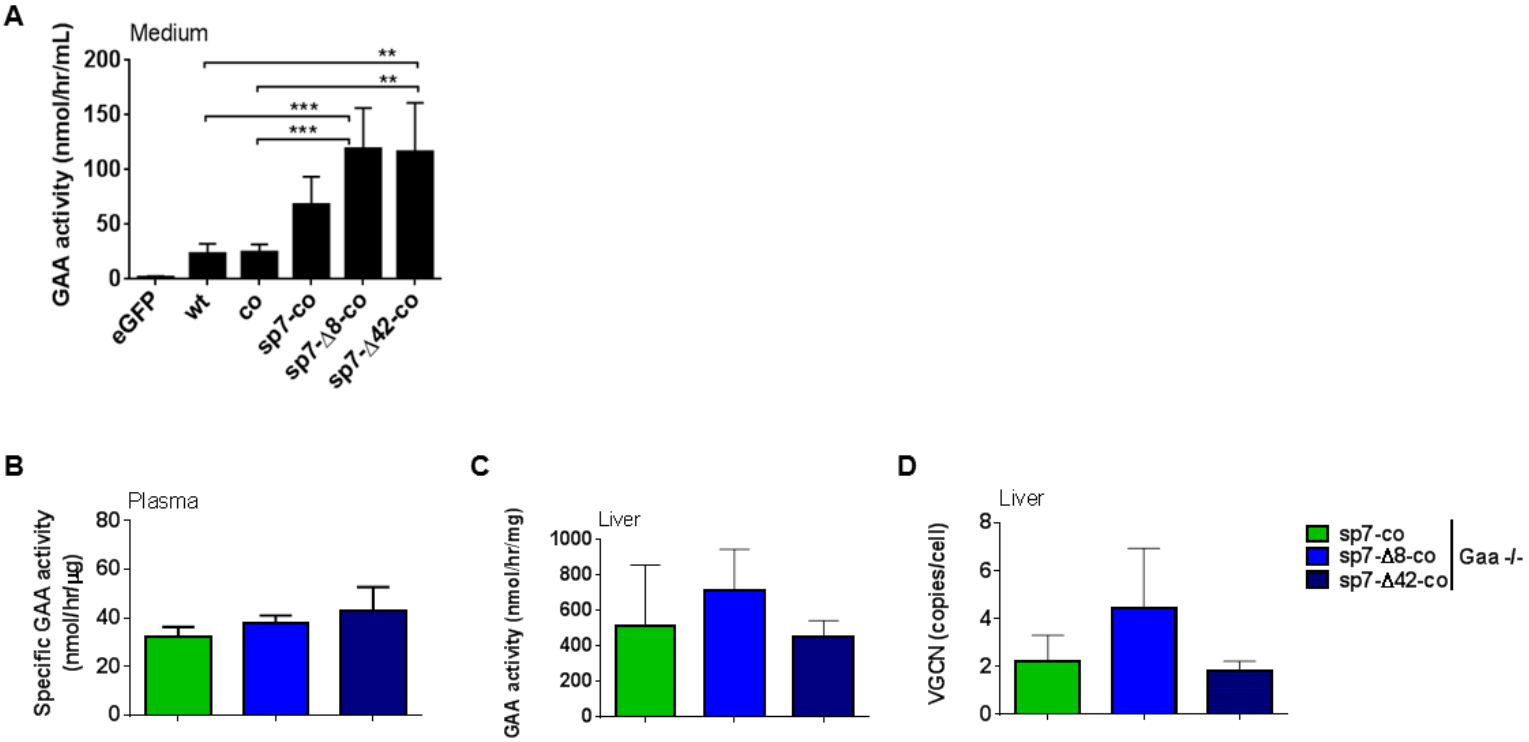

Fig S2. Selection of engineered human GAA transgenes in vitro and in vivo. *(A) GAA activity in media of HuH7 cells 48 hours after transfection with plasmids encoding for engineered human GAA transgenes. A plasmid encoding for eGFP was used as negative control. Data are shown as mean ± standard deviation of 4 independent experiments. wt, native human GAA; co, codon-optimized human GAA; sp, signal peptide; Δ, truncated human GAA. (B-D) Analysis of samples from Gaa$^{-/-}$ mice shown in Fig. 1D-F. Four-month-old mice were treated with 2x10^{12} vg/kg of AAV8 and followed for 3 months (n=3/4 per cohort). (B) Specific GAA activity of native and truncated GAA in plasma estimated by dividing the enzyme activity (Fig. 1E) by the estimated amount of GAA protein in conditioned media (Fig. 1D). Recombinant human GAA was used as standard for quantification of (C) GAA activity in the liver. (D) Vector genome copy numbers (VGCN) in the liver. (A-D) Statistical analysis: one-way ANOVA with Tukey's post hoc. Error bars represent the standard deviation of the mean.*

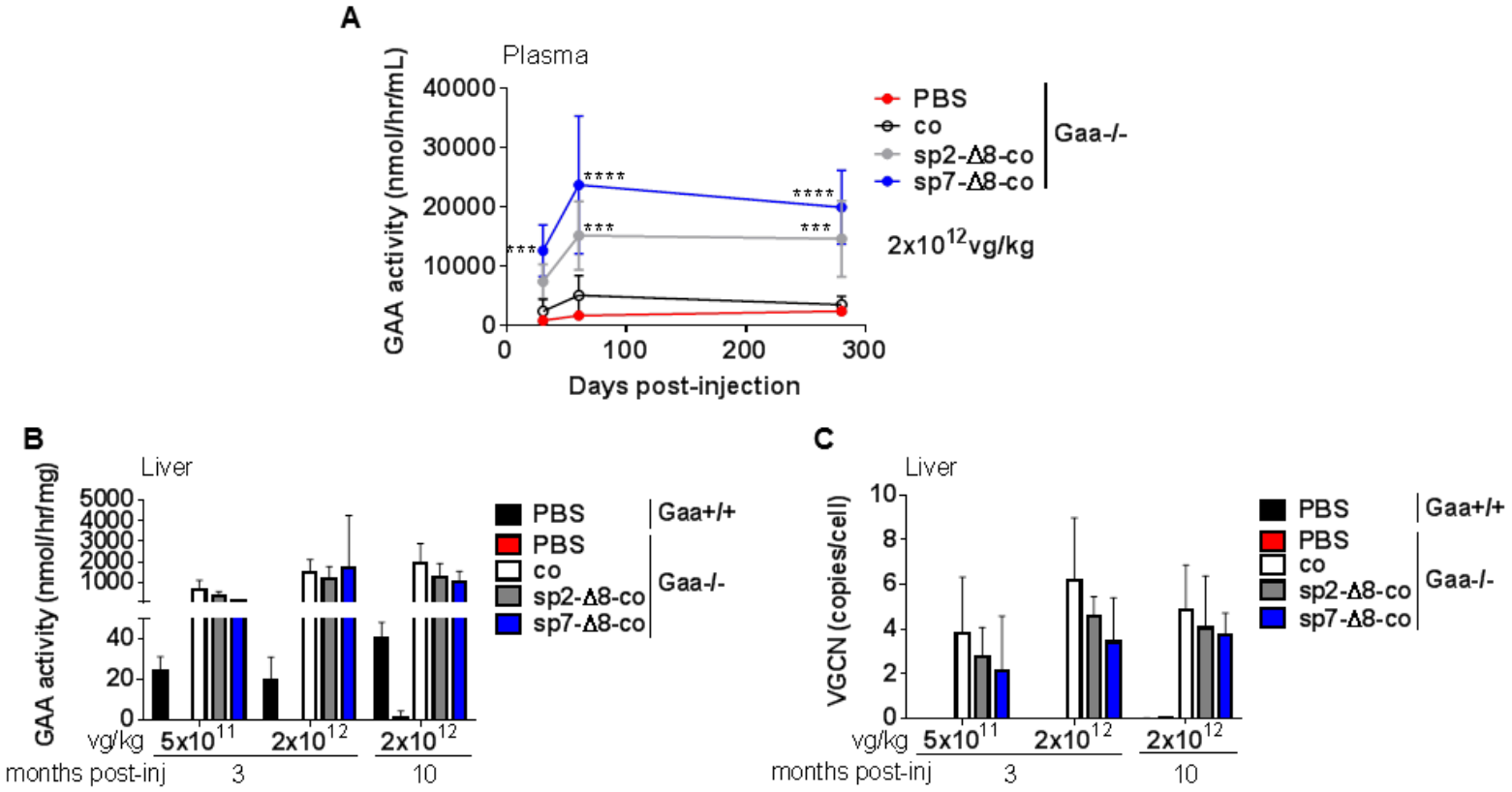

Fig S3. GAA activity levels and liver vector transduction in vivo. *(A-C) Four-month-old mice were treated with PBS or at the vector doses indicated and followed for 3 months (n=4/5 per cohort) or 10 months (n=8/9 per cohort; for PBS-treated Gaa$^{-/-}$ mice, n=10 on the day of treatment, n=7 at 3 months post treatment, n=3 at 6 and 9 months after treatment). Gaa$^{+/+}$-PBS, PBS-treated wild-type littermates; Gaa$^{-/-}$-PBS. untreated control; co, AAV8-hAAT-coGAA treated Gaa$^{-/-}$ mice; sp2-Δ8-co, AAV8-hAAT-sp2-Δ8-coGAA treated Gaa$^{-/-}$ mice; sp7-Δ8-co, AAV8-hAAT-sp7-Δ8-coGAA treated Gaa$^{-/-}$ mice. co, codon-optimized human GAA; sp, signal peptide; Δ, truncated human GAA. (A) GAA transgene activity in plasma. Statistical analysis: two-way ANOVA with Tukey's post hoc (treatment, time). Stars (*) indicate significant differences vs. Gaa$^{-/-}$ treated with AAV8-hAAT-coGAA. (B) GAA transgene activity in liver. (C) Vector genome copy numbers (VGCN) in liver. (B-C) Statistical analysis: two-way ANOVA with Tukey's post hoc (treatment, dose). (A-C) Error bars represent the standard deviation of the mean. vg, viral genome.*

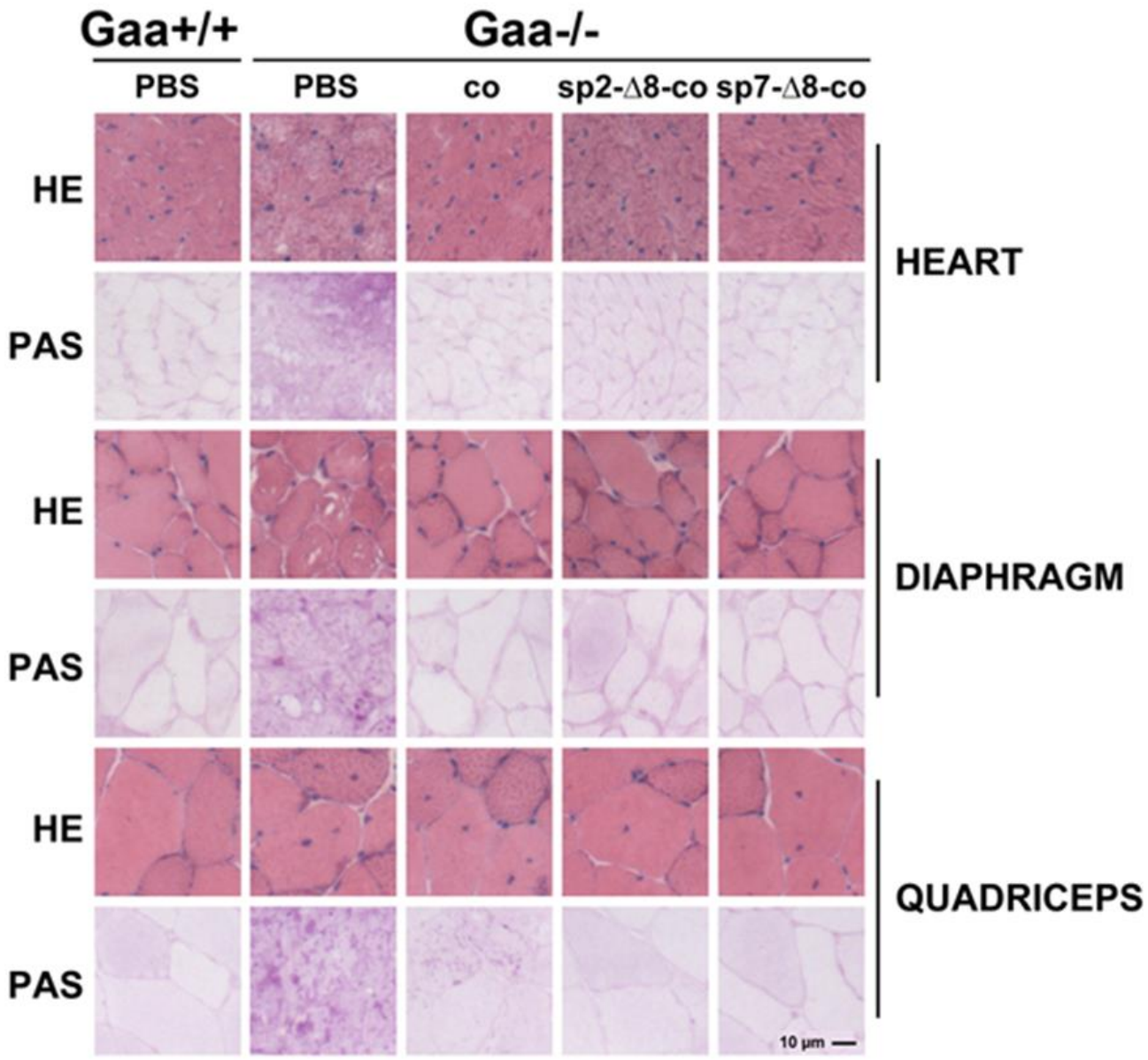

Fig. S4. Histological evaluation of hearth, diaphragm, and quadriceps of treated *Gaa*$^{-/-}$ mice and controls. *Analysis of muscle 10 months after treatment. Gaa*$^{+/+}$*-PBS, PBS-treated wild-type littermates; Gaa*$^{-/-}$*-PBS, untreated control; co, AAV8-hAAT-coGAA treated Gaa*$^{-/-}$ *mice; sp2-Δ8-co, AAV8-hAAT-sp2-Δ8-coGAA treated Gaa*$^{-/-}$ *mice; sp7-Δ8-co, AAV8-hAAT-sp7-Δ8-coGAA treated Gaa*$^{-/-}$ *mice. Vector dose used was 2x10*^{12} *vg/kg. co, codon-optimized human GAA; sp, signal peptide; Δ, truncated human GAA. Representative images of hematoxylin and eosin (HE, top panels) and periodic acid-Schiff (PAS, bottom panels) staining. The scale bar is depicted.*

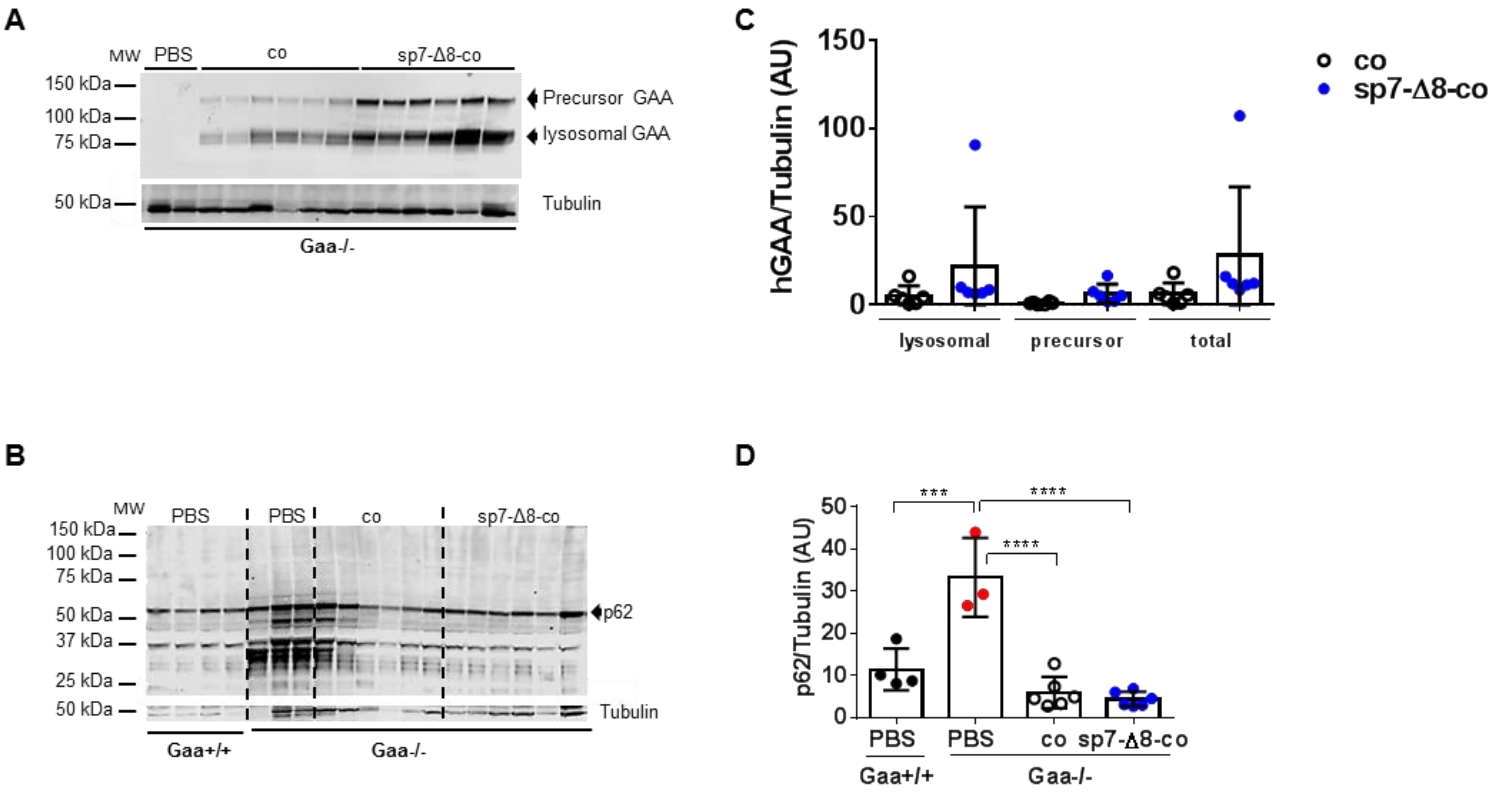

Fig. S5. GAA uptake and autophagic build-up in quadriceps of Pompe mice. *(A-B). Analysis of muscle 10 months after treatment. Gaa$^{+/+}$-PBS, PBS-treated wild-type littermates; Gaa$^{-/-}$-PBS, untreated control; co, AAV8-hAAT-coGAA treated Gaa$^{-/-}$ mice; sp7-Δ8-co, AAV8-hAAT-sp7-Δ8-coGAA treated Gaa$^{-/-}$ mice. Vector dose: 2x10^{12} vg/kg. co, codon-optimized human GAA; sp, signal peptide; Δ, truncated human GAA. (A-B). Western blot analysis of quadriceps lysates using anti-GAA (A) or anti-p62 (B) monoclonal antibodies. An anti-tubulin antibody was used as loading control. MW, molecular weight marker. (C-D) Quantification of GAA (C) or p62 (D) bands from the corresponding blots. Error bars represent standard deviation of the mean. Statistical analysis: (C) multiple t-tests with Sidak-Bonferroni post hoc. Gaa$^{-/-}$-PBS, n=2; Gaa$^{-/-}$-co, n=6; Gaa$^{-/-}$-sp7-Δ8-co, n=6. (D) one-way ANOVA with Tukey's post hoc, Gaa$^{+/+}$-PBS, n=4; Gaa$^{-/-}$-PBS, n=3; Gaa$^{-/-}$-co, n=6; Gaa$^{-/-}$- sp7-Δ8-co, n=6.*

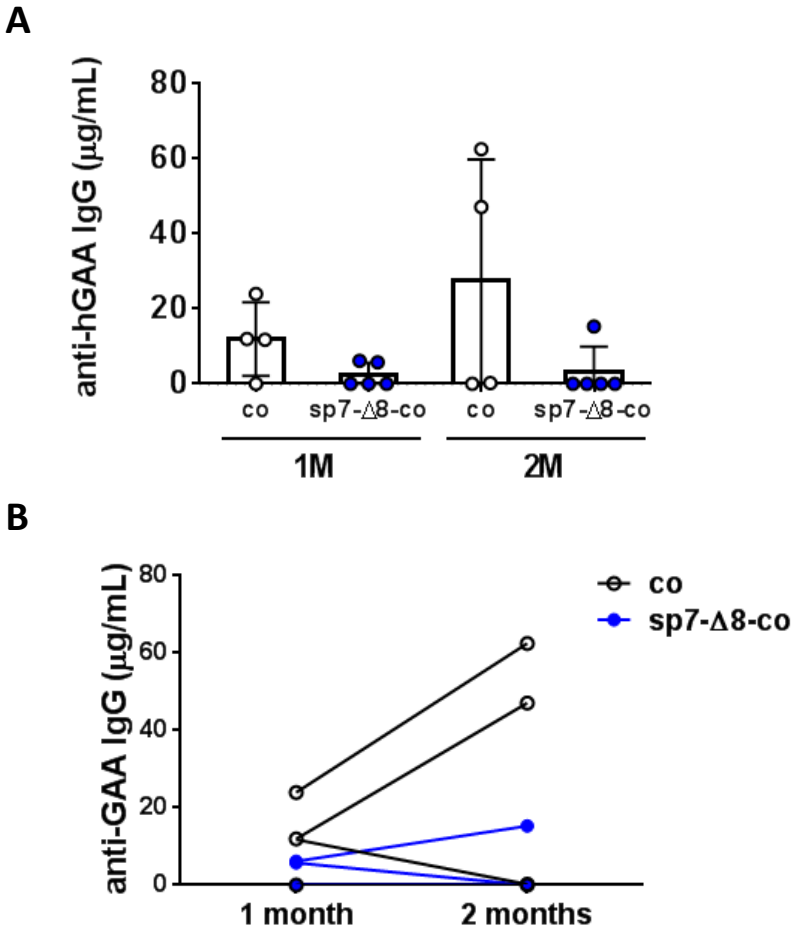

Fig. S6. Anti-human GAA transgene humoral immune responses in Gaa$^{-/-}$ mice. *(A) Analysis of anti-hGAA in plasma samples from Gaa$^{-/-}$ mice treated with AAVrh74 vectors at 2x10^{12} vg/kg. co, AAVrh74-SpC5-12-coGAA treated mice; sp7-Δ8-co, AAVrh74-SpC5-12-sp7-Δ8-coGAA treated mice. (B) Analysis of anti-hGAA in plasma samples from Gaa$^{-/-}$ mice showed in (A) plotting single mouse value. n=4/5 per cohort. co, codon-optimized human GAA; sp, signal peptide; Δ, truncated human GAA. Mice were all treated at 4 months of age, samples were analyzed 1 and 2 months (1M, 2M) post treatment. Statistical analysis: one-way ANOVA with Tukey's post hoc. Error bars represent the standard deviation of the mean.*

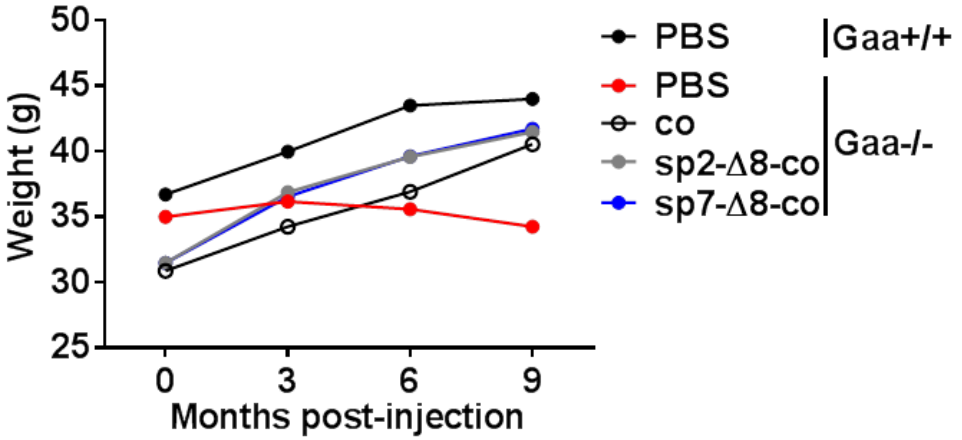

Fig. S7. Weight of treated Gaa$^{-/-}$ mice and controls. *Gaa$^{+/+}$-PBS, PBS-treated wild-type littermates; Gaa$^{-/-}$-PBS, untreated control; co, AAV8-hAAT-coGAA treated Gaa$^{-/-}$ mice; sp2-Δ8-co, AAV8-hAAT-sp2-Δ8-coGAA treated Gaa$^{-/-}$ mice; sp7-Δ8-co, AAV8-hAAT-sp7-Δ8-coGAA treated Gaa$^{-/-}$ mice. Vector dose was 2x10^{12} vg/kg. Mean mouse weight over time is depicted. For PBS-treated Gaa$^{-/-}$ mice, n=10 on the day of treatment, n=7 at 3 months post treatment, n=3 at 6 and 9 months after treatment. Statistical analysis: two-way ANOVA (treatment, time).*

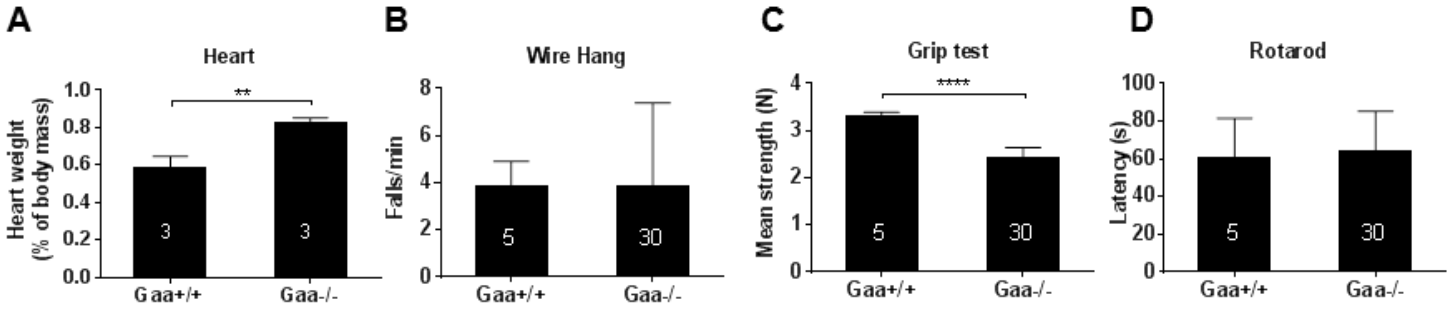

Fig. S8. Baseline measurements in Gaa$^{-/-}$ mice and controls. *Gaa$^{+/+}$, wild-type littermates; Gaa$^{-/-}$, affected mice. (A) Cardiac hypertrophy showed as heart weight expressed as percentage of body mass. (B) Wire hang test shown as falls/minute. (C) Grip test shown as mean strength. (D) Latency to fall from the rod. (A-D) Statistical analysis: unpaired t-test. The number of animals per cohort is shown in the histogram bars. Error bars represent the standard deviation of the mean.*

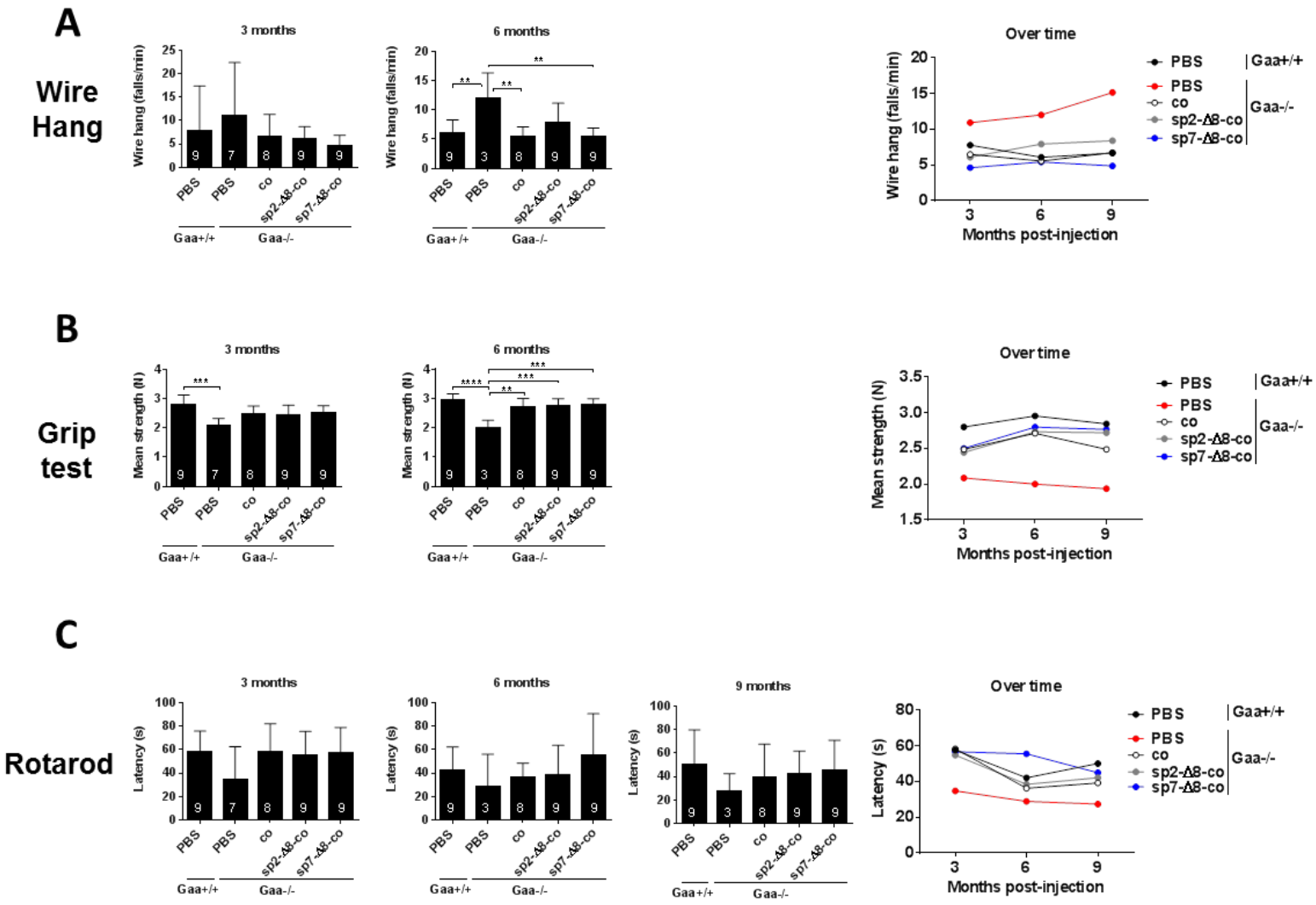

Fig. S9. Long-term outcome of gene therapy in treated Gaa$^{-/-}$ mice and controls. *(A-C) Gaa$^{+/+}$-PBS, PBS-treated wild-type littermates; Gaa$^{-/-}$-PBS, untreated control; co, AAV8-hAAT-coGAA treated Gaa$^{-/-}$ mice; sp2-Δ8-co, AAV8-hAAT-sp2-Δ8-coGAA treated Gaa$^{-/-}$ mice; sp7-Δ8-co, AAV8-hAAT-sp7-Δ8-coGAA treated Gaa$^{-/-}$ mice. Vector dose was 2x10^{12} vg/kg. (A) Wire hang test shown as falls/minute. (B) Grip test as mean three independent measurements. (C) Time spent on rotarod. (A-C) Statistical analysis: one-way ANOVA with Tukey's. The number of animals per cohort is shown in the histogram bars. Error bars represent the standard deviation of the mean. The mean value of each functional test over time is shown as linear plots in panels A-C.*

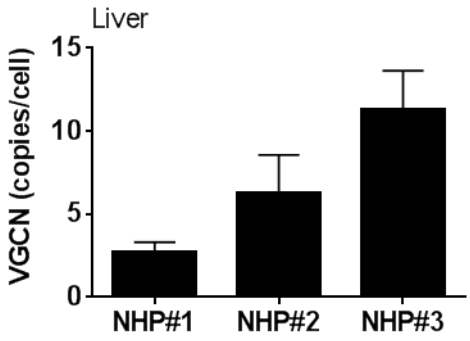

Fig. S10. Liver transduction of non-human primates treated with AAV8 encoding for the engineered sp7-Δ8-co GAA transgene. *Vector genome copy numbers (VGCN) in monkey liver 3 months after treatment. Wedge biopsies were collected from different liver lobes and VGCN measured with qPCR. Error bars represent the standard deviation of the mean of multiple biopsies analyzed.*

Supplementary Tables

Table S1. GAA activity and glycogen content in Pompe mice 3 months after treatment at a vector dose of $5x10^{11}$ vg/kg.

		Plasma	Liver	Heart		Diaphragm		Triceps		Quadriceps		Brain	
Genotype	*Treatment (n)*	*GAA Activity*	*GAA Activity*	*GAA Activity*	*Glycogen*	*GAA Activity*	*Glycogen*	*GAA Activity*	*Glycogen*	*GAA Activity*	*Glycogen*	*GAA Activity*	*Glycogen*
$Gaa^{+/+}$	**PBS (n=5)**	875 ± 749	24 ± 7	25 ± 4	0.03 ± 0.04	9.2 ± 3.7	0.03 ± 0.03	17.1 ± 3.1	0.2 ± 0.05	22.5 ± 4.1	0.2 ± 0.1	74.2 ± 12.3	0
$Gaa^{-/-}$	**PBS (n=5)**	1437 ± 346	0	0	17.1 ± 3.5	1 ± 1.4	3.6 ± 0.5	0.8 ± 0.6	3.7 ± 0.4	0.7 ± 1.4	4.7 ± 0.9	0	0.6 ± 0.1
	co (n=5)	1899 ± 674	621 ± 484	24 ± 36	7.4 ± 7.7	37 ± 40	2.1 ± 1.8	2.7 ± 2.8	2.9 ± 2	2.3 ± 2.8	2.7 ± 2.1	0	0.6 ± 0.2
	sp2-Δ8-co (n=5)	4055 ± 1807	357 ± 210	130 ± 119	0.1 ± 0.1	16 ± 12	0.9 ± 0.7	9 ± 4.3	2.5 ± 1.5	9.9 ± 6.9	2.7 ± 1.6	0	0.5 ± 0.2
	sp7-Δ8-co (n=4)	3279 ± 2462	118 ± 28	83 ± 97	0.2 ± 0.1	14 ± 19	1.6 ± 0.8	11.3 ± 10.3	2 ± 1	3.8 ± 2	2 ± 0.4	0	0.5 ± 0.1

$Gaa^{+/+}$-PBS, PBS-treated wild-type littermates; $Gaa^{-/-}$-PBS, untreated controls. GAA activity: plasma (nmol/hr/mL), tissue (nmol/hr/mg). Glycogen (mmol glucose/ g protein). Values are shown as mean ± standard deviation.

Table S2. GAA activity and glycogen content in Pompe mice 3 months after treatment at a vector dose of $2x10^{12}$ vg/kg.

		Plasma	Liver	Heart		Diaphragm		Triceps		Quadriceps		Brain	
Genotype	*Treatment (n)*	*GAA Activity*	*GAA Activity*	*GAA Activity*	*Glycogen*	*GAA Activity*	*Glycogen*	*GAA Activity*	*Glycogen*	*GAA Activity*	*Glycogen*	*GAA Activity*	*Glycogen*
$Gaa^{+/+}$	**PBS (n=5)**	1076 ± 452	19 ± 2 [a]	20 ± 2	0.04 ± 0.01	10 ± 1	0.2 ± 0.1	26 ± 3	0.5 ± 0.2	15 ± 1	0.3 ± 0.1	95 ± 17	0
$Gaa^{-/-}$	**PBS (n=5)**	985 ± 452	0	0.6 ± 2	14 ± 1	1 ± 1	5 ± 0.2	2 ± 2	5 ± 1	0	5 ± 1	2 ± 2	0.6 ± 0.1
	co (n=4)	1873 ± 744	1444 ± 663	40 ± 19	0.4 ± 0.2	65 ± 71	0.8 ± 0.5	8 ± 2	2 ± 0.2	12 ± 12	1 ± 1	9 ± 7	0.6 ± 0.1
	sp2-Δ8-co (n=4)	8412 ± 3496	1201 ± 577	363 ± 353	0.2 ± 0.1	101 ± 37	0.5 ± 0.3	85 ± 39	1 ± 1	41 ± 14	1 ± 1	9 ± 5	0.4 ± 0.1
	sp7-Δ8-co (n=5)	13043 ± 15138	1722 ± 2540	352 ± 544	0.3 ± 0.2	122 ± 183	0.7 ± 0.2	64 ± 85	2 ± 2	52 ± 74	1 ± 1	11 ± 7	0.6 ± 0.2

$Gaa^{+/+}$-PBS, PBS-treated wild-type littermates; $Gaa^{-/-}$-PBS, untreated controls. GAA activity: plasma (nmol/hr/mL), tissue (nmol/hr/mg). Glycogen (mmol glucose/ g protein). Values are shown as mean ± standard deviation

Table S3. GAA activity and glycogen content in Pompe mice 10 months after treatment at a vector dose of $2x10^{12}$ vg/kg.

		Plasma	Liver	Heart		Diaphragm		Triceps		Quadriceps		Brain	
Genotype	*Treatment (n)*	*GAA Activity*	*GAA Activity*	*GAA Activity*	*Glycogen*	*GAA Activity*	*Glycogen*	*GAA Activity*	*Glycogen*	*GAA Activity*	*Glycogen*	*GAA Activity*	*Glycogen*
$Gaa^{+/+}$	**PBS (n=9)**	N.D.	41 ± 8	10 ± 4	0.1 ± 0.04	8 ± 2.4	0.2 ± 0.1	10 ± 1	0.2 ± 0.1	19 ± 2	0.2 ± 0.1	34 ± 3	0.002 ± 0.002
$Gaa^{-/-}$	**PBS (n=3)**	2667 ± 591	2 ± 2	0	5.6 ± 0.8	0	2 ± 1	0.01 ± 0.02	2 ± 1	1 ± 2	3 ± 0.2	0.1 ± 0.2	2 ± 0.1
	co (n=8)	3552 ± 1446	1940 ± 946	53 ± 45	0.1 ± 0.1	49 ± 43	0.2 ± 0.1	7 ± 5	0.3 ± 0.2	9 ± 3	0.4 ± 0.3	3 ± 3	1 ± 0.1
	sp2-Δ8-co (n=9)	14602 ± 6406	1225 ± 702	264 ± 130	0.1 ± 0.1	129 ± 128	0.2 ± 0.1	23 ± 11	0.3 ± 0.2	31 ± 12	0.3 ± 0.2	4 ± 2	1 ± 0.2
	sp7-Δ8-co (n=9)	19917 ± 6189	1016 ± 520	326 ± 191	0.1 ± 0.1	122 ± 133	0.2 ± 0.1	25 ± 12	0.2 ± 0.1	36 ± 21	0.2 ± 0.2	3 ± 1	0.8 ± 0.2

$Gaa^{+/+}$-PBS, PBS-treated wild-type littermates; $Gaa^{-/-}$-PBS, untreated controls. GAA activity: plasma (nmol/hr/mL), tissue (nmol/hr/mg). Glycogen (mmol glucose/ g protein). Values are shown as mean ± standard deviation. N.D. Not determined.

Table S4. Long-term outcome of respiratory functions after gene therapy in treated Gaa$^{-/-}$ mice and controls.

Tidal volume (mL)			
Genotype	*Treatment (n)*	*3 months post-injection*	*6 months post-injection*
Gaa$^{+/+}$	**PBS (n=9)**	0.21 ± 0.03	0.24 ± 0.02
Gaa$^{-/-}$	**PBS**	0.19 ± 0.02 (n=7)	0.22 ± 0.005 (n=3)
	co (n=8)	0.2 ± 0.02	0.21 ± 0.02
	sp2-Δ8-co (n=9)	0.21 ± 0.02	0.22 ± 0.03
	sp7-Δ8-co (n=9)	0.22 ± 0.02	0.24 ± 0.03*

*Gaa$^{+/+}$-PBS, PBS-treated wild-type littermates; Gaa$^{-/-}$-PBS, untreated controls. Values are shown as mean ± standard deviation. Statistical analysis was performed with one-way ANOVA with Dunnett's post hoc (*p<0.05 vs. co 6 months).*

4. Materials and Methods

4.1 GAA expression cassettes and AAV vectors

The GAA transgene expression cassettes used in this study contained either the wild-type or the codon-optimized CDS encoding for the native or engineered forms of human GAA (**Fig. S1A**). Codon-optimization was performed using a commercial algorithm (Thermo Fisher Scientific, Waltham, MA). Transgene sequences were cloned into an AAV vector backbone under the transcriptional control of the apolipoprotein E (hepatocyte control region enhancer and the human alpha 1-antitrypsin (hAAT) promoter [151], the SpC5-12 promoter [157], or the CMV enhancer/chicken β-actin promoter (CAG) promoter. All DNA sequences used in the study were synthetized either by GeneCust (Dudelange, Luxemburg) or (Thermo Fisher Scientific, Waltham, MA).

AAV vectors used in this study were produced using an adenovirus-free transient transfection method as described earlier [181]. Titers of AAV vector stocks were determined using quantitative real-time PCR (qPCR) and confirmed by SDS-PAGE followed by SYPRO Ruby protein gel stain and band quantification using ImageJ software. All vector preparations used in the studies were quantified side-by-side at least 3 times before injection. The AAV serotypes, AAVLK03 [159], and AAVNP59 [162] are derived by shuffling. AAVNP59 is a novel shuffled capsid with high human hepatocyte transduction and favorable humoral neutralization. NP59 was derived through a multiplexed set of sequential directed evolution screens in humanized liver mice in vivo followed by on-bead selection against pools of human immunoglobulins.

4.2 In vitro experiments

Human hepatoma cells (HuH7) were transfected using Lipofectamine 2000® (Thermo Fisher Scientific, Waltham, MA) accordingly to manufacturer's instructions. 48 hours after transfection, cells and conditioned media were harvested and analyzed for GAA activity and Western blot. Each experiment was repeated at least 3 times. For transduction experiments in primary non-human primate and human hepatocytes (Biopredic International, Rennes, France), cells seeded in 96-well plates at $5x10^4$ cells/well were infected at a multiplicity of infection (MOI) of 10^5. 48 hours after infection, cells and media were harvested and analyzed for GAA activity.

4.3 In vivo studies

Mouse studies were performed according to the French and European legislation on animal care and experimentation (2010/63/EU) and approved by the local institutional ethical board (protocol n° 2015-008). The mouse procedures involving the administration of recombinant human GAA were performed at Duke University and approved by the local Institutional Animal Care and Use Committee. $Gaa^{-/-}$ mice were previously described [19]. AAV vectors were administered intravenously via the tail vein to 4-month-old male mice.

An initial screening study was performed in $Gaa^{-/-}$ mice for the evaluation of the different native or engineered GAA transgenes (n=4 per group). Two additional short-term studies in $Gaa^{-/-}$ mice and controls were conducted at low ($5x10^{11}$ vg/kg) and high ($2x10^{12}$ vg/kg) vector dose, respectively, and treated animals were followed for 3 months post-treatment (n=5 per treatment group). In one long-term study, $Gaa^{-/-}$ mice and controls were treated at a vector dose of $2x10^{12}$ vg/kg and followed for 10 months (n=8/9 per treatment group).

For the immunogenicity study in the context of muscle gene transfer, $Gaa^{-/-}$ mice (n=4 per group) were treated with $2x10^{12}$ vg/kg of vector injected intravenously.

The kinetic of clearance of the GAA enzyme in heart and triceps was evaluated in two-month old $Gaa^{-/-}$ mice after two intravenous injections of rhGAA at 100 mg/kg one week apart. Groups of 4-5 mice were sacrificed 1, 3, 7, 14, 28, and 42 days after the second injection and heart and triceps were analyzed for residual GAA activity.

For the non-human primate study, three AAV8 seronegative [182] male animals (*Macaca Fascicularis*) were included in the study. Animals were housed and *in vivo* procedures were conducted at the Nantes-Atlantic National College of Veterinary Medicine, Food Science and Engineering (Oniris, Nantes, France). Animals were handled according to French and European legislation on animal care 2010/63/EU. The protocol was approved by the local institutional ethical board (APAFIS#2651-2015110216583210v5). AAV vectors were administered by systemic injection into the saphenous vein of anesthetized animals. Vector was infused in a volume of 24 ml over the course of 1 hour. Two of the three animals received one intravenous infusion of 2 mg/kg of rapamycin the day of vector infusion.

As baseline readout of GAA enzyme activity in tissues of wild-type NHPs, tissues from a control monkey were used. For plasma, basal GAA activity from 8 untreated animals was averaged.

4.4 Vector genome copy number analysis

Vector genome copy number was determined using qPCR as previously described [151]. The PCR primers used in the reaction were located on the hAAT promoter, forward 5'-GGCGGGCGACTCAGATC-3', reverse 5'-GGGAGGCTGCTGGTGAATATT-3', for the expression cassettes. For the internal control has been used mouse titin gene, sequence of the forward and reverse primers were 5'-AAAACGAGCAGTGACGTGAGC-3' and 5'-TTCAGTCATGCTGCTAGCGC-3', respectively.

4.5 Measurement of GAA activity and glycogen content

GAA activity was measured as previously described [165]. Briefly, 10 µL of sample, either tissue homogenate or cell medium, was incubated for 1 hour at 37°C with 20 µL of 4-Methylumbelliferyl α-D-glucopyranoside (3mM) diluted in acetate buffer solution, pH 4.65 (Sigma Aldrich). Standard curve was prepared using 4-Methylumbelliferone diluted in 0.5M of carbonate solution, pH 10.5. Reaction was stopped using the carbonate solution and the fluorescence (λ_{ex} 360nm/λ_{em} 449nm) was read at the EnSpire alpha plate reader (Perkin-Elmer, Waltham, MA).

Glycogen content was measured indirectly in tissue homogenates as the glucose released after total digestion with *Aspergillus Niger* amyloglucosidase (Sigma Aldrich, Saint Louis, MO). Samples were incubated for 5 min at 95°C and then cooled at 4°C; 25 µL of amyloglucosidase diluted 1:50 in 0.1M potassium acetate pH 5.5 were then added to each sample. A control reaction without amyloglucosidase was prepared for each sample. Both sample and control reactions were incubated at 37°C for 90 minutes. The reaction was stopped by incubating samples for 5 min at 95°C. The glucose released was determined using a glucose assay kit (Sigma Aldrich, Saint Louis, MO) and by measuring resulting absorbance at the EnSpire alpha plate reader (Perkin-Elmer, Waltham, MA) at 540 nm.

4.6 Western blot analyses

HuH7 cell lysates were prepared using 10mM PBS (pH 7.4) containing 1% of Triton-X100 and protease inhibitors (Roche Diagnosis, Basel, Switzerland). Western blot on mouse and NHP plasma was performed on samples diluted 1:4 in radioimmunoprecipitation assay (RIPA) buffer.

Mouse tissues were mechanically homogenate in H_2O using lysing matrix tubes (MP Biomedicals). NHP tissues were lysed in PBS (10mM, pH7.4) containing 1% of Triton-X and protease inhibitors (Roche Diagnosis, Basel, Switzerland) freshly added to the samples.

Protein concentration was determined using the BCA Protein Assay (Thermo Fisher Scientific, Waltham, MA).

SDS-page electrophoresis was performed in a 4-15% gradient polyacrylamide gel. After transfer, the membrane was blocked with Odyssey buffer (Li-Cor Biosciences, Lincoln, NE) and incubated with an anti-GAA antibody (mouse monoclonal, sc-373745, SantaCruz Biotechnology, Santa Cruz, CA or rabbit monoclonal ab137068, Abcam, Cambridge, MA), anti-p62 (mouse monoclonal ab56416, Abcam, Cambridge, MA), anti-actin (mouse monoclonal, sc-8432, SantaCruz Biotechnology), or anti-tubulin (mouse monoclonal, T9026, Sigma Aldrich, Saint Louis, MO). The membrane was washed and incubated with the appropriate secondary antibody (Li-Cor Biosciences), and visualized by Odyssey imaging system (Li-Cor Biosciences).

4.7 Anti-GAA antibody detection

Anti-GAA antibody measurement was performed according to a published protocol (*61*). Briefly, maxisorp 96 wells plates (Thermo Fisher Scientific, Waltham, MA) were coated with 2 µg/ml of rhGAA. Standard curves of mouse (Sigma Aldrich, Saint Louis, MO) or monkey (Fitzgerald, Acton, MA) recombinant IgG were coated to the wells. Anti-mouse (Southern biotech, Birmingham, AL) or anti-monkey (Fitzgerald, Acton, MA) IgG secondary antibodies conjugated with horseradish peroxidase (HRP) were used. After incubation with o-phenylenediamine dihydrochloride (OPD), the reaction was stopped adding HCl 2.5N, and the absorbance was read at the EnSpire alpha plate reader at 492nm.

4.8 Histological evaluation

For muscle histology, after euthanasia triceps brachii, quadriceps femoris, diaphragm, and heart were snap-frozen in isopentane previously chilled in liquid nitrogen. Serial 8 µm cross-sections were cut in a Leica CM3050 S cryostat (Leica Biosystems, Nussloch, Germany). To minimize sampling error, 3 sections of each specimen were obtained and stained with hematoxylin-eosin (HE) and periodic acid-Schiff (PAS) according to standard procedures.

For spinal cord staining, after being explanted spinal cords were fixed in in 4% PFA transferred in a 30% PBS-sucrose solution and finally embedded in Tissue-Tek OCT (Sakura Finetek, Alphen aan den Rijn, the Netherlands), and frozen in cold isopentane. Fourteen micrometer-thick cryosections were cut using a cryostat (Leica Biosystems, Nussloch, Germany). Spinal cord sections were fixed with 4% PFA, permeabilized in 0.1% Triton X-100 in PBS and stained with the primary antibodies: anti-ChAT (choline acetyltransferase,

Merck Millipore, Billerica, MA), rabbit anti GFAP (glial fibrillary acidic protein, Agilent Technologies, Santa Clara, CA) and rabbit anti Iba1 (Ionized Calcium-Binding Adapter Molecule 1, Wako Chemicals GmbH, Neuss, Germany). After washing, tissues were incubated with the appropriate fluorescent conjugated secondary antibodies (all from Thermo Fisher Scientific, Waltham, MA) combined with DAPI staining.

ChAT-positive motor neurons (with a diameter > 20 μm) were manually counted in the ventral horn of the cervical, thoracic, and lumbar spinal cord segments using an epifluorescence microscope (Leica Microsystems, Buffalo Grove, IL). Astroglial reaction was evaluated by measuring the fluorescence intensity of the GFAP staining in the gray matter of the spinal cords using the ImageJ software. Microglial activation was evaluated by counting the Iba-1 positive cells in the grey matter of spinal cord sections. Cell counting and morphological analyses were blinded.

4.9 Functional assessment

Respiratory function during quiet breathing was evaluated as already reported [155]. Briefly, a flow-through (0.5 L/min) plethysmograph (EMKA technologies, Paris, France) was used to measure the breathing pattern in treated $Gaa^{-/-}$ mice and controls. The instrument was calibrated with known airflow and pressure signals before data collection. Signals were analyzed by using the IOX2 software (EMKA technologies). Tidal volume was evaluated over a 5 minutes period. Animals were allowed for acclimation into the plethysmograph chamber before testing. During both acclimation and data acquirement, mice were breathing normoxic air (21% O2, 79% N2).

Forelimbs wire-hanging test was performed as already reported [183]. A 4-mm wire was used to record the number of falls over a period of 3 minutes. The number of falls per minute was reported.

Grip strength was measured as already reported [183]. Using a grip strength meter, (Columbus instruments, San Diego, CA) three independent measurements of the four limbs strength were calculated. Mean values of the grip strength were reported.

Rotarod testing was performed as already reported [134] using a LE8200 apparatus (Harvard Apparatus, Holliston, MA). An accelerating protocol 4-40 rpm in 5 minutes was used. The test was repeated three times and the average time of each animal was reported.

4.10 Statistical analysis

All the data showed in the present manuscript are reported as mean±SD. The number of sampled units, n, upon which we reported statistic is the single mouse for the in vivo experiments (one mouse is n=1) and the single independent experiment for the in vitro studies using cell lines (one independent experiments n=1). GraphPad Prism 6 software (GraphPad Software) was used for statistical analyses. p-values<0.05 were considered significant. For all the data sets, data were analyzed by parametric tests, alpha=0.05, (one-way and two-way ANOVA with Tukey's or Dunnett's post-hoc correction, and multiple t-tests with Sidak-Bonferroni post-hoc correction). Non-parametric tests were performed when only two groups were compared (unpaired t-test). The statistical analysis performed for each data set is indicated in figure legends. For all figures *p<0.05, **p<0.01, ***p<0.001, ****p<0.0001 except where different symbols are used.

CHAPTER II

Long-term exposure to Myozyme results in a decrease of anti-drug antibodies in late-onset Pompe disease patients

5.1 Results

5.1 Long-term ERT results in clearance of anti-rhGAA antibodies in LOPD patients

To understand the effect of long-term ERT on humoral responses to rhGAA, anti-rhGAA antibody data from LOPD subjects (n=24) who received ERT with Myozyme at least 3 years (three antibody measurements per year) and developed a response to the enzyme were collected and analyzed. Of these subjects, five had peak antibody titers ≥1:25,000, twelve had peak antibody titers ≥1:6,400 and <1:25,000, and seven developed peak antibody titers <1:6,400. No clear correlation between GAA gene mutations (**Table S1**) and peak antibody titers was found (data not shown). 17 out of 24 patients showed the highest antibody titer in the first 1,000 days on ERT (**Fig. 1A**), with one subject reaching a titer of >1:200,000, followed by a decrease to levels close to baseline for most subjects. Statistical analysis of data, performed by comparison of titers measured during the first 500 days of ERT (108 measurements) with those collected between 501 and 1,000 days (82 measurements), between 1,001 and 1,500 days (64 measurements), and between 1,500 and 2,000 days of ERT (46 measurements), confirmed that the changes in antibody titers were significant (**Fig. 1B**). These results indicate that long-term ERT in LOPD subjects is associated with a decrease of anti-rhGAA antibodies.

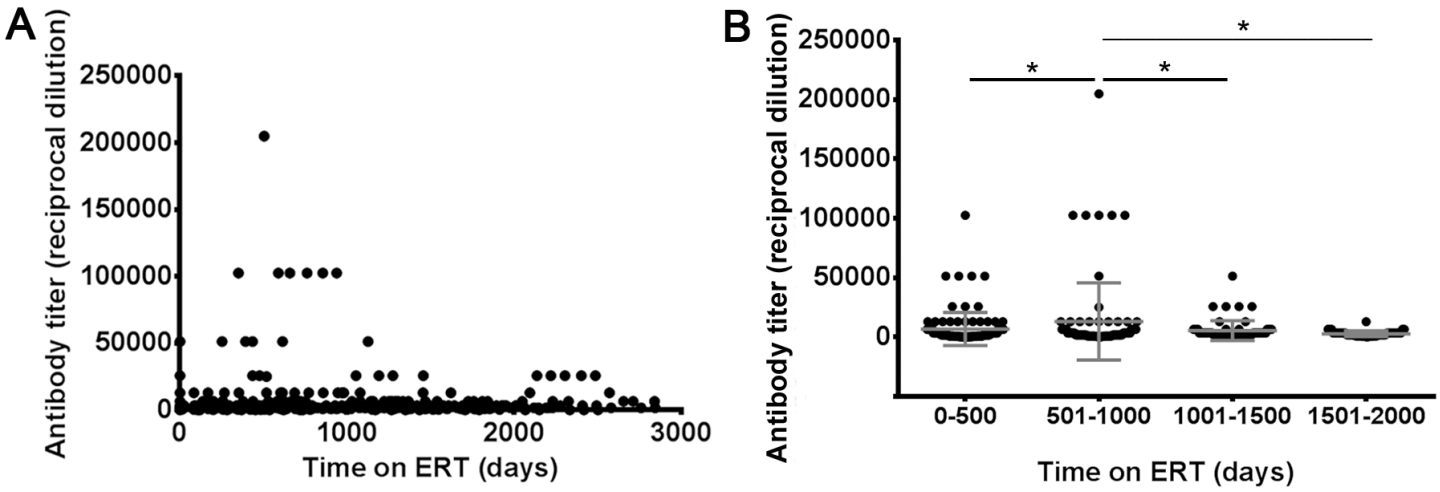

Figure 1. Long-term ERT in LOPD patients results in a decrease of anti-rhGAA antibodies. *(A) Measurement of anti-rhGAA antibody titers over time (n=24 subjects). (B) Comparison of antibody titers measured in the first 500 days of ERT (n=108 measurements) with titers measured between 500 and 1,000 days of ERT (n=82 measurements), 1,000 and 1,500 days of ERT (n=64 measurements), and 1,500 and 2,000 days of ERT (n=46 measurements). For each time period, the same number of measurements for each subject was included in the analysis. ANOVA analysis was used to compare the measurements over time (*P < 0.05). Antibody titers are expressed as reciprocal dilution as previously described* [24].

5.2 Long-term ERT in LOPD subjects results in development of non-neutralizing anti-rhGAA IgG1 and IgG4

To better understand the nature of anti-rhGAA antibody responses observed in the LOPD patients enrolled in the study, serum samples were tested using an antibody binding assay specific for anti-rhGAA IgG subclasses, IgM, and IgE (**Fig. 2**). Healthy donors (HD) and untreated LOPD subjects did not display significant levels of antibodies specific to rhGAA, whereas a subset of LOPD subjects who received long-term ERT had elevated levels of anti-rhGAA IgG1 and IgG4 antibodies (**Figs. 2A** and **2D**). No significant levels of IgG2, IgG3, IgM, and IgE antibodies were detected. As IgG4 have been reported in association with inhibitor activity [184], seven samples, displaying the highest anti-rhGAA antibody titers, were then tested for neutralizing activity on both rhGAA enzyme activity and cell uptake assays and no inhibitory activity was measured (**Fig. S1A**). In agreement with these results, follow up of six-minute walk test (6MWT) and forced vital capacity (FVC) in IgG4 positive subjects showed a similar trend to the subjects from the same cohort (**Figs. S1B, and S1C**). These results confirm the presence of anti-rhGAA antibodies in CRIM-positive LOPD

subjects even after long-term ERT. They also indicate that repeated exposures to the rhGAA antigen results in production of non-neutralizing antibodies including IgG4, an antibody subclass previously associated with activation of regulatory B cells [185], [186].

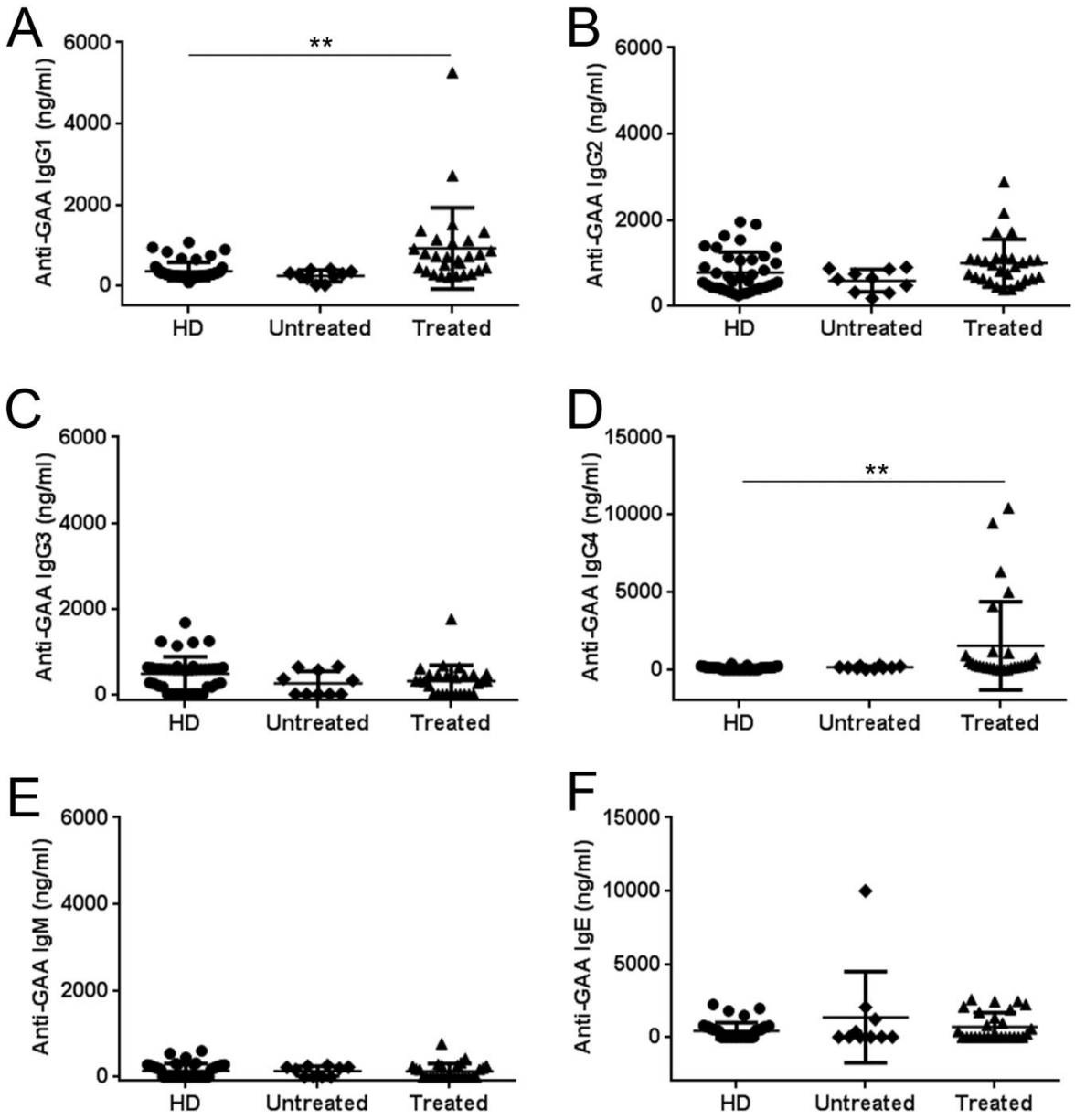

Figure 2. Anti-rhGAA IgG1 and IgG4 are the most prevalent subclasses of antibodies developed in response to long-term ERT. *(A-F) Anti-rhGAA antibodies measured with a capture assay specific for IgG1, IgG2, IgG3, IgG4, IgM, and IgE antibodies. Estimated antibody concentrations are reported for each subject. Average and standard deviation are indicated for each of the study cohorts: LOPD subjects receiving ERT (Treated, n=28), untreated LOPD subjects (Untreated, n=10), and healthy donors (HD, n=43). Unpaired two-tailed t-test was used to compare results across the study cohorts (**P < 0.01).*

5.3 DC-mediated restimulation of PBMCs results in detection of T cell reactivity to rhGAA

IgG4 production has been associated with induction of immunological tolerance [185]. To test whether a similar mechanism mediated the observed decrease in anti-GAA antibody titers in LOPD subjects undergoing ERT, and to study T cell reactivity to rhGAA in treated and untreated LOPD subjects, an IFNγ ELISpot assay specific for the enzyme was established. Initial screening of PBMCs isolated from treated LOPD subjects revealed lack of reactivity to rhGAA, even in subjects with detectable anti-rhGAA antibodies (data not shown). To enhance T cell reactivity to rhGAA, we used a dendritic cell (DC) activation protocol optimized to study low-frequency T cells [187]. Following restimulation with rhGAA and specific cytokines and chemokines prior to the ELISpot assay, we were able to measure production of IFN-γ in response to rhGAA in some subjects (**Fig. 3A**). Five out of twenty-eight treated LOPD subjects showed detectable T cell reactivity to rhGAA, however no correlation was found between production of IFN-γ and anti-rhGAA antibody titers (**Fig. 3B**). A positive T cell response to rhGAA was detected also in one untreated LOPD subject and one HD, an observation previously made for other antigens such as coagulation factor VIII in HD and in hemophilia A subjects [188]. Additional analyses of treated LOPD PBMCs restimulated in vitro with rhGAA for 48 hours followed by intracellular cytokine staining (ICS), showed a complex pattern of activation of CD4+ T cells, with production of IFNγ, TNFα, IL2, and IL17 in some subjects (**Figs. 3C-F**). No response to rhGAA was detectable in CD8+ T cells (data not shown). These results indicate that circulating GAA-reactive T cells can be found in peripheral blood, although detectable only after restimulation with the antigen [189].

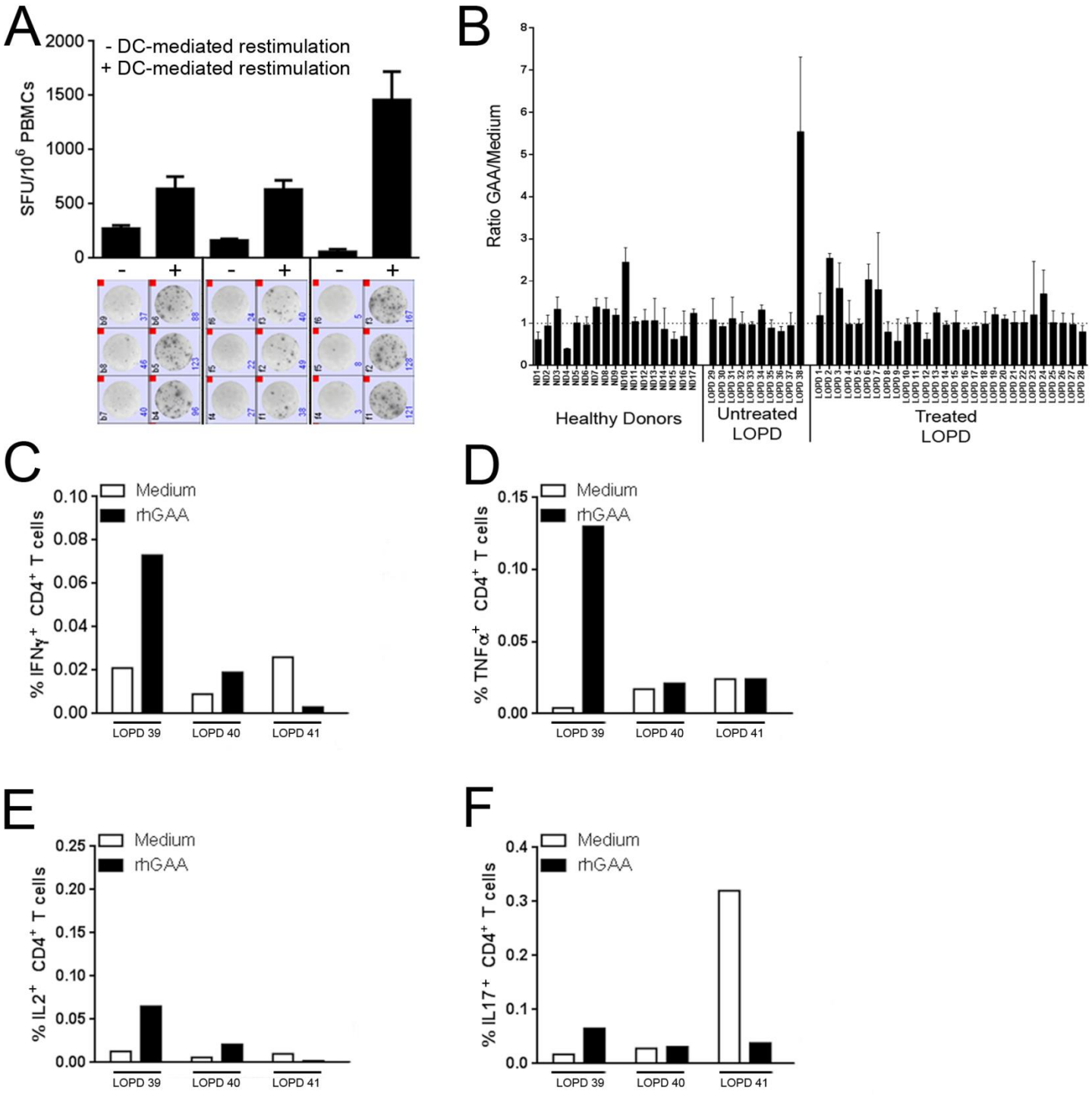

Figure 3. T cell reactivity to rhGAA is detectable after restimulation of PBMCs with the antigen. *(A) Comparison of IFNγ ELISpot count in PBMCs isolated from LOPD subjects receiving ERT before and after DC-mediated restimulation. Cells were either directly plated in the ELISpot assay (-) or restimulated in vitro with 10 µg/ml of rhGAA prior to the assay (+). Results are expressed in spot forming units (SFU) per 10^6 cells. Results are reported as average of triplicate testing +/- standard deviation. Images of the test wells in the IFNγ ELISpot assay are shown below the histogram plot. (B) Combined results for all subjects*

screened with the IFNγ ELISpot assay after PBMC restimulation. PBMCs from LOPD subjects receiving ERT (Treated, n=28), untreated LOPD subjects (Untreated, n=10), and HD (n=15) were tested in the assay. Results are expressed as ratio between SFU/10^6 cells in rhGAA-restimulated cells vs. medium control. (C-F) PBMCs from LOPD subjects receiving ERT (n=3) were restimulated with 10 μg/ml of rhGAA for 48h and then stained intracellularly for IFNγ, TNFα, IL2, and IL17. Results are reported as percentage of $CD4^+$ T cells secreting a given cytokine.

5.4 IL2 is the cytokine signature of T cell reactivity to rhGAA in treated LOPD subjects

To better define the profile of T cells reactive to rhGAA in all subjects studied, we collected supernatant from PBMCs after DC-mediated restimulation and tested them against an array of cytokines and chemokines using the Luminex platform (**Figs. 4** and **Fig. S2**). In this assay, significantly elevated levels of IL2 were detected only in treated LOPD subjects (**Fig. 4A**). IL10 was also slightly upregulated in subjects receiving ERT, although not at significant levels (**Fig. 4B**). Conversely, significant amounts of cytokines were found in both treated and untreated LOPD subjects compared with HD (**Figs. 4C-L**). A Spearman correlation matrix was used to analyze the data deriving from the cytokine and chemokine production in treated and untreated LOPD subject and the data deriving from the HD, confirming the presence of a correlation among cytokines in responses to rhGAA in both treated and untreated LOPD subjects (**Fig. 4M**). These results may reflect the proinflammatory state associated with the disease [42], [190], which was previously described in infantile Pompe patients [191]. Alternatively, the reactivity detected against rhGAA in both treated and untreated LOPD patients may be reflect an underlying immune response resulting from the expression of the endogenous mutant GAA protein.

The secretion of IL2 after DC-mediated restimulation only in treated LOPD subjects possibly reflects a state of anergy of reactive T cells deriving from long-term exposure to rhGAA [192]. Alternatively, the detection of slightly elevated levels of IL10 in treated LOPD subjects may also be evidence of equilibrium between proinflammatory and tolerogenic signals. To address this point, the untouched CD25neg fraction of PBMCs was isolated from three LOPD subjects displaying high anti-rhGAA IgG4 levels. Following a 48-hour restimulation with rhGAA, both the untouched PBMC and the CD25neg fraction of PBMC was co-cultured with autologous DCs pulsed with rhGAA. Cells were tested for reactivity to rhGAA in an IFNγ

ELISpot assay, showing enhanced T cell reactivity to rhGAA in the CD25neg fraction of PBMC (**Fig. 4N**), suggesting that the induction of peripheral tolerance contributed to the unresponsiveness to the rhGAA antigen. Similarly, to investigate the role of suppressive IL10-expressing B cells [185], [193], we depleted CD19+CD24hiCD38hi B cells in PBMC collected from six treated LOPD subjects. The remaining untouched PBMC fraction was co-cultured with autologous DCs pulsed with rhGAA antigen and then tested for reactivity to rhGAA in an IFNγ ELISpot assay. Depletion of regulatory B cells resulted in a slight enhancement of T cell reactivity to rhGAA in only 1/6 subjects (**Fig. 4O**), not supporting the involvement of CD19+CD24hiCD38hi B cells in the observed hyporesponsiveness to rhGAA.

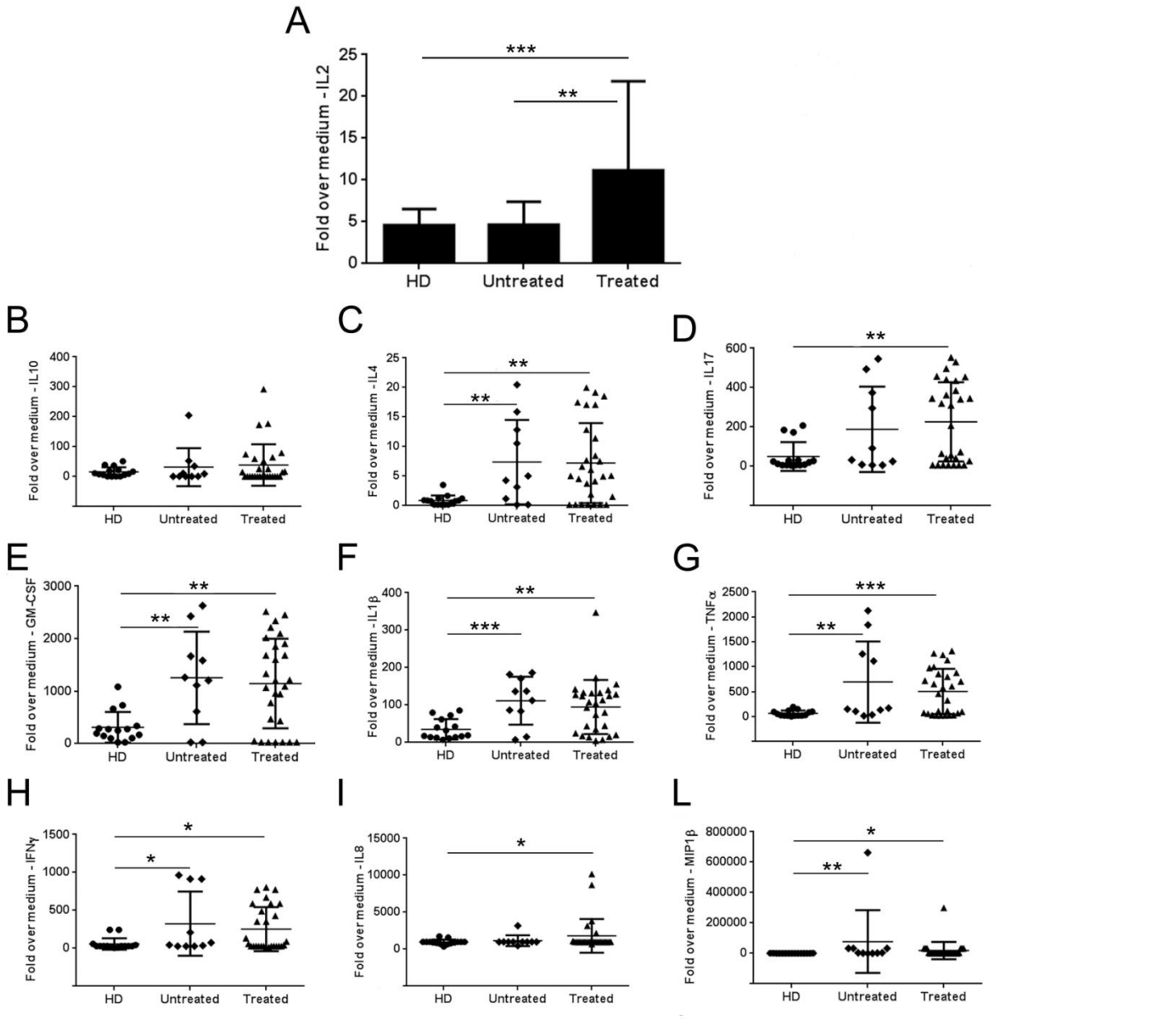

M

	IL4	IL17	GM-CSF	TNFα	IFNγ	IL1β	MIP1β	IL10	IL2
IL4		0.84 ****	0.83 ****	0.68 ****	0.71 ****	0.61 ****	0.07 NS	0.36 **	0.16 NS
IL17	0.84 ****		0.64 ****	0.78 ****	0.83 ****	0.62 ****	0.01 NS	0.31 *	0.26 NS
GM-CSF	0.83 ****	0.64 ****		0.62 ****	0.56 ****	0.73 ****	0.20 NS	0.39 **	0.07 NS
TNFα	0.68 ****	0.78 ****	0.62 ****		0.85 ****	0.80 ****	0.39 **	0.17 NS	0.19 NS
IFNγ	0.71 ****	0.83 ****	0.56 ****	0.85 ****		0.57 ****	0.09 NS	0.22 NS	0.12 NS
IL1β	0.61 ****	0.62 ****	0.73 ****	0.80 ****	0.57 ****		0.49 ***	0.32 *	0.12 NS
MIP1β	0.07 NS	0.01 NS	0.20 NS	0.39 **	0.09 NS	0.49 ***		-0.03 NS	-0.03 NS
IL10	0.36 **	0.31 *	0.39 **	0.17 NS	0.22 NS	0.32 *	-0.03 NS		-0.01 NS
IL2	0.16 NS	0.26 NS	0.07 NS	0.19 NS	0.12 NS	0.12 NS	-0.03 NS	-0.01 NS	

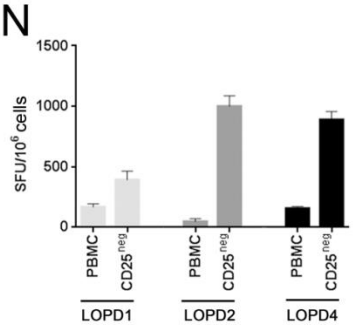

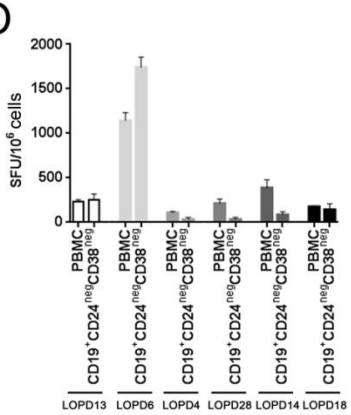

Figure 4. Cytokine profiling of supernatant from PBMCs restimulated with rhGAA. *Supernatants from cells restimulated with rhGAA were collected after 48 hours of restimulation in vitro and assayed for cytokine and chemokine production. (A) Levels of IL2 measured in conditioned media in LOPD subjects receiving ERT (Treated, n=28), untreated LOPD subjects (Untreated, n=10), and healthy donors (HD, n=17). Error bars represent the standard deviation of the mean. Mann-Whitney test was used to compare data across the study groups. (B-L) Cytokine and chemokine concentration in media measured with the Luminex array technology; shown are individual values measured in LOPD subjects receiving ERT (Treated, n=28), untreated LOPD subjects (Untreated, n=10), and healthy donors (HD, n=17). Error bars represent the average of a cohort +/- standard deviation. Mann-Whitney test was used to compare data across the study groups. (M) Pearson correlation matrix comparing measurements of cytokine and chemokine production in responses to rhGAA in treated (n=28) and untreated (n=10) LOPD subjects, and HD (n=15). Numbers in the table represent the correlation coefficient between two variables with the relative p value (t-test). (N) Depletion of $CD25^{+}$ in PBMCs from treated LOPD subjects. The untouched $CD25^{neg}$ PBMC fraction was co-cultured with autologous DCs pulsed with rhGAA antigen or unpulsed DCs as negative control, followed by IFNγ ELISpot. Results of the IFNγ ELISpot assay are shown as average of spot forming units (SFU) per 10^6 cells plated in the assay +/- standard deviation of triplicate testing. (O) Sorted untouched $CD19^{+}CD24^{neg}CD38^{neg}$ PBMC fraction from treated LOPD subjects co-cultured with autologous DCs pulsed with rhGAA antigen (or negative control) followed by IFNγ ELISpot. Results of are shown as average SFU/10^6 cells +/- standard deviation of triplicate testing (*P < 0.05; **P < 0.01; ***P < 0.001; **** P < 0.0001, NS, not significant).*

5.5 Infusion of rhGAA in LOPD subjects is associated with systemic upregulation of cytokines and chemokines

To test whether rhGAA infusion is associated with systemic activation of the immune system, we performed a study in ten LOPD subjects undergoing ERT in which we monitored serum cytokines and chemokine levels. For each subject, a serum sample was collected immediately before the infusion of rhGAA and one additional sample was collected at the end of the infusion, after flushing the intravenous line with saline solution. rhGAA administration resulted in a significant upregulation of several cytokines and chemokines, including IL8, monocyte chemotactic protein 1 (MCP1), macrophage inflammatory protein 1 beta (MIP1β), IL7, and IL13 (**Fig. 5**). Additional cytokines were upregulated, although the changes measured were not significant; these included IL6, TNFα, IL1β, IFNγ, IL4, IL5, and granulocyte macrophage colony-stimulating factor (GM-CSF) (**Fig. S3**). No clear correlation between reactivity to rhGAA and baseline measurements of humoral or cellular responses to rhGAA was evident in the subjects studied (data not shown). These results indicate that administration of rhGAA results in early activation of immunity.

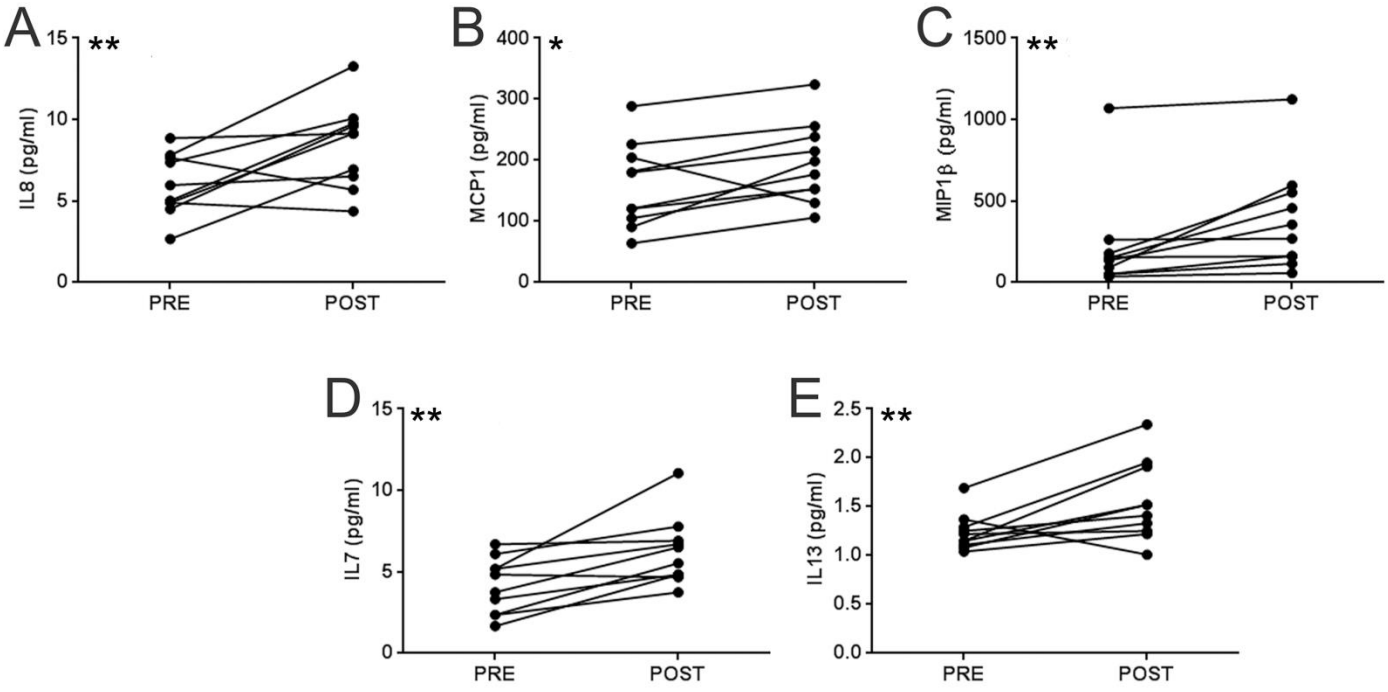

Figure 5. Serum cytokine and chemokine profiling of LOPD subjects before and after ERT. *(A-E) Luminex cytokine and chemokine measurements before (PRE) and immediately after (POST) rhGAA administration (over the course of four hours) in LOPD subjects (n=10). Shown are cytokines for which a significant change in serum levels was measured at the end*

*of ERT. Paired t-test was used to compare data analysis PRE vs. POST infusion (*P < 0.05; **P < 0.01).*

5.6 Long-term clinical outcome of ERT does not correlate with immune responses to rhGAA

Follow-up measurements of six-minute walk test (6MWT) and forced vital capacity (FVC) in the cohort of treated LOPD subjects (**Figs. 6A and 6B** respectively) showed an initial improvement or stabilization of both measurements followed by a downward trend. This finding, which possibly reflecting a worsening of the disease despite ERT in a subset of patients, will need to be confirmed in larger studies. Notably, a recently published meta-analysis of clinical trials involving LOPD patients undergoing ERT also showed a marked improvement in 6MWT and FVC in the first year of treatment, followed by a subsequent stabilization or decline in performance [23].

In our analysis, no correlation was found between the evolution of FVC and 6MWT and the measurements of immune responses to rhGAA after long-term ERT (**Fig. 6C**), consistent with the fact that no neutralizing antibody response was detected after long-term ERT. These results confirm that, after long-term ERT, no relationship between clinical endpoints of disease progression and immune responses to rhGAA is found.

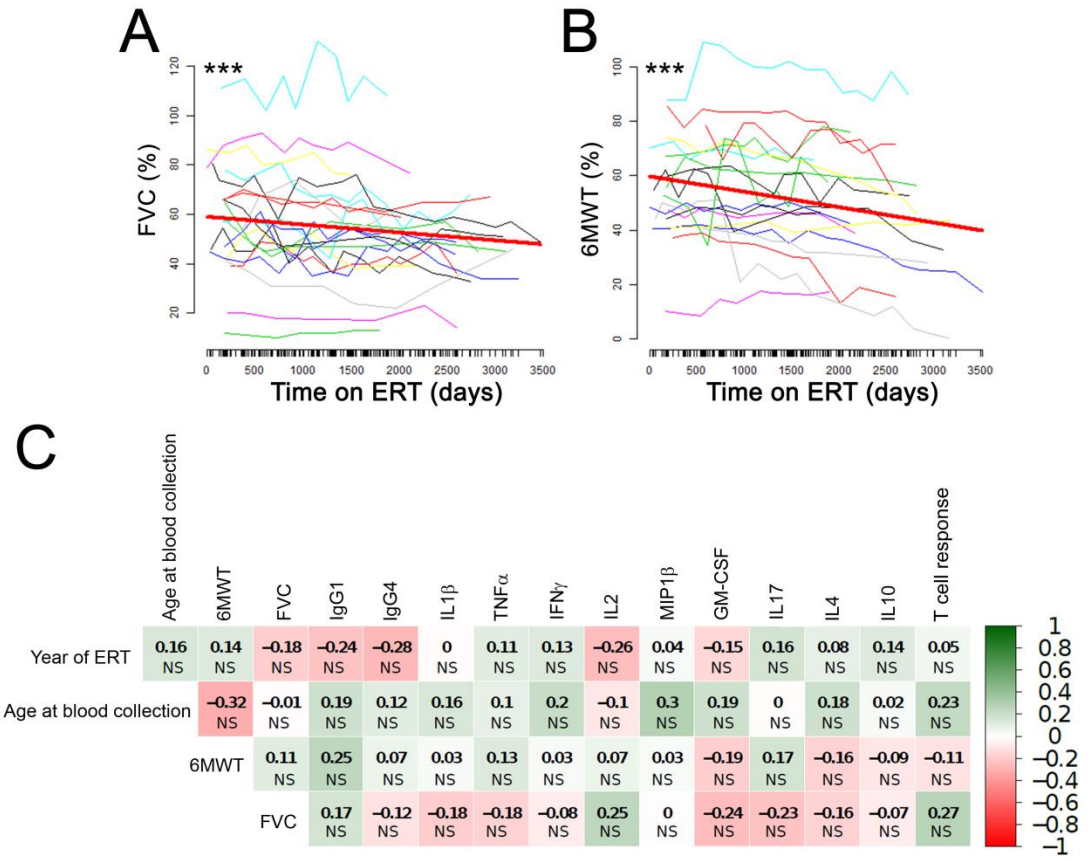

Figure 6. Clinical outcome measures and statistical analysis of results. *(A) % forced vital capacity (FVC) measurements, expressed as % predicted in healthy individuals, over a period of 4 years in 21 treated LOPD subjects; the red line represents the average evolution of the measurement. The estimated slope is -1.16% per year; the estimated intercept is 58.9%; p value is given by linear mixed models (see Methods). The following equations were used to calculate the % FVC: [FVC predicted for males = 0.060 * height - 0,0214 * age – 4.65]; [FVC predicted for females = 0.0491 * height - 0.0216 * age – 3.59]; [FVC (%) = FVC observed / FVC predicted * 100] (B) Six-minute walk test (6MWT), expressed as % predicted in healthy individuals, measured over a period of 4 years in 19 subjects, the red line represents the average evolution of the measurement. The estimated slope is -2.06% per year; the estimated intercept is 59.6%; p value is given by linear mixed models (see Methods) (***P<0.001). The following equations were used to calculate the % 6MWT: [6MWT predicted for males = -309 - 5.02 * age - 1.76 * weight + 7.57 * height]; [6MWT predicted for females = 667 - 5.78 * age - 2.29 * weight + 2.11 * height]; [6MWT (%) = 6MWT observed / 6MWT predicted * 100]. (C) Spearman correlation of measurements of immune responses to rhGAA with clinical outcome measures recorded at the time of blood collection. The numbers in the table represent the correlation coefficient between two variables with the relative p value (t-test) (NS, not significant).*

6. Discussion

Immunogenicity of protein-replacement therapeutics represents a major hurdle in the treatment of genetic [194] and acquired [195] disorders. Several factors contribute to shape the immune responses to an antigen, including the genetic background of the host [35], [196], the immunogenicity of the therapeutic protein [197], polymorphisms in genes regulating immune responses [198], and presence of contaminants in the drug substance that can exert an adjuvant effect on immune responses [197]. Additionally, underlying inflammation associated with some diseases can enhance immune responses against protein and gene therapeutics [111], [199]. To date, the mechanisms driving the immunogenicity of rhGAA in ERT for Pompe disease are largely unknown.

Here we presented a comprehensive characterization of immune responses to rhGAA in a cohort of subjects affected by LOPD, either untreated or undergoing long-term ERT. The data presented demonstrate that in this patient population, despite the presence of residual GAA antigen endogenously expressed [200], antibodies responses are elicited by ERT, in some cases reaching high titers (Fig. 1A and [36], [201]). Unlike for other genetic diseases [196], no clear correlation with the underlying mutation in the disease-causative gene was found, reflecting the fact that LOPD subjects are typically CRIM-positive, and suggesting that other genetic factors [202] may contribute to shape the response to rhGAA. To this end, secretion of cytokines in response to rhGAA by PBMC collected both from treated and untreated LOPD subjects indicate the existence of an underlying proinflammatory condition associated with the disease, regardless of ERT. This is possibly the consequence of impaired autophagy [203] that characterizes Pompe disease and other lysosomal storage diseases [204], [205]. Alternatively, as previously observed in Duchenne muscular dystrophy patients [199], residual expression of the endogenous GAA in these subjects may also result in an increased immunogenicity of rhGAA. These results were also confirmed *in vivo*, as we showed that infusion of rhGAA in LOPD patients triggered immediate systemic secretion of several cytokines and chemokines.

In our cohort of subjects, despite the fact that some subjects reached anti-rhGAA antibody titers >1:200,000 during the first ~1,000 days of ERT, long-term exposure to rhGAA in the absence of immunomodulatory interventions resulted in a marked decrease in antibody levels, with no late occurrence of antibodies, except for non-neutralizing IgG1 and IgG4. This outcome of ERT is markedly different that observed in infantile Pompe patients, who need

adjuvant immunomodulatory therapy to prevent or eradicate immune responses to rhGAA [206]–[208].

Differently from ERT in hemophilia A, where detection of IgG4 is typically associated with presence of inhibitor [184], [209], [210], the presence of increased levels of non-neutralizing IgG4 antibodies, in the absence of IgE antibodies, in treated LOPD subjects compared with HD and untreated LOPD subjects possibly reflects the desensitization to the immunogen [185], [211]–[213]. Alternatively, the production of GAA-specific IgG4 may simply reflect the chronic exposure to antigen [214]. Whether the residual anti-rhGAA IgG titers found in our patient cohort affect clearance or bioavailability of the protein, remain to be established [215].

Immune tolerance associated with ERT has been previously described in humans affected by diseases like mucopolysaccharidosis type I [216], [217] and hemophilia B [210]. Studies in mice [38], [218] support the idea that $CD4^+$ T helper cells are key to the development of humoral responses to rhGAA, confirmed by the fact that targeting these cells with non-depleting monoclonal antibodies results in avoidance of antibody formation to the protein [219]. In our study, detection of $CD4^+$ T cell reactivity only after mature DC-mediated restimulation [187] of PBMCs highlights a state of hyporesponsiveness of T cells, which can produce large amounts of proinflammatory cytokines when encountering the rhGAA antigen in the context of the appropriate stimulus. IL2, in particular appears to be the cytokine signature in LOPD subjects on ERT. Production of IgG4 antibodies has been associated with the presence of IL10-secreting B regulatory 1 (Br1) cells [185]. Detection of slightly elevated levels of IL10 following PBMC restimulation may indicate the existence of some mechanism of active suppression of immune responses to rhGAA that contributes to the development of immune tolerance to the antigen. Indeed, depletion of $CD4^+CD25^+$ T cells from PBMCs did resulted in enhanced T cell reactivity to rhGAA, while little to no effect was observed when $CD24^{hi}CD38^{hi}$ B cells [193] were depleted. While these results are preliminary, they support the role of regulatory T cells in the development of peripheral tolerance to rhGAA following ERT. More detailed studies will also help to fully address the role of $CD73^-CD25^+CD71^+$ Br1 cells [185] in Pompe disease patients undergoing ERT.

Finally, it is not surprising that the measurements of immune responses after long-term exposure to ERT do not correlate with the longitudinal analysis of 6MWT and FVC. This is likely to be the results of multiple factors, including 1) all subjects after long-term ERT had low residual levels of anti-rhGAA antibodies which were not neutralizing, 2) the fact that the immune responses measured were more consistent with a state of unresponsiveness, rather

than immunity, to rhGAA and 3) the fact that the immune assays were performed far in time from the peak of antibody responses to rhGAA.

In summary, exposure to rhGAA via ERT in LOPD subjects results in early development of antibodies to the protein, which subsequently mostly disappear over time. The presence of residual levels of non-neutralizing rhGAA-specific IgG4 antibodies, and the T cell activation profile consistent with hyporesponsiveness to the antigen, reflect an immunomodulatory effect mediated by the long-term exposure to the antigen, possibly via the induction of regulatory T cells. These data indicate that antibody formation induced by long-term ERT is not a major concern in LOPD patients. Immune tolerance induction protocols based on high-dose antigen exposure [220], [221] and/or pharmacological interventions [222] are valuable tools to manage detrimental humoral immune responses encountered in ERT. Conversely, in LOPD patients, acute reactions to the enzyme are among the most relevant immune complications of ERT [223], [224], thus not warranting the use of immunomodulatory strategies to eradicate anti-GAA antibodies.

Supplementary Table

	LOPD	Age	Sex	Years of ERT	Mutations		Clinical Outcome	
					Allele 1	Allele 2	6MWT (meters)	FVC (%)
Treated	1	69	M	8	c.-32-13T>G	c.3G>A	467	61
	2	68	F	5	c.-32-13T>G	c.1629C>G	275	116
	3	72	F	4	c.-32-13T>G	c.2481+102_2646+31del	264	56
	4	50	M	9	c.-32-13T>G	c.-32-13T>G	140	34
	5	57	M	2	c.-32-13T>G	c.546+1G>T	461	49
	6	65	M	8	c.-32-13T>G	c.2481+102_2646+31del	95	36
	7	58	F	9	c.-32-13T>G	c.2041-1G>A	N/A*	14
	8	54	M	8	c.-32-13T>G	c.1888+1G>A	300	33
	9	34	F	6	c.1655T>C	c.1688A>T	452	76
	10	80	M	7	c.-32-13T>G	c.1927G>A	220	44
	11	57	M	9	c.-32-13T>G	c.525del	210	31
	12	45	M	5	c.-32-13T>G	c.655G>A	301	13
	13	30	F	7	c.-32-13T>G	c.525del	520	50
	14	69	F	9	c.-32-13T>G	c.118C>T	200	51
	15	54	F	8	c.-32-13T>G	c.1717A>C	229	39
	16	61	F	7	c.-32-13T>G	c.693-1G>C	392	52
	17	49	F	2	c.-32-13T>G	c.1548G>A	314	54
	18	66	M	9	c.-32-13T>G	c.1047del	290	45
	19	57	M	8	c.-32-13T>G	c.1819_1836del	273	77
	20	63	F	9	c.1748 C>T	c.2014C>T	10	57
	21	49	F	8	c.-32-13T>G	c.1819_1836del	N/A*	59
	22	46	F	3	c.-32-13T>G	c.1819_1836del	73	68

	23	77	M	2	c.-32-13T>G	c.925G>A	120	40
	24	48	F	9	c.-32-13T>G	c.2481+102_2646+31del	180	67
	25	67	M	4	c.-32-13C>G	c.-32-3C>G	172	49
	26	65	F	5	c.-32-13T>G	c.1548G>A	N/A*	57
	27	71	M	0.3	c.-32-13T>G	c. 2608C>T	348	53
	28	49	F	6	c.-32-13T>G	c.799-803delinsA	251	109
Untreated	29	50	F	N/A	c.-32-13T>G	c.2481+102_2646+31del	354	116
	30	37	M	N/A	N/A	N/A	487	80
	31	45	F	N/A	c.-32-13T>G	c.1636+1G>C	457	99
	32	45	F	N/A	c.-32-13T>G	c.1888+1G>A	533	77
	33	79	F	N/A	c.-32-13T>G	c.1560C>G	312	113
	34	46	M	N/A	c.-32-13T>G	c.1888+1G>A	383	73
	35	26	M	N/A	c.-32-13T>G	c.655G>A	645	101
	36	69	F	N/A	c.-32-13T>G	c.854C>G	252	87
	37	62	F	N/A	c.-32-13T>G	c.2481+102_2646+31del	475	94
	38	75	M	N/A	c.-32-13T>G	c.1560C>G	246	N/A

N/A, not available; *, unable to perform the test

Supplementary Table S1. Characteristics of the study cohorts of treated and untreated LOPD subjects. *Patients ID, age of patients, sex, years of ERT, mutations (the nucleotide numbering reflects cDNA numbering with +1 corresponding to the A of the ATG initiation codon in RefSeq NM_000152.3; the amino acid numbering is according to NP 000143.2) and clinical outcome (6MWT and FVC) at the latest follow up visit.*

Supplementary figures

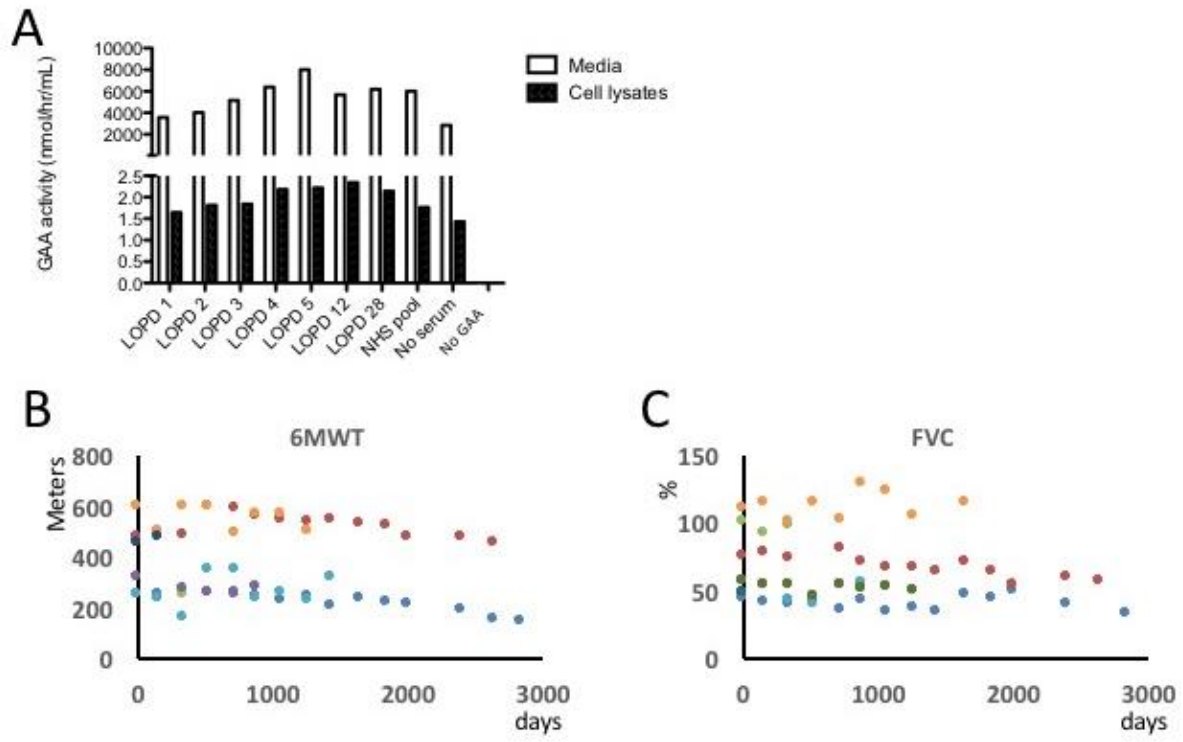

Supplementary Figure S1. Anti-GAA neutralizing antibody assay and follow up of 6MWT and FVC in LOPD subjects with high anti-GAA IgG4 titers. *(A) GAA uptake inhibition assay, GAA activity levels are shown in medium and cell lysates following incubation of Pompe fibroblasts with GAA and LOPD sera positive for anti-GAA IgG4 (LOPD1, 2, 3, 4, 5, 12, and 28), pooled healthy donor serum samples (NHS pool), medium only (No serum). Cells incubated with medium without GAA (No GAA) were used as negative/background control. Shown is the results of one of three replicate experiments. (B) 6MWT follow up in LOPD1, 2, 3, 4, 5, 12, and 28. (C) FVC follow up in LOPD1, 2, 3, 4, 5, 12, and 28.*

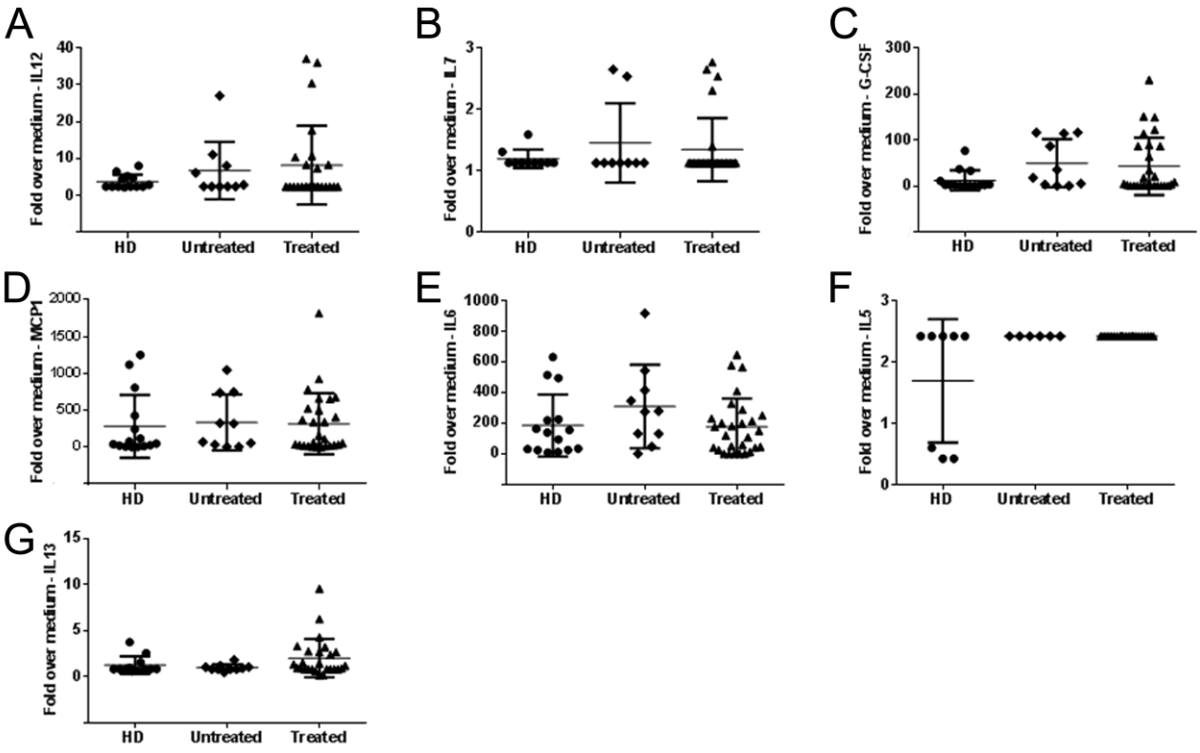

Supplementary Figure S2. Luminex assay for cytokine and chemokine production in supernatant of PBMCs restimulated with rhGAA. *(A-G) Shown are levels of IL12, IL7, G-CSF, MCP1, IL6, IL5, and IL13. The Mann-Whitney test was used to compare data analysis across study groups.*

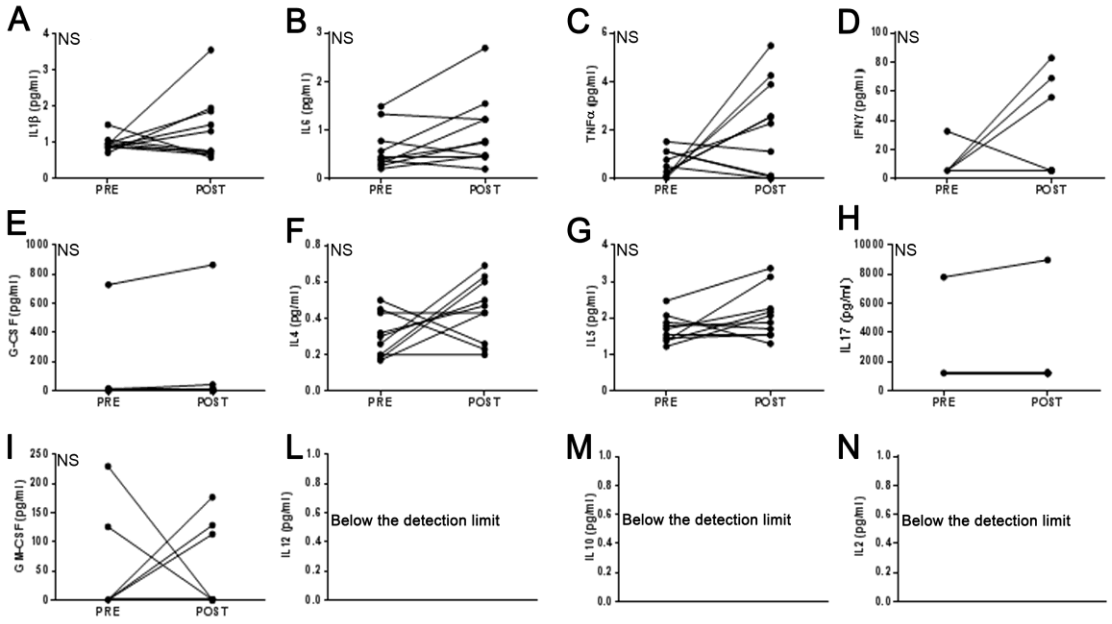

Supplementary Figure S3. Serum cytokine and chemokine profile of LOPD subjects receiving ERT. *(A-N) Measurement of cytokines and chemokines in serum samples collected from each subject before (PRE) and at the end (POST) of rhGAA infusion. Paired t-test was used to compare data analysis PRE vs. POST infusion (NS, not significant).*

7. Materials and methods

7.1 Human samples

LOPD subjects included in this study were part of the French registry of adult Pompe disease patients. Approvals from the competent health authorities and the local Ethical Committee of the Pitie-Salpetriere Hospital, Paris, were obtained prior to the initiation of the study (CNIL N/Ref MMS/CWR/AR155497; CCTIRS N: 14.520; CCP approval 25/06/2014). Informed consent was given by each participant prior to inclusion in the study. All the experiments were carried out in accordance with the relevant guidelines for clinical investigation in France and Europe. Study inclusion criteria were diagnosis of PD defined as deficiency of GAA enzyme activity measured in blood or skin fibroblasts. PD diagnosis was confirmed by *GAA* gene sequencing. Exclusion criteria were age older than 80 years, ongoing or recent (less than 3 months) immunosuppressive treatment, malignancy not in remission, immunodeficiency, or autoimmunity. Blood samples were collected via venipuncture in heparin tubes and used to isolate serum and PBMCs.

Medical history was collected at the time of study inclusion, which included measurements of disease progression such as 6MWT and FVC [24], [225], for which data were collected through validated testing across all clinical centers participating to the study. Historical measurements of anti-rhGAA antibodies were also collected. Samples from 28 LOPD subjects receiving biweekly infusion with rhGAA at 20 mg/kg (Treated LOPD) were collected. Treated LOPD (average age 58.2 years, standard deviation 2.4 years; median 57.5 years) were on ERT for 6.5 years on average (standard deviation 2.4; median 7), 13 males and 15 females participated to the study. Additional samples from 10 LOPD subjects (4 males and 6 females) who were not on ERT (Untreated LOPD, average age 53.4 years, standard deviation 17.2 years; median 48 years) were also collected, together with 43 healthy donors (HD). Almost all the LOPD subjects carried the mutation c.32-13T>G in at least one allele. Details of the LOPD subjects enrolled in this study are given in Supplementary Table S1. De-identified HD blood samples (n=43) were collected through the French blood bank (Etablissement Française du Sang, EFS). De-identified PD patient fibroblasts lacking GAA activity were obtained from the Coriell Institute repository (Camden, NJ, USA) and used in the rhGAA uptake assay.

7.2 Antibody assays

Antibody titers over time in treated subjects were determined as previously described [24]. To study the IgG subclasses specific to GAA, 96-well Nunc Polysorp Immunoplate microplates (Dutscher, Paris, France) were coated with rhGAA to a final concentration of 1 µg/ml. A standard curve made of purified human IgG (Gamunex, Grifolds, Meyreuil, France), purified human IgG1 (Life Technologies, Saint Aubin, France), IgG2, IgG3, IgG4, IgE (Abcam, Paris, France), or IgM (Sigma-Aldrich, Lyon, France) was added directly to the plates. Plates were coated overnight at 4°C. The next day, after blocking the plates, serum samples were added at dilutions of 1:10 and 1:20 in duplicate and incubated overnight at 4°C. Monoclonal anti-human Ig biotin-conjugated antibodies specific for each subclass (all from Sigma-Aldrich, Lyon, France) were added to the plates. Binding of the secondary antibodies was detected with alkaline phosphatase-conjugated streptavidin (Sigma-Aldrich, Lyon, France). The enzymatic reaction was developed with p-nitrophenyl phosphate (Sigma-Aldrich, Lyon, France) substrate and color development was read at 405 nm using a microplate reader (MRX Relevation, DYNEX Technologies, Denkendorf, Germany). Anti-rhGAA antibody concentration was determined against the Ig subclass-specific standard curve using 4-parameters regression.

To evaluate the neutralizing activity of serum anti-rhGAA antibodies, a GAA activity assay was established as previously described [165], [226].

7.3 Short-term T cell restimulation with dendritic cell (DC) induction and cell selection

PBMCs were restimulated *in vitro* according to a protocol designed to enhance detection of antigen-specific T cell responses [187]. PBMCs from the three cohorts studied were stimulated with rhGAA to a final concentration of 10µg/ml, or medium without antigen. Cells recovered after the short-term restimulation protocols were used to perform antigen-specific T cell assays.

$CD25^+$ T cell depletion was performed prior to restimulation of PBMC with antigen using magnetic beads conjugated with anti-CD25 antibodies (Miltenyi Biotec, Bergisch Gladbach, Germany). Flow cytometry was used to assess the efficacy of depletion. PBMC depleted of $CD19^+CD24^{hi}CD38^{hi}$ B cells were obtained by staining cells with anti-CD19, CD24, and CD38 antibodies (all BD Biosciences, Le Pont de Claix, France) following by sorting on a FACSAria (BD Biosciences).

7.4 Antigen-specific T cell assays

The IFNγ ELISpot assay was performed as previously described [227]. rhGAA was used at a concentration of 10 µg/ml, medium only served as negative control, and a mix of 0.05 µg/ml of phorbol 12-myristate 13-acetate (PMA, Sigma-Aldrich, Lyon, France) and 1 µg/ml of ionomycin (Sigma-Aldrich, Lyon, France) was used as positive control. All antigens and controls were tested in triplicate.

Intracellular cytokine staining (ICS) was performed by incubating PBMCs from treated LOPD with rhGAA protein (10µg/ml). Brefeldin A (Sigma-Aldrich, Lyon, France) and monensin (GolgiStop, BD Biosciences, Le Pont de Claix, France) were added to the cultures at a concentration of 1 µg/ml and 2 µM, respectively. A mix of PMA (0.05 µg/ml) and ionomycin (1 µg/ml) was used as positive control in the ICS assay. At a 4-hour incubation with the antigen, cells were harvested and a mix of fluorescently-labeled antibodies specific for the surface markers CD4 (PerCP-Cy5.5, 1:100, eBioscience, Paris, France), and CD8 (Alexa Fluor-700, 1:100, eBioscience, Paris, France), was added to the cells. An amine-reactive aqua dye (Life Technologies, Saint Aubin, France) was used as viability stain. Cells were then fixed and permeabilized with Cytofix/Cytoperm (BD Biosciences Le Pont de Claix, France) and intracellular staining was performed using antibodies against IL2 (PE-Cy7, 1:100 dilution, eBiosciences, Paris, France), IL17 (BV785, 1:20 dilution, BD Biosciences, Paris, France), IFNγ (PE, 1:100 dilution, eBiosciences, Paris, France), TNFα (APC, 1:100 dilution, BD Biosciences, Le Pont de Claix, France). Cells were acquired on a BD LSRFortessa flow cytometer (BD Biosciences, Le Pont de Claix, France). Data analysis was performed using Flowjo software version 10 (Tree star, Ashland, OR, United States).

7.5 Cytokine and chemokine quantitation

Supernatants from PBMC restimulation *in vitro* and serum samples from LOPD subjects were used for the detection of cytokines and chemokines using a multiplexed bead immunoassay based on the Luminex technology. The levels of 17 cytokines (IL1β, IL2, IL4, IL5, IL6, IL7, IL8, IL10, IL12, IL13, IL17, G-CSF, GM-CSF, IFNγ, MCP1, MIP1β, and TNFα) were measured with the Bio-Plex Pro human cytokine 17-plex immunoassay (BioRad, Marnes-la-Coquette, France) following the manufacturer's instructions. A Bioplex 200 system (BioRad) was used to analyze the samples.

7.6 Statistical analysis

All data are shown as mean value +/- standard deviation. Data analysis was performed as indicated in figure legends using GraphPad Prism version 6 (GraphPad Software Inc., La Jolla, CA, USA). P values lower than 0.05 were considered significant.

Hierarchical clustering of the levels of cytokines and chemokines in HD and PD patients was performed with the StatistiXL software (Digital River, UK) using the Pearson correlation coefficient.

Data deriving from the immune assays (anti-rhGAA IgG levels, cytokine profiles, IFNγ ELISpot assay) and the latest measurements of clinical endpoints were used to calculate the correlation matrix using the Spearman coefficient with the free R software (Version 2.15.2, 32) and the Psych package (Version 1.5.8, Procedures for Personality and Psychological Research, Northwestern University, Evanston, Illinois, USA, http://CRAN.R-roject.org/package=psych). In both correlation matrices the correlation coefficient r was transformed to t using the formula $t=r\times [\sqrt{(n-2)}/\sqrt{(1-r2)}]$ for statistical testing and the p value adjusted for multiple comparisons using the false discovery rate method.

Only LOPD with a minimum of four years of clinical follow-up for 6MWT and FVC were included in the longitudinal analysis of clinical data. Subjects with a follow-up of <4 years or who started and then discontinued ERT were excluded from the analysis (FVC, n=21; 6MWT, n=19). A linear mixed model was used to take into account the within-patient correlation and the between-patient variability as previously described [228] with the free R software (Version 2.15.2, 32) and the nlme package (Version 3.1-125, Linear and Nonlinear Mixed Effects Models, https://cran.r-project.org/web/packages/nlme/index.html).

Conclusions

Results presented here investigated the limitations of the enzyme replacement therapy in Pompe disease patients by studying immunological reaction in LOPD subjects and described a new promising approach to treat the disease by AAV-based gene therapy targeting the liver. The investigation of the immune response in LOPD patients undergoing ERT for a long time allowed us to investigate the immunological consequences of long-term exposure to rhGAA. In particular, we established that sustained exposure to the rhGAA antigen results in a decrease of antibody titer via mechanism(s) that resemble tolerance induction. In the case of LOPD patients, immune response to the therapeutic enzyme do not seem prevent efficacy of ERT a. However, the immunogenicity of rhGAA still remains a major concern and limitation in terms of both safety and efficacy of ERT in infantile Pompe patients, who are at high risk of developing neutralizing antibody responses to the infused rhGAA protein. This is a major issue in Pompe disease and an unmet medical need, particularly for CRIM-negative patients. Here we also proposed a novel approach based on an engineered secretable GAA transgene expressed in the liver, which mediates cross-correction body-wide. One advantage of our gene therapy approach is to reduce immunogenicity of the GAA protein by exploiting the tolerogenic properties of the liver, further enhanced in the context of secretable proteins. This represents a very promising step to overcome the potentially harmful immune responses both in LOPD and IOPD patients and may lead to an improved therapeutic efficacy. The exact mechanisms underlying the lower immunogenicity of the secretable GAA transgenes we developed are currently object of further investigations in the lab.

To this end we hope to translate into the clinic this gene therapy approach in order to treat both the most severe (IOPD) and the milder (LOPD) forms of the pathology. As first target of patient population we may ideally choose to treat LOPD since being CRIM-positive, the risk that they develop immune reactions to GAA is minimal and the liver is not in active proliferative phase. Thus, in LOPD patients we expect long-term expression of the GAA transgene derived from the liver. One of the challenges to address moving forward to treat infantile subjects is that the liver proliferates rapidly during the first years of life and, due to the episomal nature of the AAV genome, the transgene expression could be in part lost. In some cases, therefore re-administration of the AAV vector would be needed to restore the protein expression in hepatocytes, however generation of neutralizing antibodies against the

capsid would hamper liver transduction. This phenomenon is currently being intensively studied in our laboratory, and a clinical trial of liver gene therapy with AAV vectors in pediatric subjects, promoted by our team and expected to start later this year, will in part address this point.

Nevertheless, recently studies carried out in our team, demonstrated that the co-administration of an AAV vector together with immunomodulatory nanoparticles ablated the formation of neutralizing antibodies and allowed a second administration of the vector with consequent stable transgene expression. This technology is currently being tested in humans and will be also tested in AAV gene transfer trials in the near future.

The design of a future clinical trial must take into account concerns and challenges emerged in the past gene therapy trials. As already mentioned, in the recent and successful Hemophilia B trial, patients have been treated with corticosteroids in order to alleviate the cell-mediated response to hepatocytes expressing FIX. Moreover, during the trial it has been demonstrated that this response depends on the dose of vector injected.

Thus, in order to reduce hepatotoxicity due to the high dose of vector, a novel generation of AAV with enhanced transduction potency is needed. Recently, a large number of novel AAV serotypes have been isolated and described to target human hepatocytes more efficiently than those already used in the clinic. In our study, we tested some of these serotypes, confirming their higher efficiency in human hepatocytes transduction compared with AAV8 vectors, the gold standard of liver gene transfer. Thus, identifying novel AAV capsid able to deliver therapeutic levels of expression at lower doses is a major goal in liver gene transfer and the direction towards which the field is moving. This because this maneuver can help escaping potentially detrimental immune responses to the capsid, thus resulting in long lasting transgene expression. Additionally, it may help achieving full therapeutic efficacy in diseases requiring high and widespread liver gene transfer, for example primary hyperoxaluria and glycogen storage disease type I.

Taken together, these findings will be instrumental for the design of a future clinical trial aimed at the safe and efficacious treatment of patients affected by Pompe disease.

[1] J.-A. Lim, L. Li, and N. Raben, "Pompe disease: from pathophysiology to therapy and back again.," *Front. Aging Neurosci.*, vol. 6, no. July, p. 177, 2014.

[2] H. a Wisselaar, M. a Kroos, M. M. Hermans, J. van Beeumen, and a J. Reuser, "Structural and functional changes of lysosomal acid alpha-glucosidase during intracellular transport and maturation.," *J. Biol. Chem.*, vol. 268, no. 3, pp. 2223–2231, 1993.

[3] S. Kornfeld, "Structure and function of the mannose 6-phosphate/insulinlike growth factor II receptors.," *Annu. Rev. Biochem.*, vol. 61, pp. 307–30, Jan. 1992.

[4] M. M. Hermans, H. A. Wisselaar, M. A. Kroos, B. A. Oostra, and A. J. Reuser, "Human lysosomal alpha-glucosidase: functional characterization of the glycosylation sites.," *Biochem. J.*, vol. 289 (Pt 3, pp. 681–6, Feb. 1993.

[5] R. J. Moreland *et al.*, "Lysosomal acid ??-glucosidase consists of four different peptides processed from a single chain precursor," *J. Biol. Chem.*, vol. 280, no. 8, pp. 6780–6791, Feb. 2005.

[6] A. T. van der Ploeg and A. J. Reuser, "Pompe's disease," *Lancet*, vol. 372, no. 9646, pp. 1342–1353, 2008.

[7] D. Güngör and A. J. J. Reuser, "How to describe the clinical spectrum in Pompe disease?," *Am. J. Med. Genet. Part A*, vol. 161, no. 2, pp. 399–400, 2013.

[8] B. L. Thurberg *et al.*, "Characterization of pre- and post-treatment pathology after enzyme replacement therapy for Pompe disease.," *Lab. Invest.*, vol. 86, no. 12, pp. 1208–20, Dec. 2006.

[9] J. L. Van Hove, H. W. Yang, J. Y. Wu, R. O. Brady, and Y. T. Chen, "High-level production of recombinant human lysosomal acid alpha-glucosidase in Chinese hamster ovary cells which targets to heart muscle and corrects glycogen accumulation in fibroblasts from patients with Pompe disease.," *Proc. Natl. Acad. Sci.*, vol. 93, no. 1, pp. 65–70, 1996.

[10] R. Lüllmann-Rauch, "Lysosomal glycogen storage mimicking the cytological picture of Pompe's disease as induced in rats by injection of an alpha-glucosidase inhibitor. I.

Alterations in liver.," *Virchows Arch. B. Cell Pathol. Incl. Mol. Pathol.*, vol. 38, no. 1, pp. 89–100, Jan. 1981.

[11] R. Lüllmann-Rauch, "Lysosomal glycogen storage mimicking the cytological picture of Pompe's disease as induced in rats by injection of an alpha-glycosidase inhibitor. II. Alterations in kidney, adrenal gland, spleen and soleus muscle.," *Virchows Arch. B. Cell Pathol. Incl. Mol. Pathol.*, vol. 39, no. 2, pp. 187–202, Jan. 1982.

[12] H. C. Walvoort, R. G. Slee, and J. F. Koster, "Canine glycogen storage disease type II. A biochemical study of an acid alpha-glucosidase-deficient Lapland dog.," *Biochim. Biophys. Acta*, vol. 715, no. 1, pp. 63–9, Mar. 1982.

[13] E. H. Seppälä, A. J. J. Reuser, and H. Lohi, "A Nonsense Mutation in the Acid α-Glucosidase Gene Causes Pompe Disease in Finnish and Swedish Lapphunds," *PLoS One*, vol. 8, no. 2, 2013.

[14] T. Matsui, S. Kuroda, M. Mizutani, Y. Kiuchi, K. Suzuki, and T. Ono, "Generalized glycogen storage disease in Japanese quail (Coturnix coturnix japonica).," *Vet. Pathol.*, vol. 20, no. 3, pp. 312–21, May 1983.

[15] H. W. Yang, T. Kikuchi, Y. Hagiwara, M. Mizutani, Y. T. Chen, and J. L. Van Hove, "Recombinant human acid alpha-glucosidase corrects acid alpha-glucosidase-deficient human fibroblasts, quail fibroblasts, and quail myoblasts.," *Pediatr. Res.*, vol. 43, no. 3, pp. 374–80, Mar. 1998.

[16] S. Tsujino *et al.*, "Adenovirus-mediated transfer of human acid maltase gene reduces glycogen accumulation in skeletal muscle of Japanese quail with acid maltase deficiency.," *Hum. Gene Ther.*, vol. 9, no. 11, pp. 1609–16, Jul. 1998.

[17] C.-Y. Lin, C.-H. Ho, Y.-H. Hsieh, and T. Kikuchi, "Adeno-associated virus-mediated transfer of human acid maltase gene results in a transient reduction of glycogen accumulation in muscle of Japanese quail with acid maltase deficiency.," *Gene Ther.*, vol. 9, no. 9, pp. 554–63, May 2002.

[18] A. J. McVie-Wylie *et al.*, "Multiple muscles in the AMD quail can be 'cross-corrected' of pathologic glycogen accumulation after intravenous injection of an [E1-,

polymerase-] adenovirus vector encoding human acid-alpha-glucosidase.," *J. Gene Med.*, vol. 5, no. 5, pp. 399–406, May 2003.

[19] N. Raben *et al.*, "Targeted disruption of the acid alpha-glucosidase gene in mice causes an illness with critical features of both infantile and adult human glycogen storage disease type II.," *J. Biol. Chem.*, vol. 273, no. 30, pp. 19086–19092, 1998.

[20] R. L. Sidman *et al.*, "Temporal neuropathologic and behavioral phenotype of 6neo/6neo Pompe disease mice.," *J. Neuropathol. Exp. Neurol.*, vol. 67, no. 8, pp. 803–18, Aug. 2008.

[21] B. Sun *et al.*, "Immunomodulatory gene therapy prevents antibody formation and lethal hypersensitivity reactions in murine pompe disease.," *Mol. Ther.*, vol. 18, no. 2, pp. 353–60, Feb. 2010.

[22] P. S. Kishnani *et al.*, "Recombinant human acid [alpha]-glucosidase: major clinical benefits in infantile-onset Pompe disease.," *Neurology*, vol. 68, no. 2, pp. 99–109, Jan. 2007.

[23] B. Schoser *et al.*, "Survival and long-term outcomes in late-onset Pompe disease following alglucosidase alfa treatment: a systematic review and meta-analysis.," *J. Neurol.*, Jul. 2016.

[24] A. T. van der Ploeg *et al.*, "A randomized study of alglucosidase alfa in late-onset Pompe's disease.," *N. Engl. J. Med.*, vol. 362, no. 15, pp. 1396–406, Apr. 2010.

[25] S. N. Prater *et al.*, "The emerging phenotype of long-term survivors with infantile Pompe disease.," *Genet. Med.*, vol. 14, no. 9, pp. 800–10, Sep. 2012.

[26] A. Chakrapani, A. Vellodi, P. Robinson, S. Jones, and J. E. Wraith, "Treatment of infantile Pompe disease with alglucosidase alpha: the UK experience.," *J. Inherit. Metab. Dis.*, vol. 33, no. 6, pp. 747–50, Dec. 2010.

[27] S. N. Prater *et al.*, "Skeletal muscle pathology of infantile Pompe disease during long-term enzyme replacement therapy.," *Orphanet J. Rare Dis.*, vol. 8, p. 90, Jun. 2013.

[28] D. Güngör *et al.*, "Quality of life and participation in daily life of adults with Pompe

disease receiving enzyme replacement therapy: 10 years of international follow-up," *J. Inherit. Metab. Dis.*, vol. 39, no. 2, pp. 253–260, 2016.

[29] K. M. Stepien, C. J. Hendriksz, M. Roberts, and R. Sharma, "Observational clinical study of 22 adult-onset Pompe disease patients undergoing enzyme replacement therapy over 5years.," *Mol. Genet. Metab.*, vol. 117, no. 4, pp. 413–8, Apr. 2016.

[30] N. Sayeed, P. Sharma, M. Abdelhalim, and R. Mukherjee, "Effect of enzyme replacement therapy (ERT) added to Home Mechanical Ventilation (HMV) in Adult Pompe disease.," *Respirol. case reports*, vol. 3, no. 4, pp. 159–61, Dec. 2015.

[31] T. A. Kanters, I. Hoogenboom-Plug, M. P. M. H. Rutten-Van Mölken, W. K. Redekop, A. T. van der Ploeg, and L. Hakkaart, "Cost-effectiveness of enzyme replacement therapy with alglucosidase alfa in classic-infantile patients with Pompe disease.," *Orphanet J. Rare Dis.*, vol. 9, p. 75, May 2014.

[32] P. S. Kishnani and A. A. Beckemeyer, "New therapeutic approaches for Pompe disease: enzyme replacement therapy and beyond.," *Pediatr. Endocrinol. Rev.*, vol. 12 Suppl 1, pp. 114–24, Sep. 2014.

[33] T. Fukuda *et al.*, "Autophagy and mistargeting of therapeutic enzyme in skeletal muscle in Pompe disease.," *Mol. Ther.*, vol. 14, no. 6, pp. 831–9, Dec. 2006.

[34] B. J. Ebbink *et al.*, "Cognitive decline in classic infantile Pompe disease: An underacknowledged challenge.," *Neurology*, vol. 86, no. 13, pp. 1260–1, Mar. 2016.

[35] P. S. Kishnani *et al.*, "Cross-reactive immunologic material status affects treatment outcomes in Pompe disease infants.," *Mol. Genet. Metab.*, vol. 99, no. 1, pp. 26–33, Jan. 2010.

[36] J. M. de Vries *et al.*, "High antibody titer in an adult with Pompe disease affects treatment with alglucosidase alfa.," *Mol. Genet. Metab.*, vol. 101, no. 4, pp. 338–45, Dec. 2010.

[37] M. Kroos *et al.*, "Update of the Pompe disease mutation database with 107 sequence variants and a format for severity rating.," *Hum. Mutat.*, vol. 29, no. 6, pp. E13-26, Jun. 2008.

[38] S. Nayak, R. Sivakumar, O. Cao, H. Daniell, B. J. Byrne, and R. W. Herzog, "Mapping the T helper cell response to acid α-glucosidase in Pompe mice," *Mol. Genet. Metab.*, vol. 106, no. 2, pp. 189–195, 2012.

[39] P. A. Doerfler, S. Nayak, M. Corti, L. Morel, R. W. Herzog, and B. J. Byrne, "Targeted approaches to induce immune tolerance for Pompe disease therapy.," *Mol. Ther. Methods Clin. Dev.*, vol. 3, no. August 2015, p. 15053, 2016.

[40] C. M. van Gelder, M. Hoogeveen-Westerveld, M. A. Kroos, I. Plug, A. T. van der Ploeg, and A. J. J. Reuser, "Enzyme therapy and immune response in relation to CRIM status: the Dutch experience in classic infantile Pompe disease," *J. Inherit. Metab. Dis.*, pp. 305–314, 2014.

[41] A. H. El-Gharbawy *et al.*, "An individually, modified approach to desensitize infants and young children with Pompe disease, and significant reactions to alglucosidase alfa infusions.," *Mol. Genet. Metab.*, vol. 104, no. 1–2, pp. 118–22, Jan. .

[42] M. Banati, Z. Hosszu, A. Trauninger, L. Szereday, and Z. Illes, "Enzyme replacement therapy induces T-cell responses in late-onset Pompe disease.," *Muscle Nerve*, vol. 44, no. 5, pp. 720–6, Nov. 2011.

[43] J. Wang *et al.*, "Neutralizing antibodies to therapeutic enzymes: considerations for testing, prevention and treatment.," *Nat. Biotechnol.*, vol. 26, no. 8, pp. 901–8, Aug. 2008.

[44] M. S. Joly *et al.*, "Transient low-dose methotrexate generates B regulatory cells that mediate antigen-specific tolerance to alglucosidase alfa.," *J. Immunol.*, vol. 193, no. 8, pp. 3947–58, Oct. 2014.

[45] N. J. Mendelsohn, Y. H. Messinger, A. S. Rosenberg, and P. S. Kishnani, "Elimination of antibodies to recombinant enzyme in Pompe's disease.," *N. Engl. J. Med.*, vol. 360, no. 2, pp. 194–5, Jan. 2009.

[46] P. A. Doerfler, S. Nayak, R. W. Herzog, L. Morel, and B. J. Byrne, "BAFF blockade prevents anti-drug antibody formation in a mouse model of Pompe disease," *Clin. Immunol.*, vol. 158, no. 2, pp. 140–147, 2015.

[47] F. B. Vincent, D. Saulep-Easton, W. A. Figgett, K. A. Fairfax, and F. Mackay, "The BAFF/APRIL system: emerging functions beyond B cell biology and autoimmunity.," *Cytokine Growth Factor Rev.*, vol. 24, no. 3, pp. 203–15, Jun. 2013.

[48] J. J. Limon and D. A. Fruman, "Akt and mTOR in B Cell Activation and Differentiation.," *Front. Immunol.*, vol. 3, p. 228, Jan. 2012.

[49] M. E. Elder *et al.*, "B-Cell depletion and immunomodulation before initiation of enzyme replacement therapy blocks the immune response to acid alpha-glucosidase in infantile-onset Pompe disease.," *J. Pediatr.*, vol. 163, no. 3, p. 847–54.e1, Sep. 2013.

[50] T. Ohashi *et al.*, "Administration of anti-CD3 antibodies modulates the immune response to an infusion of α-glucosidase in mice.," *Mol. Ther.*, vol. 20, no. 10, pp. 1924–31, Oct. 2012.

[51] B. Sun *et al.*, "Non-depleting anti-CD4 monoclonal antibody induces immune tolerance to ERT in a murine model of Pompe disease.," *Mol. Genet. Metab. reports*, vol. 1, pp. 446–450, Jan. 2014.

[52] D. M. Markusic *et al.*, "Effective gene therapy for haemophilic mice with pathogenic factor IX antibodies.," *EMBO Mol. Med.*, vol. 5, no. 11, pp. 1698–709, Nov. 2013.

[53] X. Wang *et al.*, "Mechanism of oral tolerance induction to therapeutic proteins.," *Adv. Drug Deliv. Rev.*, vol. 65, no. 6, pp. 759–73, Jun. 2013.

[54] J. Su, A. Sherman, P. A. Doerfler, B. J. Byrne, R. W. Herzog, and H. Daniell, "Oral delivery of Acid Alpha Glucosidase epitopes expressed in plant chloroplasts suppresses antibody formation in treatment of Pompe mice.," *Plant Biotechnol. J.*, vol. 13, no. 8, pp. 1023–32, Oct. 2015.

[55] M. Cremel, N. Guérin, F. Horand, A. Banz, and Y. Godfrin, "Red blood cells as innovative antigen carrier to induce specific immune tolerance.," *Int. J. Pharm.*, vol. 443, no. 1–2, pp. 39–49, Feb. 2013.

[56] M. Cremel *et al.*, "Innovative approach in Pompe disease therapy: Induction of immune tolerance by antigen-encapsulated red blood cells," *Int. J. Pharm.*, vol. 491, no. 1–2, pp. 69–77, 2015.

[57] B. Balakrishnan and G. R. Jayandharan, "Basic biology of adeno-associated virus (AAV) vectors used in gene therapy.," *Curr. Gene Ther.*, vol. 14, no. 2, pp. 86–100, Jan. 2014.

[58] R. Calcedo *et al.*, "Adeno-associated virus antibody profiles in newborns, children, and adolescents.," *Clin. Vaccine Immunol.*, vol. 18, no. 9, pp. 1586–8, Sep. 2011.

[59] K. Erles, P. Sebökovà, and J. R. Schlehofer, "Update on the prevalence of serum antibodies (IgG and IgM) to adeno-associated virus (AAV).," *J. Med. Virol.*, vol. 59, no. 3, pp. 406–11, Nov. 1999.

[60] C. Li *et al.*, "Neutralizing antibodies against adeno-associated virus examined prospectively in pediatric patients with hemophilia.," *Gene Ther.*, vol. 19, no. 3, pp. 288–94, Mar. 2012.

[61] J. F. Wright, "Manufacturing and characterizing AAV-based vectors for use in clinical studies.," *Gene Ther.*, vol. 15, no. 11, pp. 840–8, Jun. 2008.

[62] J. C. Grieger and R. J. Samulski, "Adeno-associated virus vectorology, manufacturing, and clinical applications.," *Methods Enzymol.*, vol. 507, pp. 229–54, Jan. 2012.

[63] T. Matsushita *et al.*, "Adeno-associated virus vectors can be efficiently produced without helper virus.," *Gene Ther.*, vol. 5, no. 7, pp. 938–45, Jul. 1998.

[64] G. P. Gao *et al.*, "High-titer adeno-associated viral vectors from a Rep/Cap cell line and hybrid shuttle virus.," *Hum. Gene Ther.*, vol. 9, no. 16, pp. 2353–62, Nov. 1998.

[65] M. Marek, M. M. van Oers, F. F. Devaraj, J. M. Vlak, and O.-W. Merten, "Engineering of baculovirus vectors for the manufacture of virion-free biopharmaceuticals.," *Biotechnol. Bioeng.*, vol. 108, no. 5, pp. 1056–67, May 2011.

[66] B. R. Schultz and J. S. Chamberlain, "Recombinant adeno-associated virus transduction and integration.," *Mol. Ther.*, vol. 16, no. 7, pp. 1189–99, Jul. 2008.

[67] P. N. Valdmanis, L. Lisowski, and M. A. Kay, "rAAV-mediated tumorigenesis: still unresolved after an AAV assault.," *Mol. Ther.*, vol. 20, no. 11, pp. 2014–7, Nov. 2012.

[68] H. Li *et al.*, "Assessing the potential for AAV vector genotoxicity in a murine model.,"

Blood, vol. 117, no. 12, pp. 3311–9, Mar. 2011.

[69] G. Gao, L. H. Vandenberghe, and J. M. Wilson, "New recombinant serotypes of AAV vectors.," *Curr. Gene Ther.*, vol. 5, no. 3, pp. 285–97, Jun. 2005.

[70] J. E. Rabinowitz *et al.*, "Cross-packaging of a single adeno-associated virus (AAV) type 2 vector genome into multiple AAV serotypes enables transduction with broad specificity.," *J. Virol.*, vol. 76, no. 2, pp. 791–801, Jan. 2002.

[71] A. Asokan, D. V Schaffer, and R. J. Samulski, "The AAV vector toolkit: poised at the clinical crossroads.," *Mol. Ther.*, vol. 20, no. 4, pp. 699–708, Apr. 2012.

[72] M. A. Kotterman and D. V Schaffer, "Engineering adeno-associated viruses for clinical gene therapy.," *Nat. Rev. Genet.*, vol. 15, no. 7, pp. 445–51, Jul. 2014.

[73] L. Perabo, A. Huber, S. Märsch, M. Hallek, and H. Büning, "Artificial evolution with adeno-associated viral libraries.," *Comb. Chem. High Throughput Screen.*, vol. 11, no. 2, pp. 118–26, Feb. 2008.

[74] D. Grimm, K. Pandey, H. Nakai, T. A. Storm, and M. A. Kay, "Liver transduction with recombinant adeno-associated virus is primarily restricted by capsid serotype not vector genotype.," *J. Virol.*, vol. 80, no. 1, pp. 426–39, Jan. 2006.

[75] D. M. McCarty, "Self-complementary AAV Vectors; Advances and Applications," *Mol. Ther.*, vol. 16, no. 10, pp. 1648–1656, 2008.

[76] P. E. Monahan *et al.*, "Proteasome inhibitors enhance gene delivery by AAV virus vectors expressing large genomes in hemophilia mouse and dog models: a strategy for broad clinical application.," *Mol. Ther.*, vol. 18, no. 11, pp. 1907–16, Nov. 2010.

[77] A. Ghosh and D. Duan, "Expanding adeno-associated viral vector capacity: a tale of two vectors.," *Biotechnol. Genet. Eng. Rev.*, vol. 24, pp. 165–77, Jan. 2007.

[78] J. C. Grieger and R. J. Samulski, "Packaging capacity of adeno-associated virus serotypes: impact of larger genomes on infectivity and postentry steps.," *J. Virol.*, vol. 79, no. 15, pp. 9933–44, Aug. 2005.

[79] H. Büning, "Gene therapy enters the pharma market: the short story of a long journey.,"

EMBO Mol. Med., vol. 5, no. 1, pp. 1–3, Jan. 2013.

[80] D. Gaudet *et al.*, "Efficacy and long-term safety of alipogene tiparvovec (AAV1-LPLS447X) gene therapy for lipoprotein lipase deficiency: an open-label trial.," *Gene Ther.*, vol. 20, no. 4, pp. 361–9, Apr. 2013.

[81] E. S. Stroes *et al.*, "Intramuscular administration of AAV1-lipoprotein lipase S447X lowers triglycerides in lipoprotein lipase-deficient patients.," *Arterioscler. Thromb. Vasc. Biol.*, vol. 28, no. 12, pp. 2303–4, Dec. 2008.

[82] D. Gaudet *et al.*, "Review of the clinical development of alipogene tiparvovec gene therapy for lipoprotein lipase deficiency.," *Atheroscler. Suppl.*, vol. 11, no. 1, pp. 55–60, Jun. 2010.

[83] A. C. Nathwani *et al.*, "Adenovirus-associated virus vector-mediated gene transfer in hemophilia B.," *N. Engl. J. Med.*, vol. 365, no. 25, pp. 2357–65, Dec. 2011.

[84] A. M. Maguire *et al.*, "Safety and efficacy of gene transfer for Leber's congenital amaurosis.," *N. Engl. J. Med.*, vol. 358, no. 21, pp. 2240–8, May 2008.

[85] F. Mingozzi and K. A. High, "Therapeutic in vivo gene transfer for genetic disease using AAV: progress and challenges.," *Nat. Rev. Genet.*, vol. 12, no. 5, pp. 341–55, May 2011.

[86] J. Bennett *et al.*, "AAV2 gene therapy readministration in three adults with congenital blindness.," *Sci. Transl. Med.*, vol. 4, no. 120, p. 120ra15, Feb. 2012.

[87] F. Simonelli *et al.*, "Gene therapy for Leber's congenital amaurosis is safe and effective through 1.5 years after vector administration.," *Mol. Ther.*, vol. 18, no. 3, pp. 643–50, Mar. 2010.

[88] A. V Cideciyan *et al.*, "Vision 1 year after gene therapy for Leber's congenital amaurosis.," *N. Engl. J. Med.*, vol. 361, no. 7, pp. 725–7, Aug. 2009.

[89] J. W. B. Bainbridge *et al.*, "Long-term effect of gene therapy on Leber's congenital amaurosis.," *N. Engl. J. Med.*, vol. 372, no. 20, pp. 1887–97, May 2015.

[90] A. C. Nathwani *et al.*, "Long-term safety and efficacy of factor IX gene therapy in

hemophilia B.," *N. Engl. J. Med.*, vol. 371, no. 21, pp. 1994–2004, Nov. 2014.

[91] V. Ferreira *et al.*, "Immune responses to intramuscular administration of alipogene tiparvovec (AAV1-LPL(S447X)) in a phase II clinical trial of lipoprotein lipase deficiency gene therapy.," *Hum. Gene Ther.*, vol. 25, no. 3, pp. 180–8, Mar. 2014.

[92] R. B. Moss *et al.*, "Repeated adeno-associated virus serotype 2 aerosol-mediated cystic fibrosis transmembrane regulator gene transfer to the lungs of patients with cystic fibrosis: a multicenter, double-blind, placebo-controlled trial.," *Chest*, vol. 125, no. 2, pp. 509–21, Feb. 2004.

[93] G. A. Croteau *et al.*, "Evaluation of exposure and health care worker response to nebulized administration of tgAAVCF to patients with cystic fibrosis.," *Ann. Occup. Hyg.*, vol. 48, no. 8, pp. 673–81, Nov. 2004.

[94] M. L. Aitken *et al.*, "A phase I study of aerosolized administration of tgAAVCF to cystic fibrosis subjects with mild lung disease.," *Hum. Gene Ther.*, vol. 12, no. 15, pp. 1907–16, Oct. 2001.

[95] J. A. Wagner *et al.*, "A phase I/II study of tgAAV-CF for the treatment of chronic sinusitis in patients with cystic fibrosis.," *Hum. Gene Ther.*, vol. 9, no. 6, pp. 889–909, Apr. 1998.

[96] J. A. Wagner *et al.*, "Efficient and persistent gene transfer of AAV-CFTR in maxillary sinus.," *Lancet (London, England)*, vol. 351, no. 9117, pp. 1702–3, Jun. 1998.

[97] J. A. Wagner *et al.*, "A phase II, double-blind, randomized, placebo-controlled clinical trial of tgAAVCF using maxillary sinus delivery in patients with cystic fibrosis with antrostomies.," *Hum. Gene Ther.*, vol. 13, no. 11, pp. 1349–59, Jul. 2002.

[98] T. R. Flotte *et al.*, "Phase I trial of intranasal and endobronchial administration of a recombinant adeno-associated virus serotype 2 (rAAV2)-CFTR vector in adult cystic fibrosis patients: a two-part clinical study.," *Hum. Gene Ther.*, vol. 14, no. 11, pp. 1079–88, Jul. 2003.

[99] C. S. Manno *et al.*, "Successful transduction of liver in hemophilia by AAV-Factor IX and limitations imposed by the host immune response.," *Nat. Med.*, vol. 12, no. 3, pp.

342–7, Mar. 2006.

[100] S. Worgall *et al.*, "Treatment of late infantile neuronal ceroid lipofuscinosis by CNS administration of a serotype 2 adeno-associated virus expressing CLN2 cDNA.," *Hum. Gene Ther.*, vol. 19, no. 5, pp. 463–74, May 2008.

[101] S. W. J. McPhee *et al.*, "Immune responses to AAV in a phase I study for Canavan disease.," *J. Gene Med.*, vol. 8, no. 5, pp. 577–88, May 2006.

[102] R. T. Bartus *et al.*, "Bioactivity of AAV2-neurturin gene therapy (CERE-120): differences between Parkinson's disease and nonhuman primate brains.," *Mov. Disord.*, vol. 26, no. 1, pp. 27–36, Jan. 2011.

[103] R. T. Bartus *et al.*, "Properly scaled and targeted AAV2-NRTN (neurturin) to the substantia nigra is safe, effective and causes no weight loss: support for nigral targeting in Parkinson's disease.," *Neurobiol. Dis.*, vol. 44, no. 1, pp. 38–52, Oct. 2011.

[104] C. D. Herzog, K. M. Bishop, L. Brown, A. Wilson, J. H. Kordower, and R. T. Bartus, "Gene transfer provides a practical means for safe, long-term, targeted delivery of biologically active neurotrophic factor proteins for neurodegenerative diseases.," *Drug Deliv. Transl. Res.*, vol. 1, no. 5, pp. 361–82, Oct. 2011.

[105] C. W. Christine *et al.*, "Safety and tolerability of putaminal AADC gene therapy for Parkinson disease.," *Neurology*, vol. 73, no. 20, pp. 1662–9, Nov. 2009.

[106] R. J. Hajjar *et al.*, "Design of a phase 1/2 trial of intracoronary administration of AAV1/SERCA2a in patients with heart failure.," *J. Card. Fail.*, vol. 14, no. 5, pp. 355–67, Jun. 2008.

[107] B. E. Jaski *et al.*, "Calcium upregulation by percutaneous administration of gene therapy in cardiac disease (CUPID Trial), a first-in-human phase 1/2 clinical trial.," *J. Card. Fail.*, vol. 15, no. 3, pp. 171–81, Apr. 2009.

[108] J. R. Mendell *et al.*, "A phase 1/2a follistatin gene therapy trial for becker muscular dystrophy.," *Mol. Ther.*, vol. 23, no. 1, pp. 192–201, Jan. 2015.

[109] B. Wirth, M. Barkats, C. Martinat, M. Sendtner, and T. H. Gillingwater, "Moving

towards treatments for spinal muscular atrophy: hopes and limits.," *Expert Opin. Emerg. Drugs*, vol. 20, no. 3, pp. 353–6, Sep. 2015.

[110] J. R. Mendell *et al.*, "Sustained alpha-sarcoglycan gene expression after gene transfer in limb-girdle muscular dystrophy, type 2D.," *Ann. Neurol.*, vol. 68, no. 5, pp. 629–38, Nov. 2010.

[111] J. R. Mendell *et al.*, "Dystrophin immunity in Duchenne's muscular dystrophy.," *N. Engl. J. Med.*, vol. 363, no. 15, pp. 1429–37, Oct. 2010.

[112] K. Kawecka *et al.*, "Adeno-Associated Virus (AAV) Mediated Dystrophin Gene Transfer Studies and Exon Skipping Strategies for Duchenne Muscular Dystrophy (DMD).," *Curr. Gene Ther.*, vol. 15, no. 4, pp. 395–415, Jan. 2015.

[113] F. Barthélémy, N. Wein, M. Krahn, N. Lévy, and M. Bartoli, "Translational research and therapeutic perspectives in dysferlinopathies.," *Mol. Med.*, vol. 17, no. 9–10, pp. 875–82, Jan. .

[114] T. M. Crombleholme, "Adenoviral-mediated gene transfer in wound healing.," *Wound Repair Regen.*, vol. 8, no. 6, pp. 460–72, Jan. .

[115] B. K. Smith *et al.*, "Phase I/II trial of adeno-associated virus-mediated alpha-glucosidase gene therapy to the diaphragm for chronic respiratory failure in Pompe disease: initial safety and ventilatory outcomes.," *Hum. Gene Ther.*, vol. 24, no. 6, pp. 630–40, 2013.

[116] C. Mueller *et al.*, "Human Treg responses allow sustained recombinant adeno-associated virus-mediated transgene expression.," *J. Clin. Invest.*, vol. 123, no. 12, pp. 5310–8, Dec. 2013.

[117] T. R. Flotte *et al.*, "Phase 2 clinical trial of a recombinant adeno-associated viral vector expressing α1-antitrypsin: interim results.," *Hum. Gene Ther.*, vol. 22, no. 10, pp. 1239–47, Oct. 2011.

[118] A. V Cideciyan *et al.*, "Human RPE65 gene therapy for Leber congenital amaurosis: persistence of early visual improvements and safety at 1 year.," *Hum. Gene Ther.*, vol. 20, no. 9, pp. 999–1004, Sep. 2009.

[119] R. E. MacLaren *et al.*, "Retinal gene therapy in patients with choroideremia: initial findings from a phase 1/2 clinical trial.," *Lancet (London, England)*, vol. 383, no. 9923, pp. 1129–37, Mar. 2014.

[120] P. E. Pecen and P. K. Kaiser, "Current phase 1/2 research for neovascular age-related macular degeneration.," *Curr. Opin. Ophthalmol.*, vol. 26, no. 3, pp. 188–93, May 2015.

[121] P. J. Mease *et al.*, "Local delivery of a recombinant adenoassociated vector containing a tumour necrosis factor alpha antagonist gene in inflammatory arthritis: a phase 1 dose-escalation safety and tolerability study.," *Ann. Rheum. Dis.*, vol. 68, no. 8, pp. 1247–54, Aug. 2009.

[122] P. J. Mease *et al.*, "Safety, tolerability, and clinical outcomes after intraarticular injection of a recombinant adeno-associated vector containing a tumor necrosis factor antagonist gene: results of a phase 1/2 Study.," *J. Rheumatol.*, vol. 37, no. 4, pp. 692–703, Apr. 2010.

[123] A. C. Nathwani *et al.*, "Self-complementary adeno-associated virus vectors containing a novel liver-specific human factor IX expression cassette enable highly efficient transduction of murine and nonhuman primate liver.," *Blood*, vol. 107, no. 7, pp. 2653–61, Apr. 2006.

[124] A. C. Nathwani *et al.*, "Long-term safety and efficacy following systemic administration of a self-complementary AAV vector encoding human FIX pseudotyped with serotype 5 and 8 capsid proteins.," *Mol. Ther.*, vol. 19, no. 5, pp. 876–85, May 2011.

[125] G. P. Niemeyer *et al.*, "Long-term correction of inhibitor-prone hemophilia B dogs treated with liver-directed AAV2-mediated factor IX gene therapy.," *Blood*, vol. 113, no. 4, pp. 797–806, Jan. 2009.

[126] F. Mingozzi *et al.*, "Induction of immune tolerance to coagulation factor IX antigen by in vivo hepatic gene transfer.," *J. Clin. Invest.*, vol. 111, no. 9, pp. 1347–56, May 2003.

[127] F. Mingozzi *et al.*, "Modulation of tolerance to the transgene product in a nonhuman

primate model of AAV-mediated gene transfer to liver.," *Blood*, vol. 110, no. 7, pp. 2334–41, Oct. 2007.

[128] E. Dobrzynski *et al.*, "Induction of antigen-specific CD4+ T-cell anergy and deletion by in vivo viral gene transfer.," *Blood*, vol. 104, no. 4, pp. 969–77, Aug. 2004.

[129] T. M. Cao, A. Thomas, Y. Wang, S. Tsai, K. Logronio, and J. A. Shizuru, "A chromosome 16 quantitative trait locus regulates allogeneic bone marrow engraftment in nonmyeloablated mice.," *Blood*, vol. 114, no. 1, pp. 202–10, Jul. 2009.

[130] F. Mingozzi *et al.*, "CD8(+) T-cell responses to adeno-associated virus capsid in humans.," *Nat. Med.*, vol. 13, no. 4, pp. 419–22, Apr. 2007.

[131] F. Mingozzi and H. Büning, "Adeno-Associated Viral Vectors at the Frontier between Tolerance and Immunity.," *Front. Immunol.*, vol. 6, p. 120, Jan. 2015.

[132] D. D'Avola *et al.*, "Phase I open label liver-directed gene therapy clinical trial for acute intermittent porphyria," *J. Hepatol.*, vol. 65, no. 4, pp. 776–783, 2016.

[133] B. K. Smith *et al.*, "Inspiratory muscle conditioning exercise and diaphragm gene therapy in Pompe disease: Clinical evidence of respiratory plasticity," *Exp. Neurol.*, vol. 287, pp. 216–224, 2017.

[134] B. Sun *et al.*, "Efficacy of an adeno-associated virus 8-pseudotyped vector in glycogen storage disease type II," *Mol Ther*, vol. 11, no. 1, pp. 57–65, 2005.

[135] D. J. Falk *et al.*, "Comparative impact of AAV and enzyme replacement therapy on respiratory and cardiac function in adult Pompe mice.," *Mol. Ther. Methods Clin. Dev.*, vol. 2, no. January, p. 15007, 2015.

[136] P. a Doerfler, B. J. Byrne, and N. Clément, "Copackaging of multiple adeno-associated viral vectors in a single production step.," *Hum. Gene Ther. Methods*, vol. 25, no. 5, pp. 269–76, 2014.

[137] P. A. Doerfler *et al.*, "Copackaged AAV9 Vectors Promote Simultaneous Immune Tolerance and Phenotypic Correction of Pompe Disease.," *Hum. Gene Ther.*, vol. 27, no. 1, pp. 43–59, 2016.

[138] L. M. Franco *et al.*, "Evasion of immune responses to introduced human acid ??-glucosidase by liver-restricted expression in glycogen storage disease type II," *Mol. Ther.*, vol. 12, no. 5, pp. 876–884, 2005.

[139] B. Sun *et al.*, "Packaging of an AAV vector encoding human acid ??-glucosidase for gene therapy in glycogen storage disease type II with a modified hybrid adenovirus-AAV vector," *Mol. Ther.*, vol. 7, no. 4, pp. 467–477, 2003.

[140] R. J. Ziegler *et al.*, "Ability of adeno-associated virus serotype 8-mediated hepatic expression of acid alpha-glucosidase to correct the biochemical and motor function deficits of presymptomatic and symptomatic Pompe mice.," *Hum. Gene Ther.*, vol. 19, no. 6, pp. 609–21, Jun. 2008.

[141] B. Sun *et al.*, "Enhanced Efficacy of an AAV Vector Encoding Chimeric, Highly Secreted Acid ??-Glucosidase in Glycogen Storage Disease Type II," *Mol. Ther.*, vol. 14, no. 6, pp. 822–830, 2006.

[142] F. Mingozzi and K. A. High, "Immune responses to AAV vectors: overcoming barriers to successful gene therapy.," *Blood*, vol. 122, no. 1, pp. 23–36, Jul. 2013.

[143] N. P. Van Til *et al.*, "Lentiviral gene therapy of murine hematopoietic stem cells ameliorates the Pompe disease phenotype," *Blood*, vol. 115, no. 26, pp. 5329–5337, 2010.

[144] C. St-Pierre, A. Trofimov, S. Brochu, S. Lemieux, and C. Perreault, "Differential Features of AIRE-Induced and AIRE-Independent Promiscuous Gene Expression in Thymic Epithelial Cells.," *J. Immunol.*, vol. 195, no. 2, pp. 498–506, Jul. 2015.

[145] K. Kisand, P. Peterson, and M. Laan, "Lymphopenia-induced proliferation in aire-deficient mice helps to explain their autoimmunity and differences from human patients.," *Front. Immunol.*, vol. 5, p. 51, Jan. 2014.

[146] A. Chuprin *et al.*, "The deacetylase Sirt1 is an essential regulator of Aire-mediated induction of central immunological tolerance.," *Nat. Immunol.*, vol. 16, no. 7, pp. 737–45, Jul. 2015.

[147] C. Porto *et al.*, "Pharmacological enhancement of α-glucosidase by the allosteric

chaperone N-acetylcysteine.," *Mol. Ther.*, vol. 20, no. 12, pp. 2201–11, 2012.

[148] G. Parenti *et al.*, "A Chaperone Enhances Blood α-Glucosidase Activity in Pompe Disease Patients Treated With Enzyme Replacement Therapy," *Mol. Ther.*, vol. 22, no. 11, pp. 2004–2012, 2014.

[149] A. Hille-Rehfeld, "Mannose 6-phosphate receptors in sorting and transport of lysosomal enzymes.," *Biochim. Biophys. Acta*, vol. 1241, no. 2, pp. 177–94, Jul. 1995.

[150] T. N. Petersen, S. Brunak, G. von Heijne, and H. Nielsen, "SignalP 4.0: discriminating signal peptides from transmembrane regions," *Nat. Methods*, vol. 8, no. 10, pp. 785–6, 2011.

[151] G. Ronzitti *et al.*, "A translationally optimized AAV-UGT1A1 vector drives safe and long-lasting correction of Crigler-Najjar syndrome," *Mol. Ther. — Methods Clin. Dev.*, vol. 3, no. May, p. 16049, 2016.

[152] N. Raben *et al.*, "Replacing acid ??-glucosidase in Pompe disease: Recombinant and transgenic enzymes are equipotent, but neither completely clears glycogen from type II muscle fibers," *Mol. Ther.*, vol. 11, no. 1, pp. 48–56, 2005.

[153] N. Raben *et al.*, "Suppression of autophagy in skeletal muscle uncovers the accumulation of ubiquitinated proteins and their potential role in muscle damage in Pompe disease.," *Hum. Mol. Genet.*, vol. 17, no. 24, pp. 3897–908, Dec. 2008.

[154] A. C. Nascimbeni, M. Fanin, E. Masiero, C. Angelini, and M. Sandri, "The role of autophagy in the pathogenesis of glycogen storage disease type II (GSDII).," *Cell Death Differ.*, vol. 19, no. 10, pp. 1698–708, 2012.

[155] L. R. DeRuisseau *et al.*, "Neural deficits contribute to respiratory insufficiency in Pompe disease," *Proc Natl Acad Sci U S A*, vol. 106, no. 23, pp. 9419–9424, 2009.

[156] S. M. F. Turner, A. K. Hoyt, M. K. ElMallah, D. J. Falk, B. J. Byrne, and D. D. Fuller, "Neuropathology in respiratory-related motoneurons in young Pompe (Gaa(-/-)) mice.," *Respir. Physiol. Neurobiol.*, vol. 227, pp. 48–55, 2016.

[157] X. Li, E. M. Eastman, R. J. Schwartz, and R. Draghia-Akli, "Synthetic muscle

promoters: activities exceeding naturally occurring regulatory sequences.," *Nat. Biotechnol.*, vol. 17, no. 3, pp. 241–5, Mar. 1999.

[158] M. Nielsen, C. Lundegaard, and O. Lund, "Prediction of MHC class II binding affinity using SMM-align, a novel stabilization matrix alignment method.," *BMC Bioinformatics*, vol. 8, p. 238, Jul. 2007.

[159] L. Lisowski *et al.*, "Selection and evaluation of clinically relevant AAV variants in a xenograft liver model.," *Nature*, vol. 506, no. 7488, pp. 382–6, Mar. 2014.

[160] J. B. Nietupski *et al.*, "Systemic administration of AAV8-α-galactosidase A induces humoral tolerance in nonhuman primates despite low hepatic expression.," *Mol. Ther.*, vol. 19, no. 11, pp. 1999–2011, 2011.

[161] S. Li *et al.*, "Efficient and Targeted Transduction of Nonhuman Primate Liver With Systemically Delivered Optimized AAV3B Vectors.," *Mol. Ther.*, vol. 23, no. 12, pp. 1867–76, Dec. 2015.

[162] M. A. K. N. K. Paulk, A. Dane, S. Nygaard, "Bioengineered AAV capsids with enhanced human hepatocyte transduction and unique humoral neutralization profiles for use in liver gene therapy," *Liver center annual symposium*. 2016.

[163] R. J. Desnick, "Enzyme replacement and enhancement therapies for lysosomal diseases.," *J. Inherit. Metab. Dis.*, vol. 27, no. 3, pp. 385–410, Jan. 2004.

[164] B. Sun *et al.*, "Correction of multiple striated muscles in murine Pompe disease through adeno-associated virus-mediated gene therapy.," *Mol. Ther.*, vol. 16, no. 8, pp. 1366–71, Aug. 2008.

[165] a Amalfitano *et al.*, "Systemic correction of the muscle disorder glycogen storage disease type II after hepatic targeting of a modified adenovirus vector encoding human acid-alpha-glucosidase.," *Proc. Natl. Acad. Sci. U. S. A.*, vol. 96, no. 16, pp. 8861–6, 1999.

[166] T. J. Fraites *et al.*, "Correction of the enzymatic and functional deficits in a model of Pompe disease using adeno-associated virus vectors.," *Mol. Ther.*, vol. 5, no. 5 Pt 1, pp. 571–8, May 2002.

[167] D. T. Deming, "Molecular genetics and metabolism," 2016, pp. 14–124.

[168] F. Xu *et al.*, "Modulation of disease severity in mice with targeted disruption of the acid alpha-glucosidase gene.," *J. Gene Med.*, vol. 38, no. 4, pp. 481–506, 2009.

[169] N. Raben *et al.*, "Glycogen stored in skeletal but not in cardiac muscle in acid alpha-glucosidase mutant (Pompe) mice is highly resistant to transgene-encoded human enzyme.," *Mol. Ther.*, vol. 6, no. 5, pp. 601–8, Nov. 2002.

[170] B. Sun, H. Zhang, A. Bird, S. Li, S. P. Young, and D. D. Koeberl, "Impaired clearance of accumulated lysosomal glycogen in advanced Pompe disease despite high-level vector-mediated transgene expression.," *J. Gene Med.*, vol. 11, no. 10, pp. 913–20, Oct. 2009.

[171] A. Ruzo *et al.*, "Liver production of sulfamidase reverses peripheral and ameliorates CNS pathology in mucopolysaccharidosis IIIA mice.," *Mol. Ther.*, vol. 20, no. 2, pp. 254–66, Mar. 2012.

[172] P. A. Gonzales *et al.*, "Large-scale proteomics and phosphoproteomics of urinary exosomes.," *J. Am. Soc. Nephrol.*, vol. 20, no. 2, pp. 363–79, Mar. 2009.

[173] N. W. Andrews, "Regulated secretion of conventional lysosomes.," *Trends Cell Biol.*, vol. 10, no. 8, pp. 316–21, Aug. 2000.

[174] B. Sun *et al.*, "Correction of glycogen storage disease type II by an adeno-associated virus vector containing a muscle-specific promoter.," *Mol. Ther.*, vol. 11, no. 6, pp. 889–98, Jun. 2005.

[175] B. Sun, A. Bird, S. P. Young, P. S. Kishnani, Y.-T. Chen, and D. D. Koeberl, "Enhanced response to enzyme replacement therapy in Pompe disease after the induction of immune tolerance.," *Am. J. Hum. Genet.*, vol. 81, no. 5, pp. 1042–9, 2007.

[176] O. Cao *et al.*, "Impact of the underlying mutation and the route of vector administration on immune responses to factor IX in gene therapy for hemophilia B.," *Mol. Ther.*, vol. 17, no. 10, pp. 1733–42, Oct. 2009.

[177] G. Q. Perrin *et al.*, "Dynamics of antigen presentation to transgene product-specific

CD4(+) T cells and of Treg induction upon hepatic AAV gene transfer.," *Mol. Ther. Methods Clin. Dev.*, vol. 3, no. August, p. 16083, 2016.

[178] F. M. A. Meliani, F. Boisgerault, G. Ronzitti, F. Collaud, C. Leborgne, T. K. Kishimoto, "Antigen-specific modulation of capsid immunogenicity with tolerogenic nanoparticles results in successful AAV vector readministration," *Mol. Ther. 24, Suppl. 1*, p. 34, 2016.

[179] A. Biffi, "Gene therapy for lysosomal storage disorders: a good start.," *Hum. Mol. Genet.*, vol. 25, no. R1, pp. R65-75, Apr. 2016.

[180] B. Stern, A. Optun, M. Liesenfeld, C. Gey, M. Gräfe, and I. F. Pryme, "Enhanced protein synthesis and secretion using a rational signal-peptide library approach as a tailored tool.," *BMC Proc.*, vol. 5 Suppl 8, no. Suppl 8, p. O13, 2011.

[181] E. Ayuso *et al.*, "High AAV vector purity results in serotype- and tissue-independent enhancement of transduction efficiency.," *Gene Ther.*, vol. 17, no. 4, pp. 503–510, Apr. 2010.

[182] A. Meliani, C. Leborgne, S. Triffault, L. Jeanson-Leh, P. Veron, and F. Mingozzi, "Determination of anti-adeno-associated virus vector neutralizing antibody titer with an in vitro reporter system.," *Hum. Gene Ther. Methods*, vol. 26, no. 2, pp. 45–53, Apr. 2015.

[183] P. Zhang *et al.*, "Immunodominant liver-specific expression suppresses transgene-directed immune responses in murine pompe disease.," *Hum. Gene Ther.*, vol. 23, no. 5, pp. 460–72, 2012.

[184] S. F. J. Whelan *et al.*, "Distinct characteristics of antibody responses against factor VIII in healthy individuals and in different cohorts of hemophilia A patients.," *Blood*, vol. 121, no. 6, pp. 1039–48, Mar. 2013.

[185] W. van de Veen *et al.*, "IgG4 production is confined to human IL-10-producing regulatory B cells that suppress antigen-specific immune responses.," *J. Allergy Clin. Immunol.*, vol. 131, no. 4, pp. 1204–12, Apr. 2013.

[186] F. Meiler, S. Klunker, M. Zimmermann, C. A. Akdis, and M. Akdis, "Distinct

regulation of IgE, IgG4 and IgA by T regulatory cells and toll-like receptors.," *Allergy*, vol. 63, no. 11, pp. 1455–63, Nov. 2008.

[187] E. Martinuzzi *et al.*, "acDCs enhance human antigen-specific T-cell responses.," *Blood*, vol. 118, no. 8, pp. 2128–37, Aug. 2011.

[188] G. Hu, D. Guo, N. S. Key, and B. M. Conti-Fine, "Cytokine production by CD4+ T cells specific for coagulation factor VIII in healthy subjects and haemophilia A patients.," *Thromb. Haemost.*, vol. 97, no. 5, pp. 788–94, May 2007.

[189] B. Knoechel *et al.*, "Functional and molecular comparison of anergic and regulatory T lymphocytes.," *J. Immunol.*, vol. 176, no. 11, pp. 6473–83, Jun. 2006.

[190] E. M. Moran and F. L. Mastaglia, "Cytokines in immune-mediated inflammatory myopathies: cellular sources, multiple actions and therapeutic implications.," *Clin. Exp. Immunol.*, vol. 178, no. 3, pp. 405–15, Dec. 2014.

[191] A. T. Palermo *et al.*, "Transcriptional response to GAA deficiency (Pompe disease) in infantile-onset patients.," *Mol. Genet. Metab.*, vol. 106, no. 3, pp. 287–300, Jul. 2012.

[192] C. T. Prendergast, D. E. Sanin, and A. P. Mountford, "CD4 T-cell hyporesponsiveness induced by schistosome larvae is not dependent upon eosinophils but may involve connective tissue mast cells.," *Parasite Immunol.*, vol. 38, no. 2, pp. 81–92, Mar. 2016.

[193] P. A. Blair *et al.*, "CD19(+)CD24(hi)CD38(hi) B cells exhibit regulatory capacity in healthy individuals but are functionally impaired in systemic Lupus Erythematosus patients.," *Immunity*, vol. 32, no. 1, pp. 129–40, Jan. 2010.

[194] P. S. Kishnani *et al.*, "Immune response to enzyme replacement therapies in lysosomal storage diseases and the role of immune tolerance induction.," *Mol. Genet. Metab.*, vol. 117, no. 2, pp. 66–83, Mar. 2016.

[195] M. Keiserman *et al.*, "The effect of antidrug antibodies on the sustainable efficacy of biologic therapies in rheumatoid arthritis: practical consequences.," *Expert Rev. Clin. Immunol.*, vol. 10, no. 8, pp. 1049–57, Aug. 2014.

[196] S. S. Fakharzadeh and H. H. Kazazian, "Correlation between factor VIII genotype and

inhibitor development in hemophilia A.," *Semin. Thromb. Hemost.*, vol. 26, no. 2, pp. 167–71, Jan. 2000.

[197] G. Shankar, C. Pendley, and K. E. Stein, "A risk-based bioanalytical strategy for the assessment of antibody immune responses against biological drugs.," *Nat. Biotechnol.*, vol. 25, no. 5, pp. 555–61, May 2007.

[198] G. M. Bartelds *et al.*, "Anti-adalimumab antibodies in rheumatoid arthritis patients are associated with interleukin-10 gene polymorphisms.," *Arthritis Rheum.*, vol. 60, no. 8, pp. 2541–2, Aug. 2009.

[199] K. M. Flanigan *et al.*, "Anti-dystrophin T cell responses in Duchenne muscular dystrophy: prevalence and a glucocorticoid treatment effect.," *Hum. Gene Ther.*, vol. 24, no. 9, pp. 797–806, Sep. 2013.

[200] P. S. Kishnani *et al.*, "Pompe disease diagnosis and management guideline.," *Genet. Med.*, vol. 8, no. 5, pp. 267–88, May 2006.

[201] T. T. Patel, S. G. Banugaria, L. E. Case, S. Wenninger, B. Schoser, and P. S. Kishnani, "The impact of antibodies in late-onset Pompe disease: a case series and literature review.," *Mol. Genet. Metab.*, vol. 106, no. 3, pp. 301–9, Jul. 2012.

[202] A. Wroblewska, B. M. Reipert, K. P. Pratt, and J. Voorberg, "Dangerous liaisons: how the immune system deals with factor VIII.," *J. Thromb. Haemost.*, vol. 11, no. 1, pp. 47–55, Jan. 2013.

[203] A. C. Nascimbeni, M. Fanin, E. Tasca, C. Angelini, and M. Sandri, "Impaired autophagy affects acid ??-glucosidase processing and enzyme replacement therapy efficacy in late-onset glycogen storage disease type II," *Neuropathol. Appl. Neurobiol.*, vol. 41, no. 5, pp. 672–675, 2015.

[204] A. Lucia *et al.*, "McArdle disease: another systemic low-inflammation disorder?," *Neurosci. Lett.*, vol. 431, no. 2, pp. 106–11, Jan. 2008.

[205] M. J. Allen, B. J. Myer, A. M. Khokher, N. Rushton, and T. M. Cox, "Pro-inflammatory cytokines and the pathogenesis of Gaucher's disease: increased release of interleukin-6 and interleukin-10.," *QJM*, vol. 90, no. 1, pp. 19–25, Jan. 1997.

[206] S. G. Banugaria *et al.*, "Persistence of high sustained antibodies to enzyme replacement therapy despite extensive immunomodulatory therapy in an infant with Pompe disease: need for agents to target antibody-secreting plasma cells.," *Mol. Genet. Metab.*, vol. 105, no. 4, pp. 677–80, Apr. 2012.

[207] Y. H. Messinger *et al.*, "Successful immune tolerance induction to enzyme replacement therapy in CRIM-negative infantile Pompe disease.," *Genet. Med.*, vol. 14, no. 1, pp. 135–42, Jan. 2012.

[208] S. G. Banugaria *et al.*, "Bortezomib in the rapid reduction of high sustained antibody titers in disorders treated with therapeutic protein: lessons learned from Pompe disease.," *Genet. Med.*, vol. 15, no. 2, pp. 123–31, Mar. 2013.

[209] S. A. L. Montalvão, A. C. Tucunduva, L. H. Siqueira, A. L. A. Sambo, S. S. Medina, and M. C. Ozelo, "A longitudinal evaluation of anti-FVIII antibodies demonstrated IgG4 subclass is mainly correlated with high-titre inhibitor in haemophilia A patients.," *Haemophilia*, vol. 21, no. 5, pp. 686–92, Sep. 2015.

[210] P. C. Moorehead *et al.*, "Rapid acquisition of immunologic tolerance to factor VIII and disappearance of anti-factor VIII IgG4 after prophylactic therapy in a hemophilia A patient with high-titer factor VIII inhibitor.," *J. Pediatr. Hematol. Oncol.*, vol. 37, no. 4, pp. e220-2, May 2015.

[211] C. A. Akdis and M. Akdis, "Mechanisms of immune tolerance to allergens: role of IL-10 and Tregs.," *J. Clin. Invest.*, vol. 124, no. 11, pp. 4678–80, Nov. 2014.

[212] A. Renand *et al.*, "Chronic cat allergen exposure induces a TH2 cell-dependent IgG4 response related to low sensitization.," *J. Allergy Clin. Immunol.*, vol. 136, no. 6, pp. 1627-35–13, Dec. 2015.

[213] A. F. Santos *et al.*, "IgG4 inhibits peanut-induced basophil and mast cell activation in peanut-tolerant children sensitized to peanut major allergens.," *J. Allergy Clin. Immunol.*, vol. 135, no. 5, pp. 1249–56, May 2015.

[214] R. C. Aalberse, R. van der Gaag, and J. van Leeuwen, "Serologic aspects of IgG4 antibodies. I. Prolonged immunization results in an IgG4-restricted response.," *J.*

Immunol., vol. 130, no. 2, pp. 722–6, Mar. 1983.

[215] F. Dazzi *et al.*, "High incidence of anti-FVIII antibodies against non-coagulant epitopes in haemophilia A patients: a possible role for the half-life of transfused FVIII.," *Br. J. Haematol.*, vol. 93, no. 3, pp. 688–93, Jun. 1996.

[216] P. Dickson *et al.*, "Immune tolerance improves the efficacy of enzyme replacement therapy in canine mucopolysaccharidosis I.," *J. Clin. Invest.*, vol. 118, no. 8, pp. 2868–76, Aug. 2008.

[217] R. Kakavanos, C. T. Turner, J. J. Hopwood, E. D. Kakkis, and D. A. Brooks, "Immune tolerance after long-term enzyme-replacement therapy among patients who have mucopolysaccharidosis I.," *Lancet (London, England)*, vol. 361, no. 9369, pp. 1608–13, May 2003.

[218] S. Nayak *et al.*, "Immune responses and hypercoagulation in ERT for Pompe disease are mutation and rhGAA dose dependent.," *PLoS One*, vol. 9, no. 6, p. e98336, Jan. 2014.

[219] S. Han *et al.*, "Enhanced efficacy from gene therapy in Pompe disease using coreceptor blockade.," *Hum. Gene Ther.*, vol. 26, no. 1, pp. 26–35, Jan. 2015.

[220] J. Oldenburg, R. Schwaab, and H. H. Brackmann, "Induction of immune tolerance in haemophilia A inhibitor patients by the 'Bonn Protocol': predictive parameter for therapy duration and outcome.," *Vox Sang.*, vol. 77 Suppl 1, pp. 49–54, Jan. 1999.

[221] N. J. Singh and R. H. Schwartz, "The strength of persistent antigenic stimulation modulates adaptive tolerance in peripheral CD4+ T cells.," *J. Exp. Med.*, vol. 198, no. 7, pp. 1107–17, Oct. 2003.

[222] Z. B. Kazi *et al.*, "Durable and sustained immune tolerance to ERT in Pompe disease with entrenched immune responses.," *JCI insight*, vol. 1, no. 11, pp. 1–9, 2016.

[223] S. E. Lipinski, M. J. Lipinski, A. Burnette, T. A. Platts-Mills, and W. G. Wilson, "Desensitization of an adult patient with Pompe disease and a history of anaphylaxis to alglucosidase alfa.," *Mol. Genet. Metab.*, vol. 98, no. 3, pp. 319–21, Nov. 2009.

[224] J.-S. Park, H.-G. Kim, J.-H. Shin, Y.-C. Choi, and D.-S. Kim, "Effect of enzyme replacement therapy in late onset Pompe disease: open pilot study of 48 weeks follow-up.," *Neurol. Sci.*, vol. 36, no. 4, pp. 599–605, Apr. 2015.

[225] A. T. van der Ploeg *et al.*, "Open-label extension study following the Late-Onset Treatment Study (LOTS) of alglucosidase alfa.," *Mol. Genet. Metab.*, vol. 107, no. 3, pp. 456–61, Nov. 2012.

[226] H. Galjaard, M. Mekes, D. E. Josselin de Jong JE, and M. F. Niermeijer, "A method for rapid prenatal diagnosis of glycogenosis II (Pompe's disease).," *Clin. Chim. Acta.*, vol. 49, no. 3, pp. 361–75, Dec. 1973.

[227] F. Mingozzi *et al.*, "AAV-1-mediated gene transfer to skeletal muscle in humans results in dose-dependent activation of capsid-specific T cells.," *Blood*, vol. 114, no. 10, pp. 2077–86, Sep. 2009.

[228] B. Spiessens, E. Lesaffre, G. Verbeke, K. Kim, and D. L. DeMets, "An overview of group sequential methods in longitudinal clinical trials.," *Stat. Methods Med. Res.*, vol. 9, no. 5, pp. 497–515, Oct. 2000.